11-23-2010

Recent Uplift of the Burica Peninsula, Panama and Costa Rica, Recorded by Marine Terraces

Daniel Davidson
Trinity University, ddavidso@trinity.edu

Recent Uplift of the Burica Peninsula, Panama and Costa Rica, Recorded by Marine Terraces

DANIEL DAVIDSON

A DEPARTMENT HONORS THESIS SUBMITTED TO THE
DEPARTMENT OF GEOSCIENCES AT TRINITY UNIVERSITY
IN PARTIAL FULFILLMENT OF THE REQUIREMENTS FOR
GRADUATIONWITH DEPARTMENTAL HONORS

NOVEMBER 23, 2010

_____ _____

Dr. Thomas Gardner, Thesis Advisor Dr. Glenn Kroeger, Department Chair

_____

Associate Vice President for
Academic Affairs

TABLE OF CONTENTS

LIST OF FIGURES

LIST OF TABLES

ACKNOWLEDGMENTS

I would like to thank the National Science Foundation grant EAR-4241965U from the Tectonics program, and The Tinker Family Endowment for the Geosciences for funding this project. I thank Dr. Donald Fisher at Pennsylvania State University for allowing me to use previous work on the peninsula including radiocarbon and OSL samples used in this study. I would also like to thank Kristen Morell for her field assistance, lessons in ArcGIS, and collaboration on data analysis. A special thank-you goes to Allison Teletzke for being an excellent partner to collaborate with during this project. Teletzke helped me from data analysis at school, to hiking in the mud while taking DGPS data points. I thank Dr. Leslie Bleamaster for reading and providing edits of my work. I am also thankful for the encouragement from all the faculty, staff, and students in the Trinity University Geosciences Department. A very important thank-you is needed for Thomas Gardner for not only allowing me this opportunity to complete my thesis but being a great mentor through my final semesters at Trinity. I would like to thank everyone I surround myself with everyday from my parents to my friends for always encouraging me in everything I do. Finally I would like to thank God, because through him all things are possible.

ABSTRACT

Deformation and uplift of the Burica Peninsula along the Panama-Costa Rica border results from eastward migration of the Panama Triple Junction (PTJ); the boundary between three tectonic plates. As the triple junction migrates to the southeast at ~55 mm/yr along the Middle America Trench (MAT), the Panama Fracture Zone (PFZ), separating the Cocos and Nazca plates, subducts under the Panama microplate. Differences in the thickness of the plates across the PFZ, as well as the rate and angle of subduction between the Cocos and Nazca plates, cause the Panama microplate to step up and over the Cocos plate. A flight of up to seven marine terraces are recognized on Burica, the highest of which does not exceed ~80 m. Terraces grade from thin, sediment-starved strata deposits to ~10 m thick bay-filled shelf sediments. Radiocarbon and Optical Stimulated Luminescence (OSL) ages indicate these deposits range in age from Marine Isotope Stage (MIS) 3 (45,800 ± 7,100 YBP) to latest Holocene (90 ± 50 YBP). Uplift rates calculated from terrace ages and high-precision DGPS surveys range between 2.2 mm/yr and 3.2 mm/yr. The consistent elevation of inner edges (paleo-high tide line) indicates that uplift of the Burica Peninsula is spatially uniform. The Panama microplate is being uplifted at a constant and uniform uplift rate along a north striking and eastward dipping thrust fault in response to subduction of the Cocos Ridge.

INTRODUCTION

Tectonic Setting (Properties of a subducting plate that affect deformation are age, volcanic activity, speed of subduction)

The purpose of this thesis is to determine the rates of deformation of the Burcia Peninsula that results from subduction of the Cocos plate at the Middle American Trench (MAT). The Burcia Penisula is located 20 kilometers northeast from the MAT and about 55 kilometers north of the Panama Tripple Junction (PTJ); the intersection of the Panama microplate, Nazca plate, and Cocos plate (Figure 1a). The Cocos plate is southwest of the Panama microplate and west of the Nazca plate. Both the Nazca and Cocos plates subduct beneath the Panama microplate at the MAT. However, subduction of the Cocos and Nazca plates underneath the Panama microplate result in two very different subduction regimes. The Cocos plate is younger and much thicker and has many seamounts on it created by volcanic activity at the Galapagos hot spot (Figure 1b). Also, a significant feature on the Cocos plate is the Cocos Ridge, a thick, asymmetric ridge with approximately 2000 meters of relief (Figure 1b) (Corrigan, 1990; and Sitchler et al., 2007). The thick, buoyant Cocos Ridge is very difficult to subduct under the Panama Microplate. Also, there is a boundary between the Cocos and the Nazca plates, a transform boundary called the Panama Fracture Zone (PFZ). The PFZ is a right lateral transform fault. The intersection of the PFZ and the MAT is the PTJ.

The motion of the Nazca plate is 48 mm/yr towards the east, the Cocos plate is moving at 91 mm/yr towards the northeast and the Panama microplate is moving 11 mm/yr all with respect to the Caribbean plate (Figure 2a) (DeMets, 2001). The Cocos plate is subducting underneath the Panama microplate at a rate of about 80 mm/yr, while the Nazca is only subducting obliquely underneath the Panama microplate at a rate of about 20 mm/yr. As previously mentioned, the Cocos plate is much younger, less dense, and thicker than the Nazca plate. Therefore, because of this thick, buoyant plate and high subduction velocity, the plate subducts at a much shallower angle than the Nazca plate. The Panama microplate has two very different types of subduction acting against it at once. When doing the vector calculations, as shown in Figure 2a, the conclusion is that the PTJ is migrating 55mm/yr along the MAT.

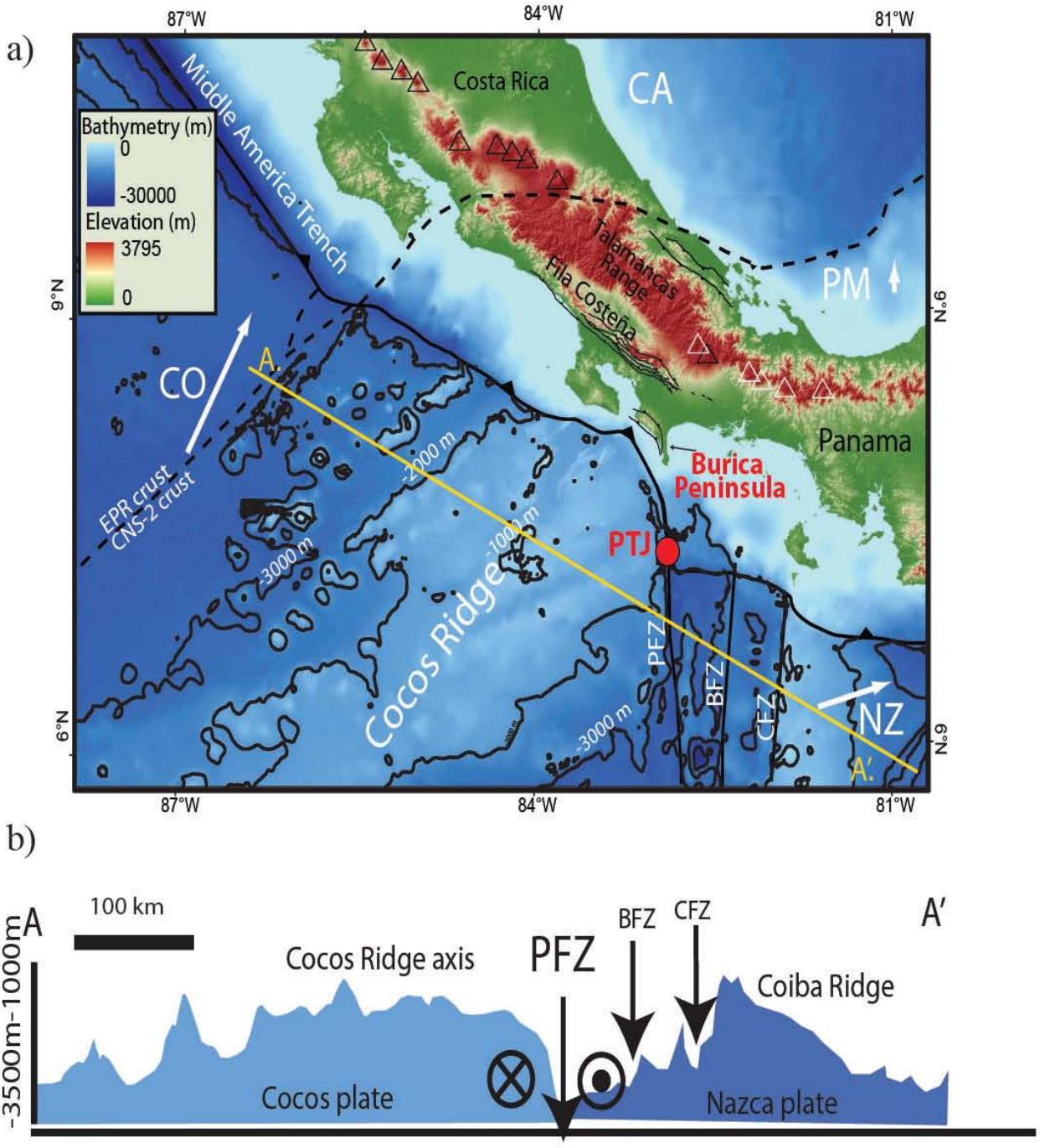

Figure 1 (Tectonic Setting) General tectonic setting shown by a DEM of the area surrounding the Panama Triple Junction. Abbreviations are: Cocos plate=CO, Nazca plate=NZ, Caribbean plate=CA, Panama microplate=PM, PFZ=Panama Fracture Zone, BFZ=Balboa Fracture Zone, CFZ=Coiba Fracture Zone and PTJ= Panama Triple Junction. Bathymetric data combined from ETOPO1 (Smith and Sandwell, 2003; and Ranero et al., 2003). Topography from SRTMv4 dataset. Black triangles indicate active volcanoes, white triangles indicate extinct volcanoes. Plate motion with respect to the Caribbean plate is indicated by arrows . b) The cross-section, A to A', shows the difference in bathymetry of the subducting Nazca and Cocos plate.

a)

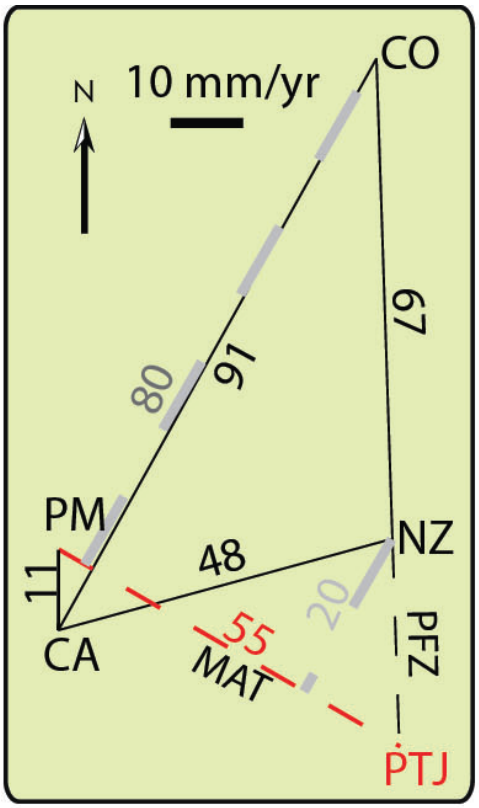

Figure 2 (Triple Junction Migration) a) A plate vector diagram in mm/yr based on velocity model NNR-NUVEL-1B (Bird, 2003; DeMets et al., 1990; DeMets et al., 2000; and Shuanggen and Zhu, 2004). Featured abbreviations are as follows: Cocos plate=CO, Nazca plate=NZ, Caribbean plate=CA, Panama microplate=PM, Panama Fracture Zone=PFZ, MAT= Middle American Trench and Panama Triple Junction=PTJ. The black solid lines are the plate motions with respect to the Caribbean plate, The grey dash lines are the subduction rates with respect to the MAT, The red dashed line is the migrating PTJ. The diagram shows the PTJ travels 55 mm/yr towards the southeast along the MAT. b) A plate reconstruction model of the region around the Panama Tripple Junction for the past 3 MA based on reconstruction of MacMillan et al. 2004. The blue dot represents a stationary point on the Panama microplate and the red dot represents the migration of the Panama Triple Junction at 55 mm/yr.

b)

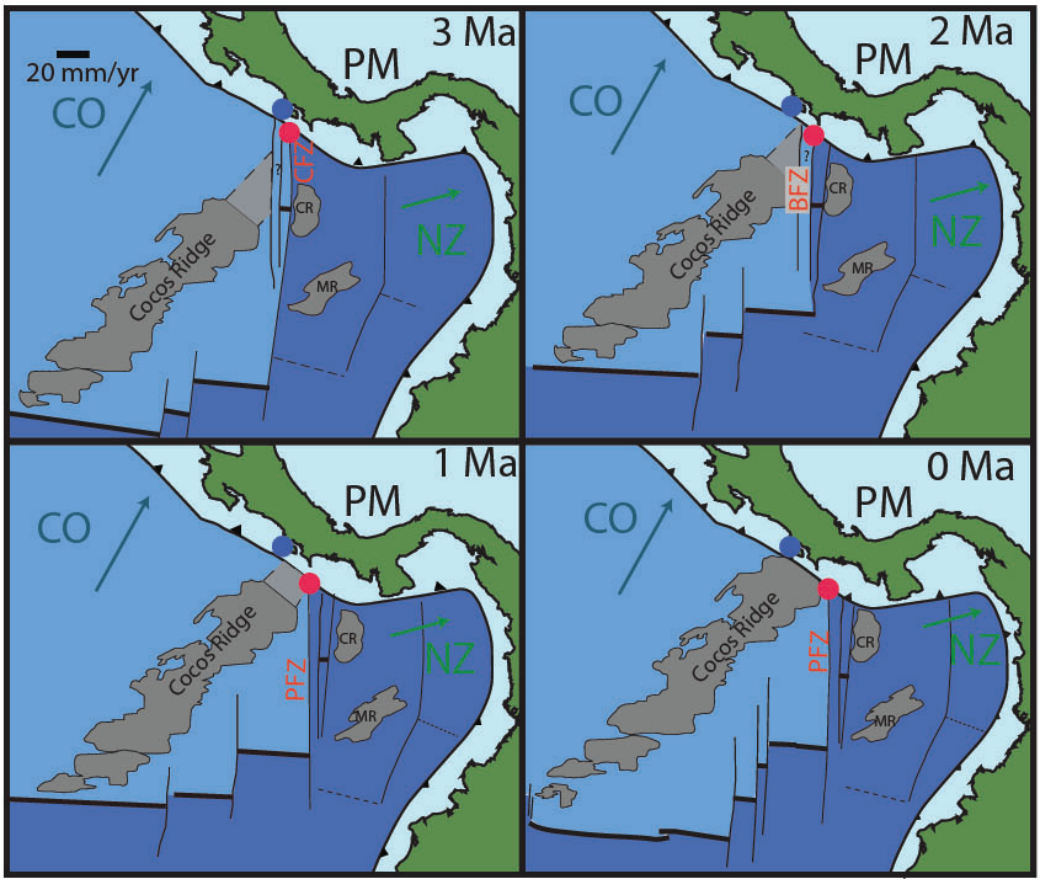

This means that the PTJ and PFZ are both migrating east at 55 mm/yr along the MAT with respect to the Panama microplate (Figure 2b). This causes the Panama microplate to be affected by a change in subduduction from the Nazca to the Cocos plate as the PTJ migrates along the MAT (Morell et al., 2008; Gardner et al., 1992; and MacMillan et al., 2004). The hypothesis of this thesis is that the Panama microplate is actively being uplifted and forced to step up and over the thick Cocos plate as the Panama Triple Junction migrates to the east along the Middle American Trench and that marine terrace deposits on the Burica Peninsula record this uplift.

The Burica Peninsula contains a series of thrust faults, which can be seen at the surface (Figure 3). The location of the thrust faults can be determined by the offset bedding, bedding tilt angle, and structural reconstruction of the Pilocene Charco Azul and Pleistocene Puerto Armuelles Formations (Morell et al., 2009; Fisher et al., 2004;). Within the Armuelles Formation are the Baru volcanic deposits, which are about 278 thousand years old as determined from recent Ar^{40}/Ar^{39} dating (Morell, pers. comm.). The thrust faults are the mechanism for the uplift of the peninsula. The faults strike to the north and dip approximately 30 degrees (average thrust angle) to the east. The marine terraces are the youngest and most recent deposits on the peninsula.

Marine sediments on the Burica Peninsula record both active uplift and changing sea levels. The Burica Peninsula extends from Central America south into the Pacific Ocean. The Burica Peninsula is separated by the Costa Rican and Panamanian border. For the purpose of this research all data will be collected on the eastern Panamanian side of the peninsula. The peninsula is made up of a large, steep range of peaks at its core rising a maximum in elevation of 350 meters. This will be referred to as the paleo-sea cliff. Also there is a stair-step coastal landscape extending from the paleo sea cliff to the coast. These stair-step landscapes are separated into risers and marine terraces. The marine terraces are old abandoned marine abrasion platforms created at sea level. In order for risers and terraces to form, the area must be tectonically active and/or sea levels must change or both.

Purpose

The purpose of this study is to:

Figure 3 (Thrust Fault Locations on the Burica Peninsula) A geologic map of the Burica Peninsula showing geology and a stratigraphy column of the Burica Peninsula. The terraces are colored acording to elevation. The marine terraces on the Burica Peninsula are composed of the youngest sediments, the Monte Verde formation. The Monteverde formation is colored by the grading of colors of all the terraces. Baru volcanic deposits are deposited no less 278 ka ago. These volcanics can be seen in the study area. From what is exposed at the surface on the Burica Peninsula and topography, thrust fault locations can be projected onto the peninsula (Morell et al., 2008). The thrust faults strike north and have a approximate 30 degree dip to the east.

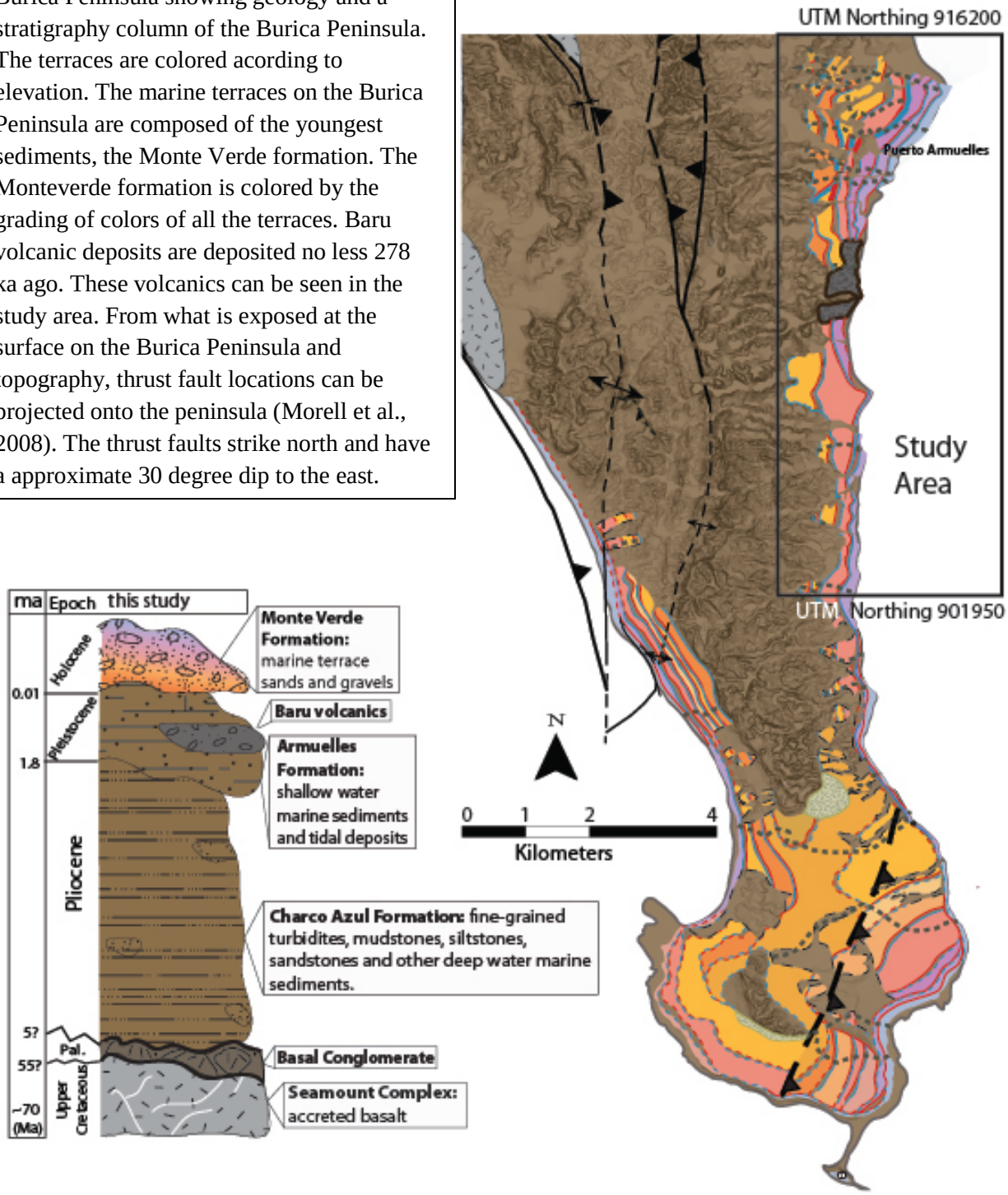

1) Create a marine terrace map of the Burica peninsula separating terraces by their elevations from Port Armuelles (a city located at the North East corner of the peninsula) to the UTM Northing coordinate 901950 (Figure 3)

2) Calculate the uplift rate of the marine terraces using dated samples, depth of deposition from paleo sea level elevations, and modern elevation.

3) Plot the marine terrace elevations and compare the data with other data south of UTM Northing coordinate 901950 (Teletzke, 2010) and see if there is any tectonic tilt.

4) Evaluate the original hypothesis: the Panama microplate (Burica Peninsula) is actively being uplifted and forced to step up and over the thick Cocos plate as the Panama Triple Junction migrates to the east along the Middle American Trench and marine terrace on the Burica Peninsula record this uplift.

Formation of a marine terrace

To constrain the amount of uplift from a marine terrace, the mode of formation and characteristic features must be known. A marine terrace is an old, nearly flat, marine, abrasion platform created by wave erosion into bedrock creating a low relief surface (Figure 4a). A bedrock sea cliff is formed where the waves erode the coastline at mean high tide or the high tide debris line (HTDL) (Figure 5) (Bradley, 1957; and Anderson et al., 1999). Beach sands are deposited on top of the gently seaward sloping marine abrasion platform. The marine terraces are composed of horizontally bedded sand deposited on top of tilted mudstone (Charco Azul and Puerto Armuelles Formations). The Charco Azul and Puerto Armuelles Formations will be referred to as the bedrock in this study. The sea-cliff is composed of either of these tilted mudstones. After the formation of the marine abrasion platform either a drop in sea level or tectonic uplift will cause the platform to be abandoned and preserve the deposits and fossils, thus forming the marine terrace (Figure 4a).

Note that for the formation of the abrasion platform, sea levels must be stable enough to erode a gently seaward sloping surface and deposit sediments. So, marine terraces are only formed during either stable high stand or low stand of the sea. The low stand marine terraces are hardly ever preserved because

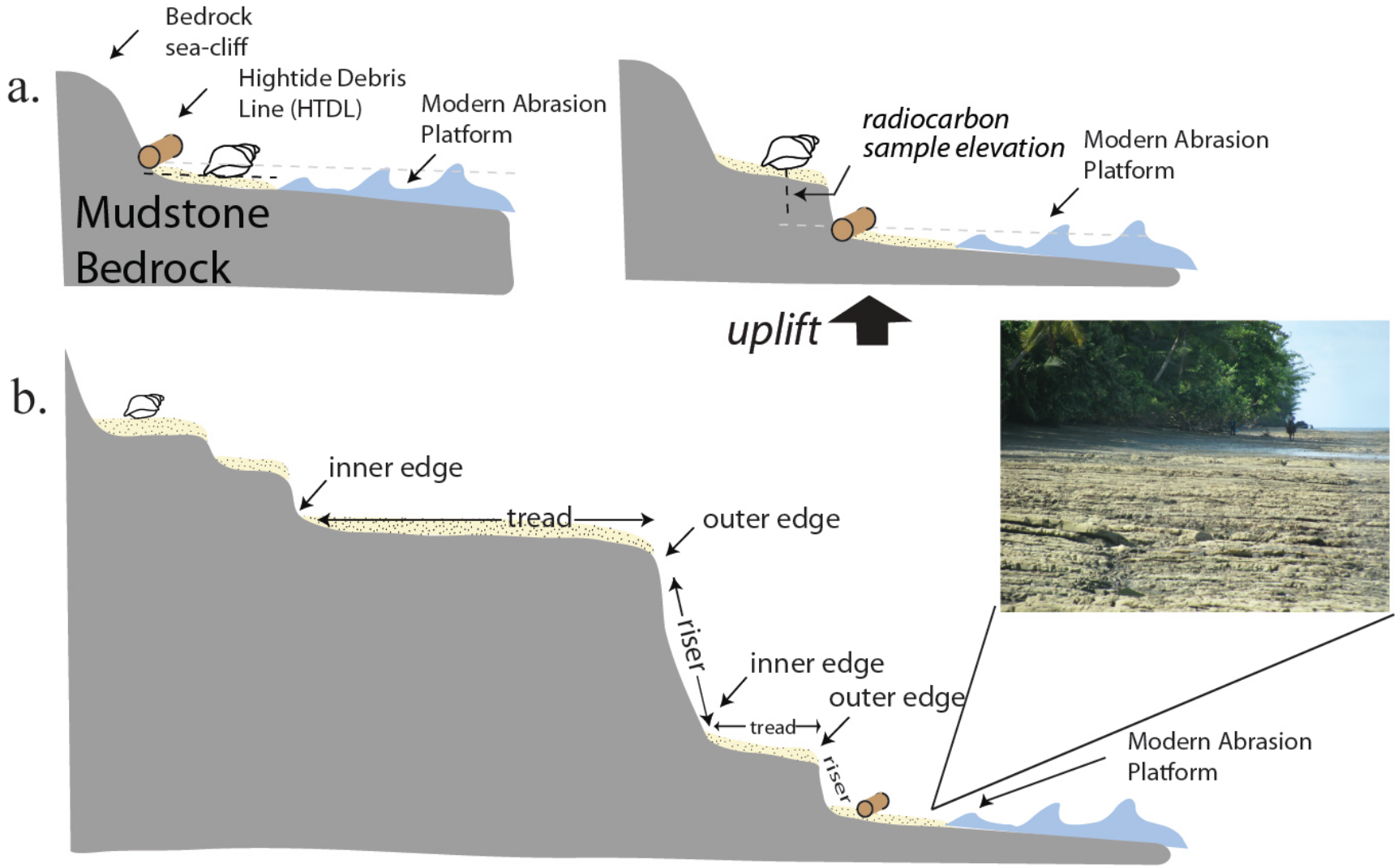

Figure 4 (Marine Terrace Generation and Features) Diagram showing formation of marine abrasion platform and a marine terrace. a) Marine abrasion platform is created when sea level is relatively stable. Uplift or sea level fall causes active abrasion platform to be abandoned and a new one begins forming. Shells are left behind in the sediment on the platform and can be dated to determine the age of the terrace. b) Over time multiple uplift events or eustatic sea level changes will cause marine terraces of varying extent to form. These terraces are separated by a riser, are bounded by an inner edge at the base of the riser and an outer edge at the top of the riser, and a relatively flat tread. Together these produce the classic stair step topography of marine terraces along the coast.

Figure 5 (High Tide Debris Line) Picture of Teletzke standing on top of marine terrace 6. The high tide debris line, is seen here at the modern inner edge (Blue Line), which is also the modern average high tide line. The red line is the modern outer edge.

subsequent higher sea levels erode any low terraces formed while creating a new marine shelf. Thus, marine terraces are a record of both highstand sea levels and tectonic uplift.

The sea cliff behind each terrace is referred to as a riser (Figure 4b). Where the riser and back of the terrace tread meet is referred to as the inner edge (IE). Modern inner edges are being formed presently where waves erode at the HTDL. The preserved inner edge records the ancient HTDL for previous beaches. Importantly, the terrace is a nearly horizontal datum and the paleo HTDL is the closest observable estimate for sea level. The nearly flat surface of the terrace is often referred to as the tread. The tread ends at the outer edge (OE) when the riser and next terrace begin. The outer edges for terraces vary in height and distance along the coast, but inner edges vary only very slightly along the coast. This is because, even today, the HTDL is relatively constant along the coast and the abrasion platform varies in distance away from the coast.

Barbados Sea Level Curve

In order to accomplish the previously listed thesis purposes, a sea level curve from previously published research is necessary to distinguish uplift from sea level changes. The paleo-sea level curve used in this paper is derived from analyses done on coral reef terraces and benthic foraminifera on the island of Barbados. The research was done by W. R. Peltier and R.G. Fairbanks (2006) from the following article, “Global glacial ice volume and Last Glacial Maximum duration from an extended Barbados sea level record”. The research used uranium and thorium ratios (234 Th/ 234 U) to date corals along the broad, exposed continental shelf of Barbados. The broad continental shelf allows for multiple datasets to be collected and therefore a very accurate sea level curve can be produced. Comparing the ages with modern elevation should give a paleo sea level curve. However, this can be inaccurate because of slight tectonic movement. The analysis of oxygen isotope ratios ($O^{18}/ {}^{16}O$) on benthic foraminifera provides an absolute low sea level during the Last Glacial Maximum. According to previous studies the ratios between these two oxygen isotopes are related to ice volume (Shackleton, 1967); (Lambeck and Chappell, 2001). When ice forms it is more likely to be composed ^{16}O, because ^{16}O is a lighter atom and is more likely to evaporate. This causes the snow creating glaciers to be ^{16}O rich while the oceans will be

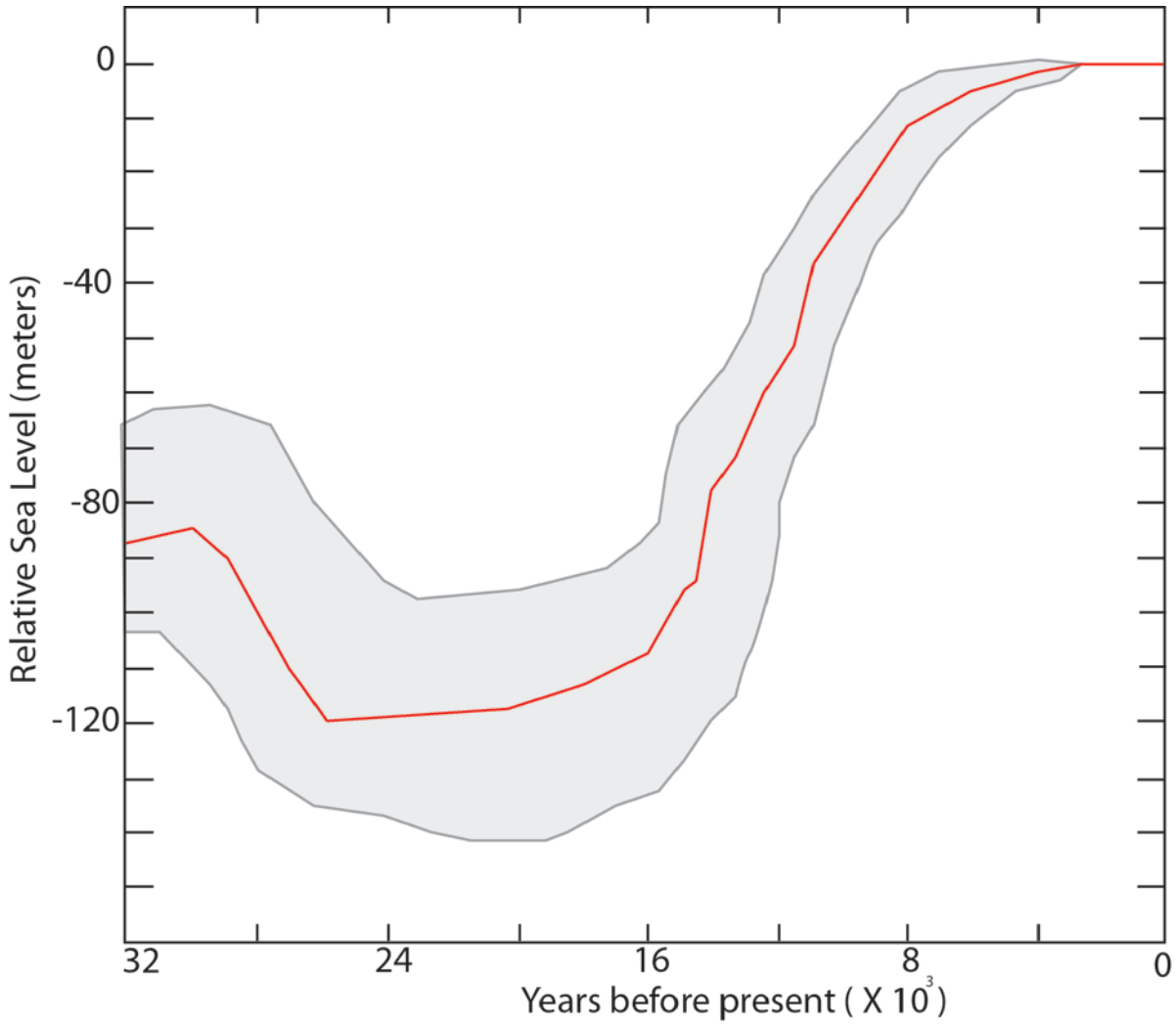

Figure 6 (Barbados Sea Level Curve) Plot showning the Barbados sea level curve (W. R. Peltier and R.G. Fairbanks, 2006). The red line is mean sea level. 0 equals modern sea level. The grey area is the error from other similar sea level research around the world.

^{18}O rich. From the $^{18}O/^{16}O$ ratio the volume of ice of the Last Maximum Glacial can be calculated. The data show that the sea level during the Last Glacial Maximum was approximately 120 m below modern sea level (Figure 6). Although the isotopic influences of bottom water temperatures can cause error in the ice volume measurements, sites sufficiently distant from areas of major glaciations confirm an approximate 120 m drop in sea level during the last glacial maximum (Shackleton, 1967). The age of the sea level minimum has been modified recently (Peltier and Fairbanks, 2006). The previously estimated time was 21,000 years ago. Calculations using this low stand sea level gave an uplift rate for Barbados of .34 mm/yr. However with the extent of recent coral dating on Barbados, the low stand at 21,000 years ago is inconsistent. Peltier and Fairbanks (2006) suggest instead the low stand occurred 26,000 years ago to better fit their data. The Barbados sea level curve used in this paper is from the extensive research from Peltier and Fairbanks(2006) on the island.

Research Objectives

The hypothesis of this thesis is that the Burica Peninsula is actively being uplifted because of the recent subduction of the Cocos plate as the PTJ migrates to the east of Burica (Figure 2b). In order to evaluate this hypothesis and solve for an uplift rate, the following objectives need to be completed:

1) Do GPS surveys of the peninsula.

2) Use GPS data, air photos, and field work to construct a terrace map and cross-sections of the peninsula.

3) From the map and cross-sections, correlate inner edge elevations along the coast to look for tilt during uplift.

4) Calculate an uplift rate using the Barbados sea level curve, depth of depositions, ages of the samples and elevations of the samples.

5) Constrain how Burica is deforming in response to the migration of the PTJ.

METHODOLOGY

GPS Goals

In order to successfully accomplish these objectives, multiple GPS elevations were collected at key locations on the marine terraces using Trimble GPS receivers. The goal was to take a data point as close to the inner edge and outer edge as possible and to take multiple points along each terrace tread and riser. This should produce an accurate transect across the landscape from the oldest paleo sea-cliff to the modern coast. The transect surveys were done in areas where a complete survey from the coast to the paleo-sea cliff could be accomplished in a relativly straight line. The inner edge and outer edge are the most important points because at these points there is a sharp break in slope. The inner edge elevation is even more important because it forms as a nearly horizontal datum at mean high tide and because the inner edge elevations will be used to correlate the terraces along the coast. GPS data were collected during July and August of 2009.

Collecting Data in the Field

Two, real-time, differentially correcting Trimble GPS receivers were used in order to achieve a precise elevation and UTM coordinates for each of the data points. The Trimble Pro XH was used as our base GPS receiver and it was stationed near camp away from hills and trees (Figure 7). The base station elevation was measured using an altimeter, zeroed at the HTDL. The reason the HTDL is used and not the mean sea level is because the HTDL is recognizable by the debris line on the beach. The mean sea level is not distinguishable along the beach, but elevations will be calculated relative to mean sea level in the Data Analysis section. The altimeter gave a reading of 4 meters above the HTDL for the base station. A GeoXT was the other Trimble GPS used as a rover. It is hand held and used to take data points out in the field. The base station allows for corrections to be made on all GPS data points taken by the rover. The GeoXT unit collected uncorrected data from satellites. The uncorrected data had a horizontal precision of decimeters (depends on the number of satellites received by the rover) but the vertical precision was not as good. Correcting the rover data with the base station gave better vertical precision, approximately 1-2 meters. This technique of correcting points taken in the field by a rover with a base station is referred as

Figure 7 (Base Station) Picture showing Gardner to the left of the GPS base station and the altimeter below the GPS base station

Differential Corrected GPS (DGPS). All data points during this research are DGPS points to give the most accurate elevation of each point.

Combined, both units were set to a specific Position Dilution of Precision (PDOP). The PDOP value is how accurate the recording is for the horizontal and vertical data. The number and positions of satellites determine the PDOP. The optimum scenario is multiple satellites spread out across the sky from horizon to horizon. The PDOP for the GPS data in this study was set to not record any data with a PDOP range in excess of 5 meters.

Getting precise elevations and UTM coordinates for some radiocarbon sample locations became a problem because of the PDOP. Shell samples were mostly found in either road cuts surrounded by trees or in river cuts surrounded by dense vegetation. If an elevation for a sample could not be determined, the elevation of the closest data point located on the same terrace was used. All DGPS data and any obtainable elevations of the samples are in Appendix A. The points off of transect used for sample elevations will have the shell sample number in the notes.

Each point has a point identification, comment, elevation in meters, UTM northing and easting, vertical precision, and max PDOP. The comments identify the type of feature the point represents on the marine terrace. Abbreviations are used to denote each feature: Inner Edge (IE), Outer Edge (OE), Riser (R), Terrace (T), Paleo Sea Cliff (PS), High Tide Debris Line (HTDL), Lahar Deposits (L), Shell (Radiocarbon Dated Shell), OSL (Sand Sediment Sample). The terraces are not perfectly flat because of erosion and depositional slope, so multiple points were taken in order to get a more accurate elevation and slope of each tread

DATA ANALYSIS

GPS data for this study can be found in Appendix A, which contains all raw DGPS data and DGPS transect cross-sections. The coordinate system used was WGS 1984, UTM Zone 17N.

Terrace Mapping

All nine DGPS surveys are shown on Plate 1. All DGPS points are plotted on geo-referenced aerial photos and can be seen in the upper left hand corner of each transect in Appendix A. The GPS data

points are coded by shape and color (see Appendix A key). The key is located on the upper left hand corner of each transect. Each terrace is assigned a unique color in Plate 1. The youngest terrace (blue) is the one closest to the coast and lowest in elevation. The oldest terrace (dark orange) is the one closest to the paleo sea cliff and highest in elevation. The riser which separates each terrace, is bedrock (Charo Azul or Armuelles Formation). Risers are composed of only bedrock and have no sediment deposition on them. The paleo sea cliff is only bedrock as well. For this reason they are being showed using the same bedrock symbol. The dissected areas are areas with extensive fluvial erosion where surface elevations no longer represent depositional elevation of marine terraces. The lahar deposit is the Baru volcanic deposit (Figure 3) forms a steep hill locally along the coast preserving no terraces younger than the fourth terrace. Marine terraces are referred to in the key as Qt. This stands for Quaternary terrace.

Terraces are assigned a unique Qt number based on the elevation of the inner edge. Plate 1 was created by comparing inner edge elevations and evaluating which terrace each inner edge belongs to. Inner edge elevations for each terrace were then plotted to see if there was any elevation overlap (Figure 8). The inner edge data was also compared to Teletzke (2010) for the data south of this study to see if there was any overlap. There is little overlap among terrace inner edge. For example, inner edges of Qt 4 do not overlap with inner edges of Qt 5 or QT 3. However the, southern inner edges were generally lower than the inner edges in the north; squares in Figure 8 tend to plot below diamonds. After each inner edge was assigned a terrace number, the terrace map (Plate 1) was created. The inner edges and outer edges were plotted on geological referenced aerial photos of the Burica Peninsula in the exact spots the GPS points were taken. Then sterophotos were used to create a 3d image of the peninsula and precisely drawn lines connecting the GPS inner edge and outer edge points for each terrace. The oil terminal shown on Plate 1 does not have any aerial photos, nor could any surveying be done in this area. To solve this problem, surveys were taken as close as possible to the terminal. In order to connect the inner edges, elevations from an SRTM (Shuttle Radar Thematic Mapping) image were used. After this was completed the terrace outline became clear and each terrace could be outlined, colored and clearly followed along the coastline. Next, the UTM coordinates for each dated sample was plotted on the terrace map. After this

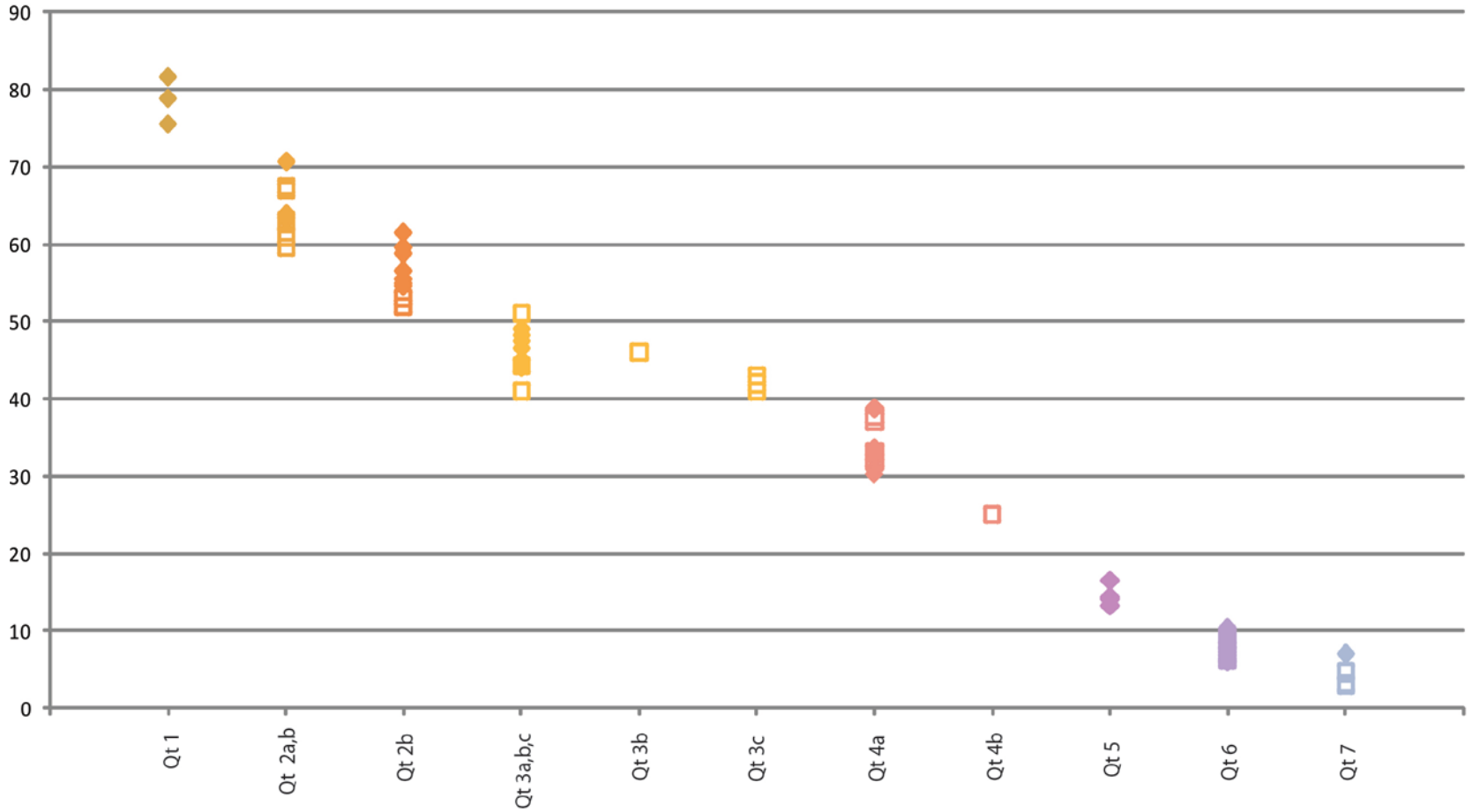

Figure 8 (Range of Inner Edge Elevations) A plot of inner edge elevations vs. marine terraces. Solid squares represent IEs recorded south of UTM Northing 901950 by Teletzke (2010). Solid diamonds represent the elevation of IEs recorded north of UTM Northing 901950. Open symbols are projected points determined by air photos and intersecting slopes from the riser and terrace. Diagram shows very little overlap between terrace IE elevations.

a few man made land marks were added to show correlation of the map to the aerial photos. These land marks include the oil reserves from the oil terminal, the only road along the coast, the main road entrance to Puerto Armuelles and the Peurto Armuelles Airport. The airport was actually strategically placed solely on one terrace because it is such a flat surface.

Transect Plots

After Plate 1 was finished, the transects seen in Appendix A were created. By plotting the DGPS elevation and local distance from the HTDL for each data point taken by the surveys. Elevation is giving by the DGPS data. The local distance however is more complicated and needed to be calculated (Figure 9). The reason for this is that the DGPS points need to be measured perpendicular to the coast. In order to successfully accomplish this, the UTM Northing and Easting needs to be used. To make this a more simple process, the UTM coordinates are adjusted to be local distances from the HTDL. Local distance for both northing and easting are calculated by finding the absolute value of the difference between UTM coordinates for the DGPS point and the UTM coordinate for the HTDL for each survey. This is done for every point on every transect. Some transects did not have a HTDL because heavy vegetation prevents a path to the coast. For these transects the distance from the coast (approximately the HTDL) to the closest DGPS survey point was measured by ruler. The distance from the coast is added after all calculations were completed to each point for the survey. The points were plotted on a graph with the local easting as the x axis and the local northing as the y axis. Next a linear regression was performed to obtain a best-fit line for all the previously plotted points. Using the negative reciprocal of the slope of the regression line, the data points can now be orthogonal projected onto the best fit line.

The equations used to find the regression line and orthogonal line are below:

Regression line: $y=mx+b_1$ $(m=m_1)$ (1)

Orthogonal line: $y=-(1/m_1)x+b_2$ $(1/m_1=m_2)$ (2)

Using these formulas we can find the calculated local distance from the coast for each data point. The formulas below give the local distance for each point:

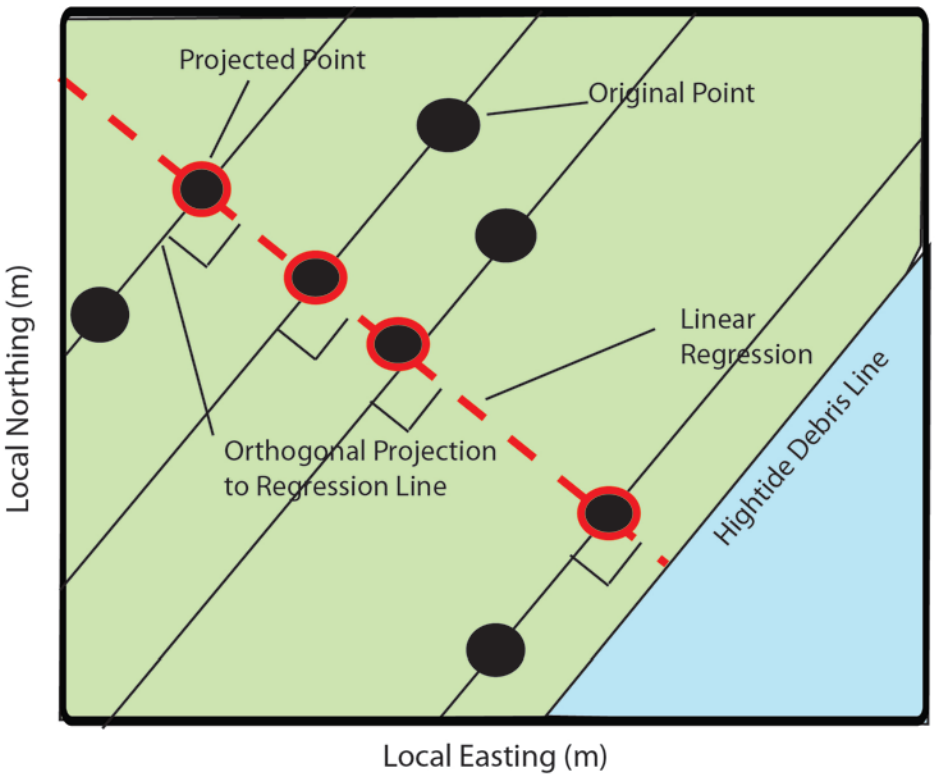

Figure 9 (Projected Point Method) This figure shows the projection method of GPS data points onto a regression line and its components. The red line in the local distance on all transects. Transects in Appendix A use the local distance from the coast along the regression line. This method, thus, reports the true perpendicular distance from the coast for each GPS point.

$m_1x + b_1 = m_2x + b_2$ (3) and $(y-b_1) / m_1 = (y-b_2)/m_2$ (4)

Using algebra to solve for *x* gives us

$x = (b_2 – b_1)/ (m_1-m_2)$ (5)

Plugging x into the original regression line will solve for *y*. To check the calculations *y* can be plugged back into equation (4). Using The Pythagorean Theorem the true local distance from the coast can be calculated.

The reason for these calculations is because using just straight easting coordinates doesn't work for many transects. The coast line is not due north and south, perpendicular to the UTM easting lines. So, transects were not going due west but more northwest. Ploting the GPS points on a UTM easting line (using the difference in UTM easting difference for local distance) would give inaccurate local distance perpendicular to the coast. In order to calculate a local distance perpendicular to the coast all points needed to be plotted on a northwestern angled line.

Now that the correct distance is calculated, the local distance and elevation can be plotted to produce transects such as Figures 10 and 11. Figure 10 shows multiple terraces that are seen on the peninsula. This is nearly the complete flight of marine terrace (Qt 2- Qt-7). Figure 11 shows the big riser that separates the predicted lower, Holocene terraces from the higher Marine Isotope Stage 3 [MIS (~30-~60ka)] terraces. This large riser can be easily seen in the photograph in Figure 12.

Calculating Uplift Rates

To complete my objectives and test my hypothesis I need to calculate uplift rates for the terraces on the peninsula. To do this I am using equation (6) The variables are:

X1) Elevation above mean sea level of sample; this includes the depth of digging to reach the sample; This was measured with a tape-measure in the field;

X2) The facies depth of the sample or depositional depth;

X3) The age; and

X4) The paleo sea level at time of deposition.

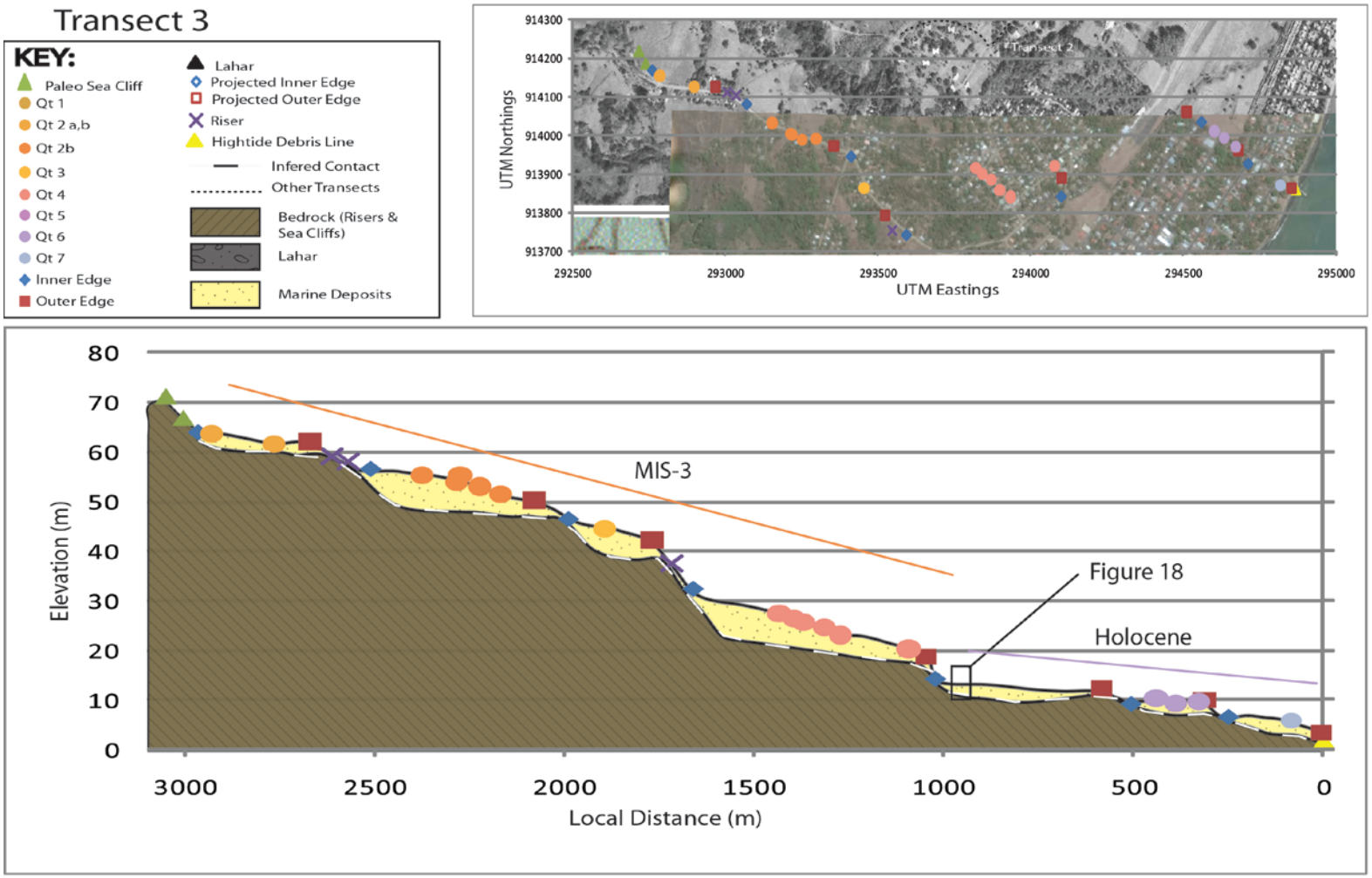

Figure 10 Geomorphic cross-section of transect 3 across the Burica Peninsula based on DGPS points. Transect location shown in Plate 1. This transect shows nearly all terraces on the Burica Peninsula. Specifically, this transect shows terraces 2 through 7. Qt1 can be seen on transect 1a, 1b, and 2 in Appendix A. The insert box shows the location of the stratigraphic column (Figure 18)

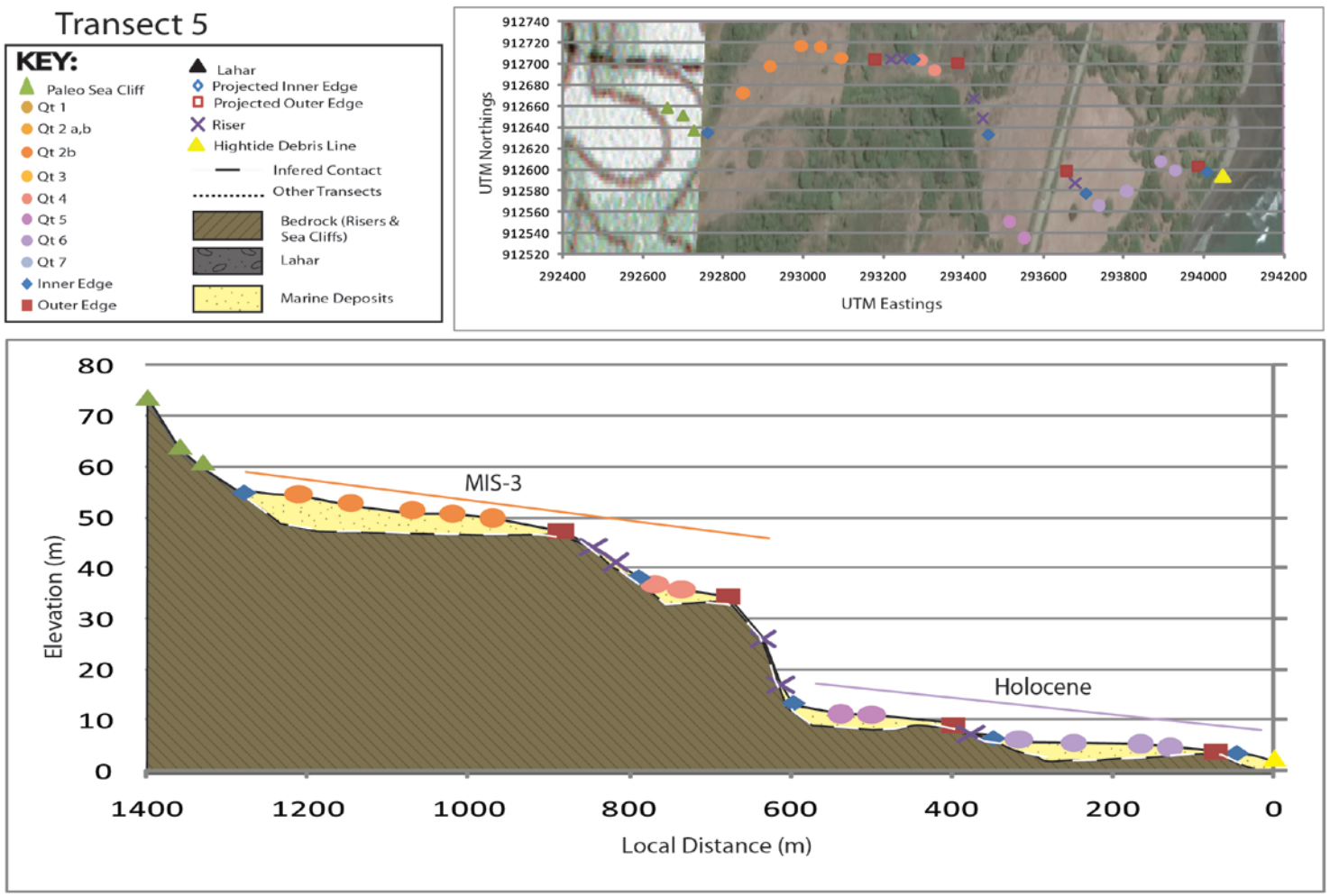

Figure 11 Geomorphic cross-section of transect 5 across the Burica Peninsula based on DGPS points. Transect location is shown in Plate 1. This transect shows the big separation between the Holocene and the Marine Isotope Stage 3 (~30-~60ka) terraces. The large riser separation is between the Qt 4 outer edge to the Qt 5 inner edge. The riser is more than 20 meters in elevation.

a.

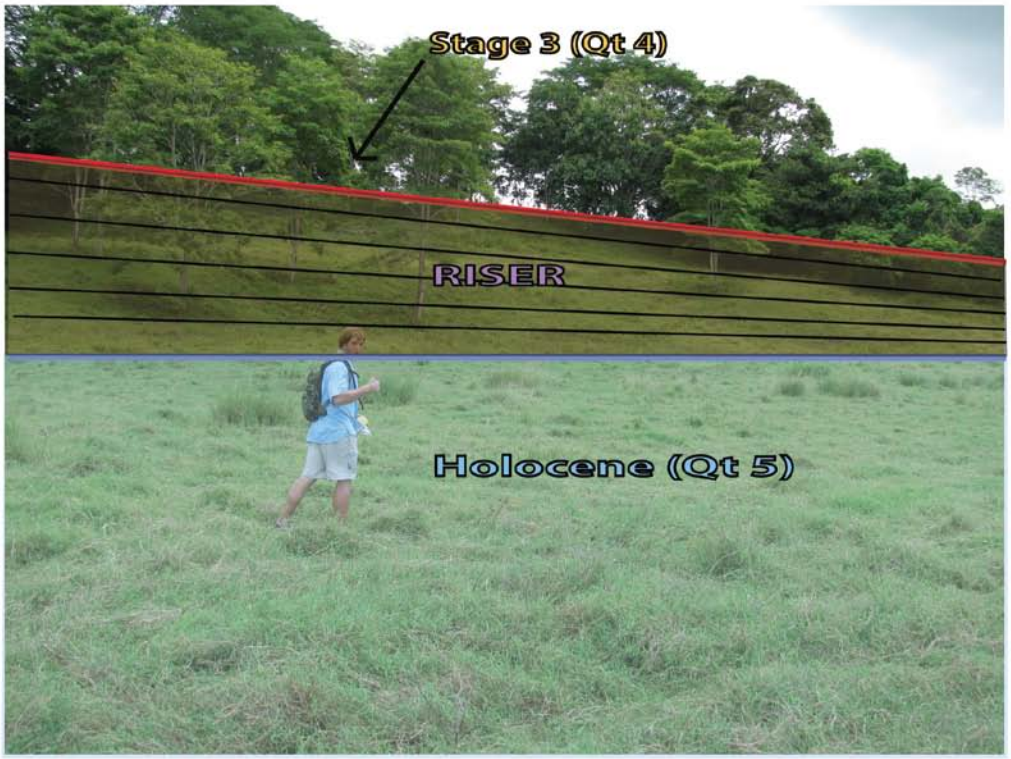

b.

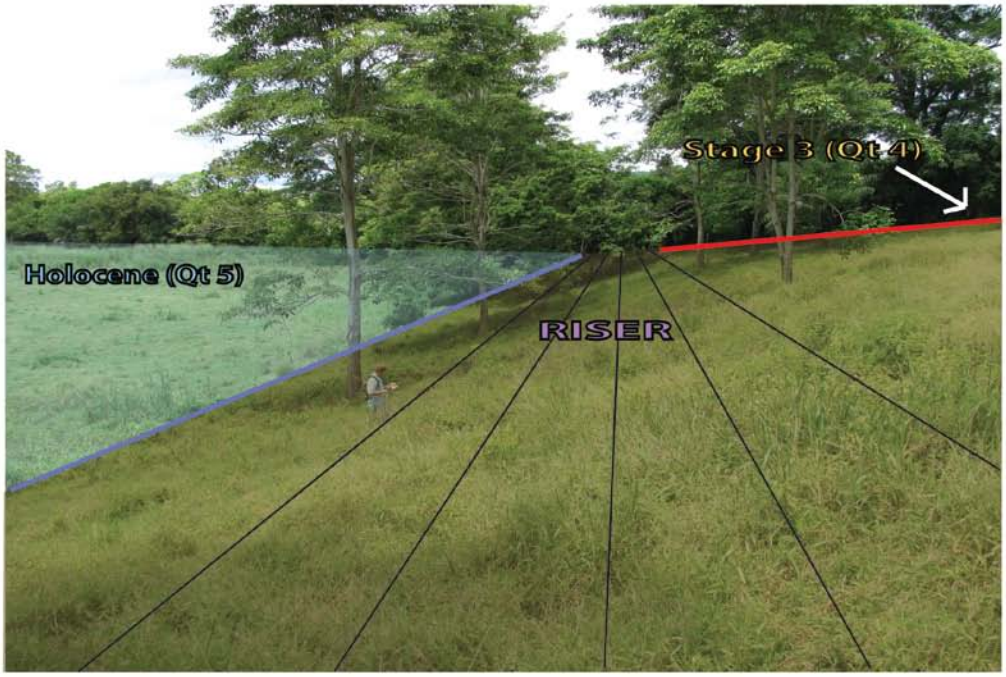

Figure 12 (Marine Terrace Morphology) a) A picture showing the riser separating the Holocene (Qt 5) and MIS-3 (Qt 4). The blue line is the inner edge and the red line is the outer edge. This picture taken is while surveying transect 7. b) Similar picture from same transect at a side view

$$\frac{[(\text{Elevation}(X1)]+[(\text{Facies Depth }(X2)]+[(\text{Paleo Sea Level at Time of Deposition }(X4)]}{[(\text{Age of Sample }(X3)]} \quad (6)$$

Elevation and Mean Sea Level (X1)

The modern coastal environment of the Burica Peninsula is a marine abrasion platform that slopes seaward from the HTDL. The HTDL is not mean sea level. Mean sea level is below the HTDL (Figure 4). In order for the uplift calculations to be correct, modern elevation measured from the DGPS surveys which used the HTDL as the datum must be adjusted for this elevation difference. To calculate mean sea level a record of high tide and low tide was obtained from mobilegeographics.com (Figure 13). The time of record used was the month during which data were collected. A best-fit linear regression was applied to the high tide and low tide data points. These lines are the high tide and low tide mean. The mean high tide is approximately the HTDL and the modern inner edge. The average of the mean high tide and mean low tide is the mean sea level. The mean sea level is approximately a 1.1 meters difference below the HTDL. 1.1 meters were added to all DGPS elevations because the GPS base station was measured from the HTDL using an altimeter and all GPS rover data were differential corrected using this base station.

Facies Depth of Samples (X2)

Samples collected for radiometric data can be separated into two facies, beach facies and wave base facies (Figure 14). The sand samples were deposited in a beach facies. The sandy beach facies is composed of a bottom gravel layer grading into a finely planar laminated, well sorted, coarse sand layers. This facies has a mean elevation of 0 meters, mean sea level. The error is the tidal range ($\pm$ 1.1m). The other facies is for the shell samples. The shell samples are deposited below the tidal range in the wave base facies. The wave base facies is composed of wavy, ripple bedded fine silty sand and clays (Port Armuelles Formation). The wave base extends to approximately 9 meters below low tide. This means that the average depth of the wave base facies is 5.6 meters below mean sea level with an error of 4.5 meters.

Sample Age (X3)

The age of samples was determined in two ways. One strategy was to collect beach facies sand from within the sand deposits on the marine terraces and use optically stimulated luminescence (OSL) to

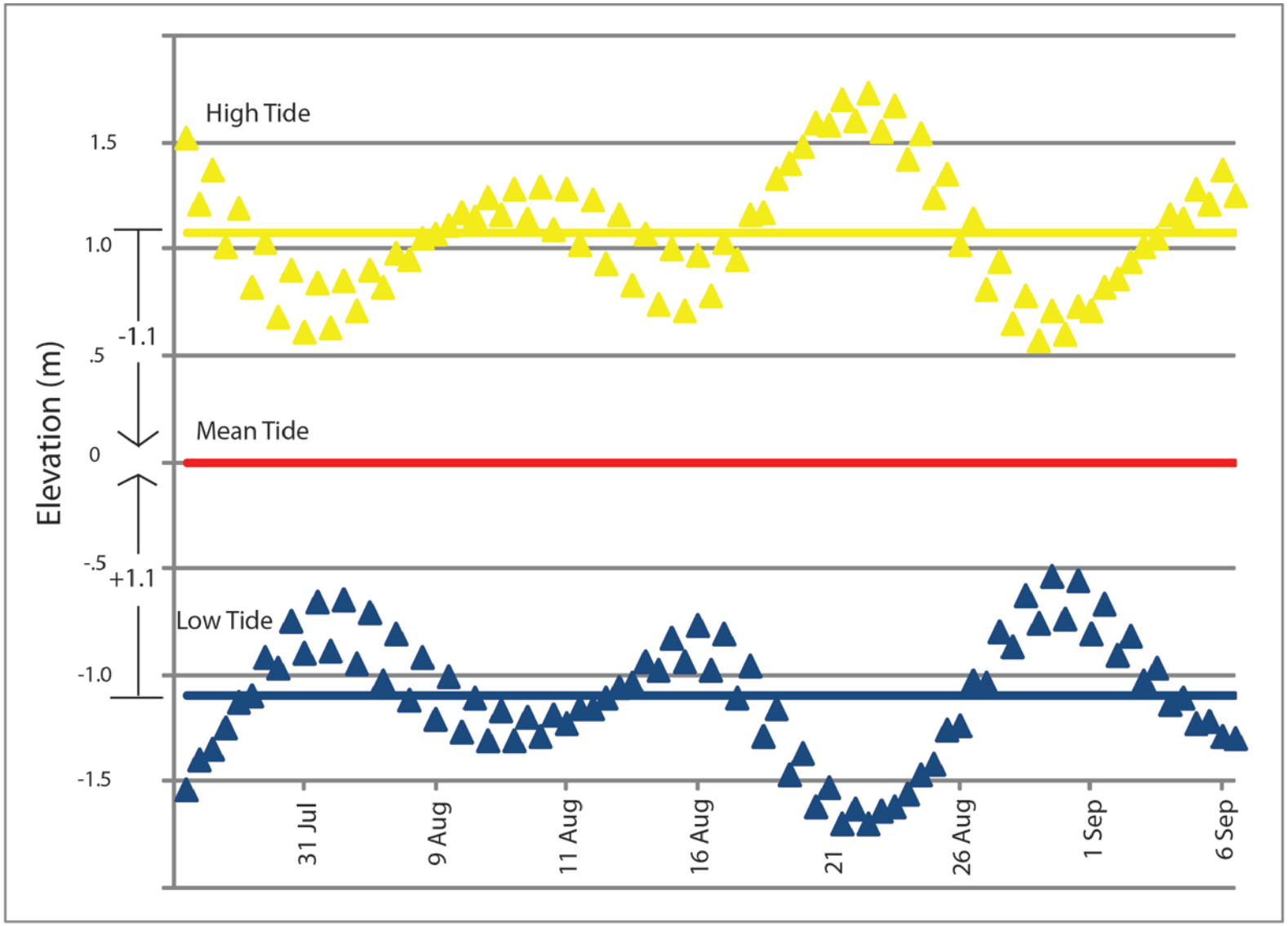

Figure 13 (Tidal Curve Analysis) A plot of the tidal cycle on the Burica Peninsula. The points plotted are the elevation of the high and low tide for 60 days surrounding the field research of late July and August, 2009. Data from mobilegeographics.com. The days used are the days that the GPS surveys were done. Tidal range is 2.2 meters. From the data presented the mean sea level is 1.1 meters below the high tide, the HTDL, or the modern inner edge.

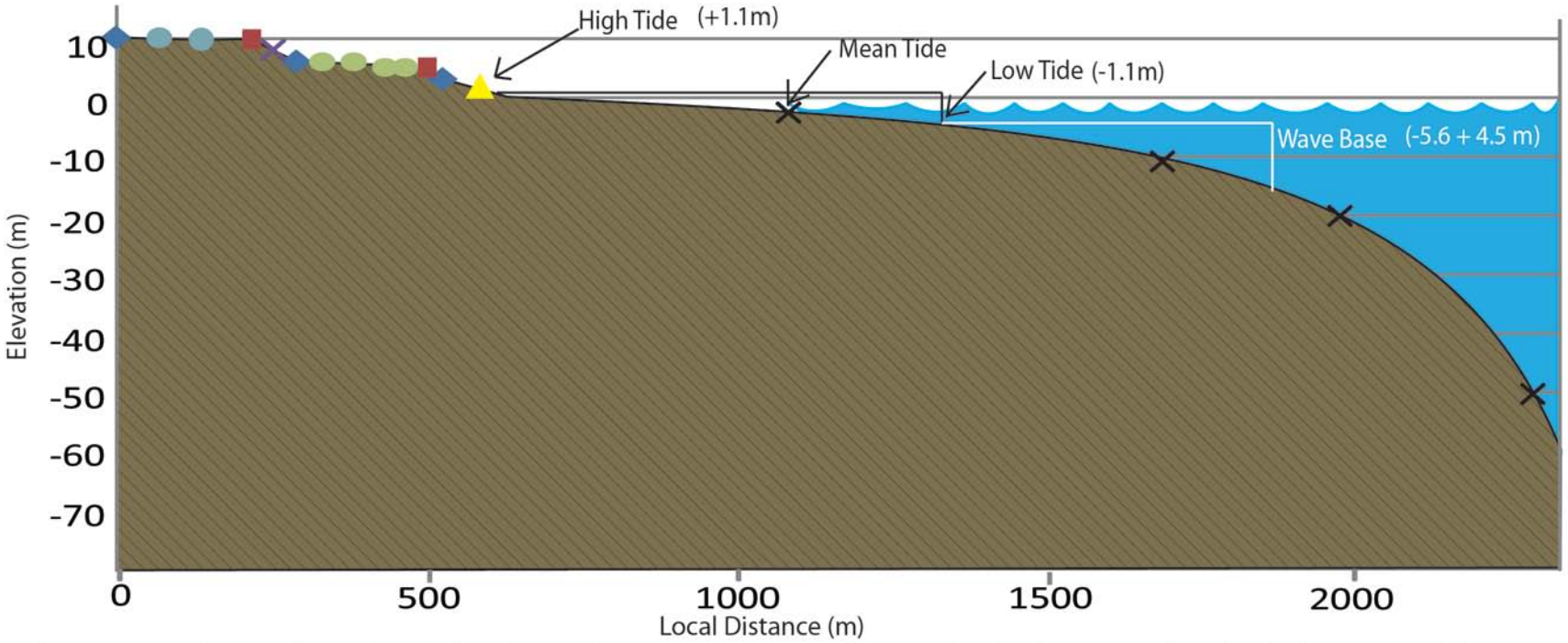

Figure 14 (Facies Depth) A plot of elevation with respect to mean modern sea level. The Xs are elevation below sea level from Puerto Armueles 1:50,000 topographic map. Elevations above sea level are from GPS transect 5. The plot shows the seaward slope of the modern abrasion platform and the facies depths associated with that platform. The range for the facies depth can be seen for wave base and the beach facies. The range for beach facies is shown by the black lines. The range for wave base elevation is shown by the white line.

date the marine terrace. OSL measure the luminescence of buried quartz grains. OSL analyses date the last time the quartz grains were exposed to sunlight. As the quartz grain is deposited and then buried, the decay of radionuclides cause electrons in silica atoms in quartz to move into and then get trapped in a higher atomic orbital within the quartz grains. As the age increase, the amount of trapped electrons increases at a constant rate. To measure the amount of trapped electrons, quartz grains are exposed to green light causing the sample to luminese because of the excited electrons falling back to a more stable and lower atomic orbital. The stronger the luminescence is, the more trapped electrons and the older the deposit.

Shell samples were dated using radiocarbon (^{14}C) dating performed by Beta Analytic Incorporate. The shell samples were deposited when the marine terrace was an active abrasion platform. The ^{14}C concentration within a shell is fixed at the time of death of the shell and then begins to decay at a constant rate. The remaining ^{14}C constrains the time of death of the shell or approximate time of deposition (assuming the shell was deposited upon death). ^{14}C is measured by using an Accelerated Mass Spectrometer (AMS). The AMS physically counts atoms of ^{14}C left within the shell and is able produce an age of deposition.

Sample correlation to sea level (X4)

Now that the age of each sample is known, the paleo sea level at the time of deposition can be determined by plotting the age of the sample on the Barbados sea level curve from Peltier and Fairbanks (2006) (Figure 15). The error accounts for the sea level error and the error for the age of each sample. The errors for age and sea level are shown by the boxes on Figure 15. This combined error is the largest error in the calculation of the uplift rate for each sample. This is because the horizontal error for the age and the vertical error for the sea level must be taken into account as the graph shows. The Discussion section will address a resolution to the large error problem.

Given X1, X2, X3, and X4, the uplift rates for the Burica Peninsula marine terraces can now be calculated.

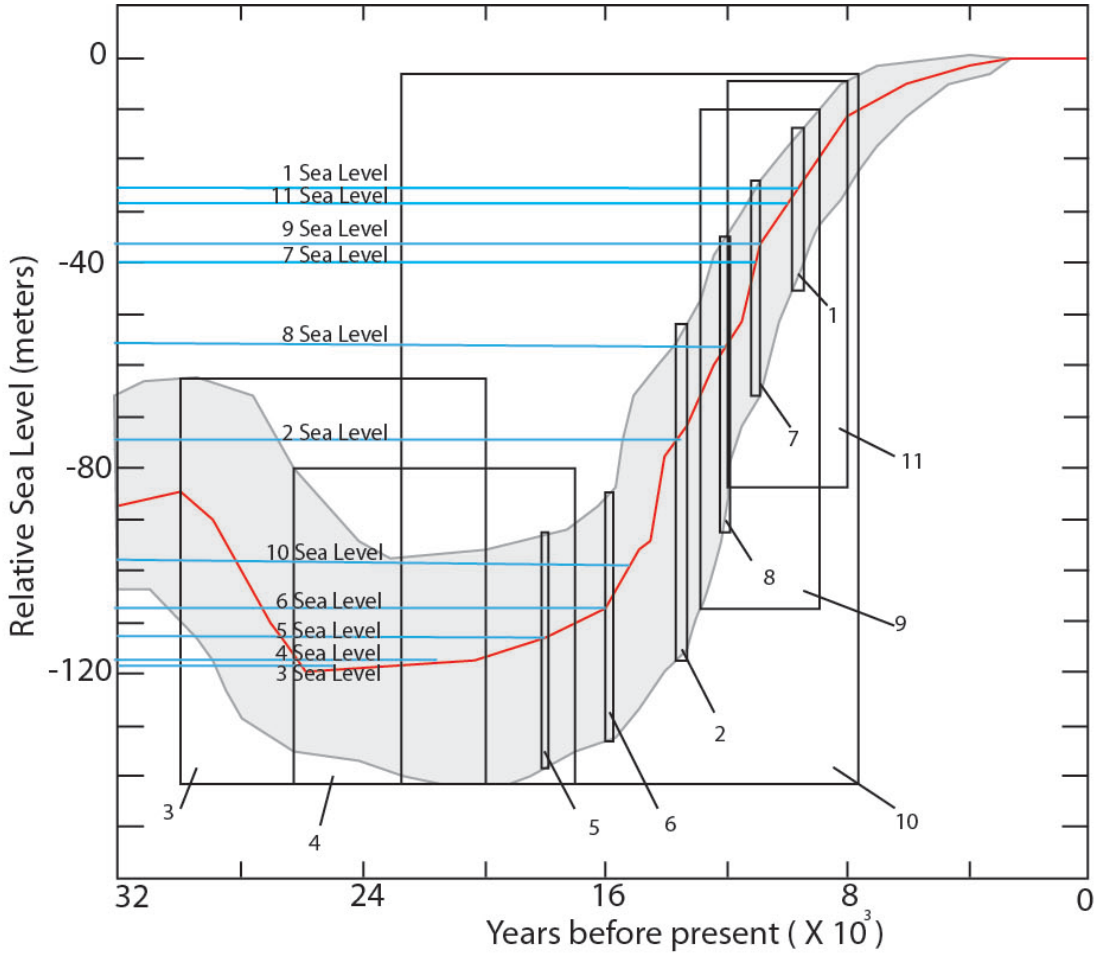

Figure 15 (Sea Level at Time of Deposition) Plot showing the Barbados sea level curve (W. R. Peltier and R.G. Fairbanks, 2006). The red line is mean sea level. 0 equals modern sea level. The grey area is the sea level curve error. The blue horizontal lines show the paleo sea level at the time of sample deposition. Sample numbers are in Table 1 and Plate 1. The boxes bound the error for age (horizontal axes) and paleo sea level (vertical axes) for each sample.

RESULTS

Terrace mapping

Seven marine terraces were identified and analyzed during this study. To create a map of the marine terraces (Plate 1) the inner edges and outer edges were correlated laterally along the Burica Peninsula through the use of transect elevations, geo-referenced stereo aerial photos, and an SRTM image. Each marine terrace was color coded according the elevation. From highest to lowest, the terraces are graded from a burnt orange to a deep blue. The inner edge lines are marked with a blue line and the outer edge lines are marked with a red line.

Plate 1 displays the spatial arrangement of the terraces along the coast of the Burica Peninsula. Along the coast there is little uniformity for any terrace extent or shape. Some terraces are discontinuous along the coast. For example, Qt 7 is only seen on transects 1 though 5 (Plate 1) and not preserved south of transect 5. Qt 3 is not preserved for approximately one kilometer around transect 5 and then becomes one of the larger terraces south of transect 5. Also, rivers have dissected terraces and volcanic deposits don't preserve the terraces well making it difficult to correlate the terraces along the coast. However, the inner edge elevations were not hard to map after a limited range of inner edge elevations for each Qt were established (Figure 8). Variations in elevation for individual terrace inner edges are minimal; the average range is less than 4 meters in elevation. For example, the elevation range for Qt 3 (~48m-~42m) and 6 (~10m-~5m) are very well confined. Thus, each terrace could be easily distinguished by elevation of the inner edgess. Correlating the inner edges from transect to transect allowed for completion of the map. The map is successful in that it shows clearly the terrace boundaries and the extent of each terrace. The location of radiometerically dated samples are plotted on the terrace map makes it possible to assign an age to each terrace. Then, uplift rates can be calculated for each dated terrace using equation (6).

The terrace map is accurate in areas where stereo aerial photos were available because of detailed examination. The area of the oil terminal, which extends from the oil tanks shown on Plate 1 to about 2.5 kilometers north, is somewhat problematic. There is no aerial photo coverage and surveying the area was not allowed. Two transects were taken as close as possible [transect 7 to the south and transect 6 to the

north (Plate 1)]. The SRTM image was used to determine terrace elevations in the area surrounding the oil terminal. The SRTM image does show elevations, however, the image shows no visual break in slope along terrace risers as do the stereo aerial photos. Thus, I could only correlate inner edge elevations and outer edge elevations using SRTM elevation data between transect 6 and 7. In order to complete a more accurate map, surveying and aerial photos would need to be used in this area.

Terrace correlation along the coast

Figure 16 shows the correlation of marine terrace inner edge elevations and the general slope for the terraces along the coast. Data from this study and from Teletzke (2010) are used to determine if there is a measurable slope or tilting of the terraces along the coast. The local distance is calculated by ruler and applied using transect 1(Plate 1) as 0 meters along the coast. The colors of the symbols and best fit regression lines match the terrace colors assigned in Plate 1. See Plate 1 for transect locations and see Appendix A for transect plots. The slope and R values are given next to the best fit lines for each terrace. The slope is not significantly different from zero for all best fit linear regression lines. However, Qt2a and Qt2b do show a decrease in inner edge elevation of apporimately 6 meters from north to south. These two terraces have a general slope of -.11 for Qt 2a and -.2 for Qt 2b, decreasing in elevation southward along the coast. This tilting could have been caused by differential slip along the thrust fault (Figure 3), which runs down the length of the peninsula. However, this possible tilting up to the north is not seen in the lower terraces.

Uplift rates

Uplift rates were calculated by using equation (6) in Data Analysis. The uplift rates and values used for calculations are given in Table 1. Table 1 gives the calculated uplift rates (last column) for every dated sample used in the area studied for this paper. The sample locations are indentified by the sample identification numbers from Plate 1. The uplift rates ranges from 4 to 10 meters per thousand years. This is a fairly large range and not the precise answer originally suspected in the purpose for this research. Also the errors for some uplift rates, especially the OSL samples are rather large. Some error ranges are

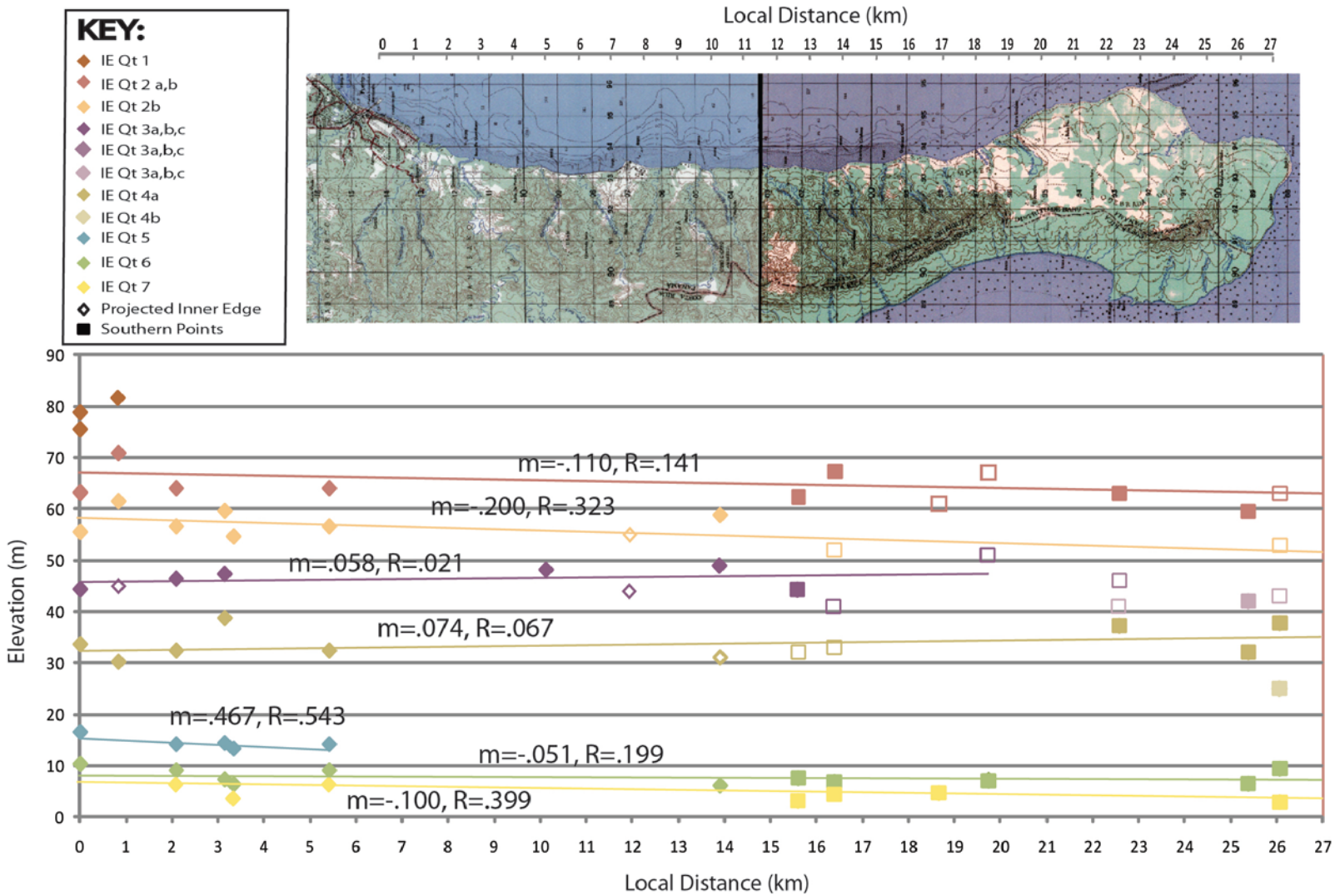

Figure 16 (Inner Edge Elevations Along the Coast) A plot of inner edge elevation vs. local distance along the coast. Squares represent points recorded south of UTM Northing 901950 by Teletzke (2010). Diamonds represent data points taken during this research. Open symbols are projected points determined from stereo air photos and projecting intersecting slopes from the riser and terrace tread. A best fit line is plotted for each terrace and the equation with slope is giving with the R value to show accuracy.

Table 1

Uplift Rates

Sample ID[#*]	Location[‡]	Age (ka) **	Modern Elevation (m)[†]	Facies depth (m) ¤◊	Sea Level (m)[%]	Uplift Rate (m/ka)[††]
1(255173)[*]	(293160, 915126)	9.795(± 0.105)	57.9 (± 1.7)	5.0(± 4)◊	25(+57, -11)	9.0(15.4-6.9)
2(247425)[*]	(293163, 915112)	13.62(± 0.13)	57.9 (± 1.7)	5.0(± 4)◊	73(+117,-52)	10.0(19.2-7.9)
3(PA 09-05)[#]	(292784, 914153)	25.8(± 4.9)	61.6 (± 1)	0(± 1.1)¤	119(+140,-62)	7.0(15.4-4.0)
4(PA 09-06)[#]	(293463, 913852)	21.7(± 4.2)	42.5 (±1)	0(± 1.1)¤	118(+140,-80)	7.4(17.3-4.7)
5(263547)[*]	(293726, 912714)	17.895(± 0.115)	6.8(± 0.9)	5.0(± 4)◊	115(+136,-91)	7.1(15.1-5.4)
6(264585)[*]	(293726, 912714)	15.86(± 0.1)	6.7(± 0.9)	5.0(± 4)◊	108(+133,-85)	7.5(16.3-5.7)
7(255932)[*]	(293532, 911187)	11.165(± 0.055)	1.1(± .25)	5.0(± 4)◊	40(+75,-32)	4.2(11.3-3.1)
8(263543)[*]	(293525, 911184)	12.425(± 0.205)	1.1(± .25)	5.0(± 4)◊	56(+64,-34)	5.0(10.7-2.9)
9(PA 09-07)[#]	(293279, 906254)	10.6(± 2.4)	16.7(± 0.9)	0(± 1.1)¤	37(+102,-10)	5.1(19.2-1.9)
10(PA 09-08)[#]	(293066, 903029)	15.6(± 7.7)	21.8(± 0.7)	0(± 1.1)¤	99(+140,-3)	7.7(33.2-1.0)
11(PA 09-09)[#]	(292956, 901670)	10.1(± 1.8)	29.1(±1.1)	0(± 1.1)¤	29.5(+82,-4)	5.8(17.2-2.6)

[*] Sample ID as show in Plate 1 with Beta Analytic number; [#] indicates OSL samples
[‡] See Plate 1 for location; UTM Zone 17 N – WGS 1984
** Calendar calibrated age and one sigma calibrated error
[†] Modern elevation from transect surveys using DGPS data; assigned errors vertical precision
¤ Beach Facies depth determined by type of sample taken, refer to text. ◊ Wave Base Facies determined by type of sample taken, refer to text.
[%] Paleo-sea-level from Peltier and Fairbanks (2006); see Figures 17
[††]Uplift rate calculated from equation 6; maximum and minimum rate from accumulated errors in other variables listed here.

more than double the calculated rate. This large error and wide range of uplift rates will be further analyzed in the Discussion section.

Figure 17 shows the uplift path for every dated sample. Each sample uplift path connects the modern elevation to the paleo elevation of deposition (sea level plus facies depth). The slope is the long term, time averaged uplift rate for each sample. The real uplift path is more likely to contain vertical jumps from seismic events and is horizontal during times of no seismicity. The sea level curve is the same curve used in Figure 6 (Peltier and Fairbanks, 2006). The figure shows the elevation of deposition including average facies depth for each sample and the modern elevation. A line is drawn connecting the two. This figure shows the wide range of measured uplift rates. For a uniform uplift rate, all uplift lines would be parallel at any given time. The terraces must have parallel uplift paths because there are no visible thrust faults separating one terrace from another. Figure 17 shows the uplift lines crossing, which is impossible. This suggests that one or multiple variables have error within the calculations.

A large problem with the uplift paths is that for multiple OSL samples (3, 4' and 10) from marine abrasion platforms would have been formed during a sea level low stand. This produces uplift rates which are not plausible and the creation of new terraces during the sea level rise of the Holocene would have eroded all previous low stand terraces. This will be discussed in the Discussion section of this paper.

The results of the research present a accurate terrace map of the Burica Peninsula showing a flight of at least 7 terraces. The peninsula shows no significant slope of the terraces. Therefore, the uplift rates must be uniform along the peninsula. The uplift rates calculated by using equation (6) show large variations and have large ranges of error. Again, this will be further discussed in the Discussion section of this paper.

DISCUSSION

The objectives successfully completed during this thesis are: completing multiple DGPS surveys, creating cross sections from the surveys showing the elevations of the multiple terraces and their features, creating a terrace map of the northern part of the Burica Peninsula showing the terrace boundaries along

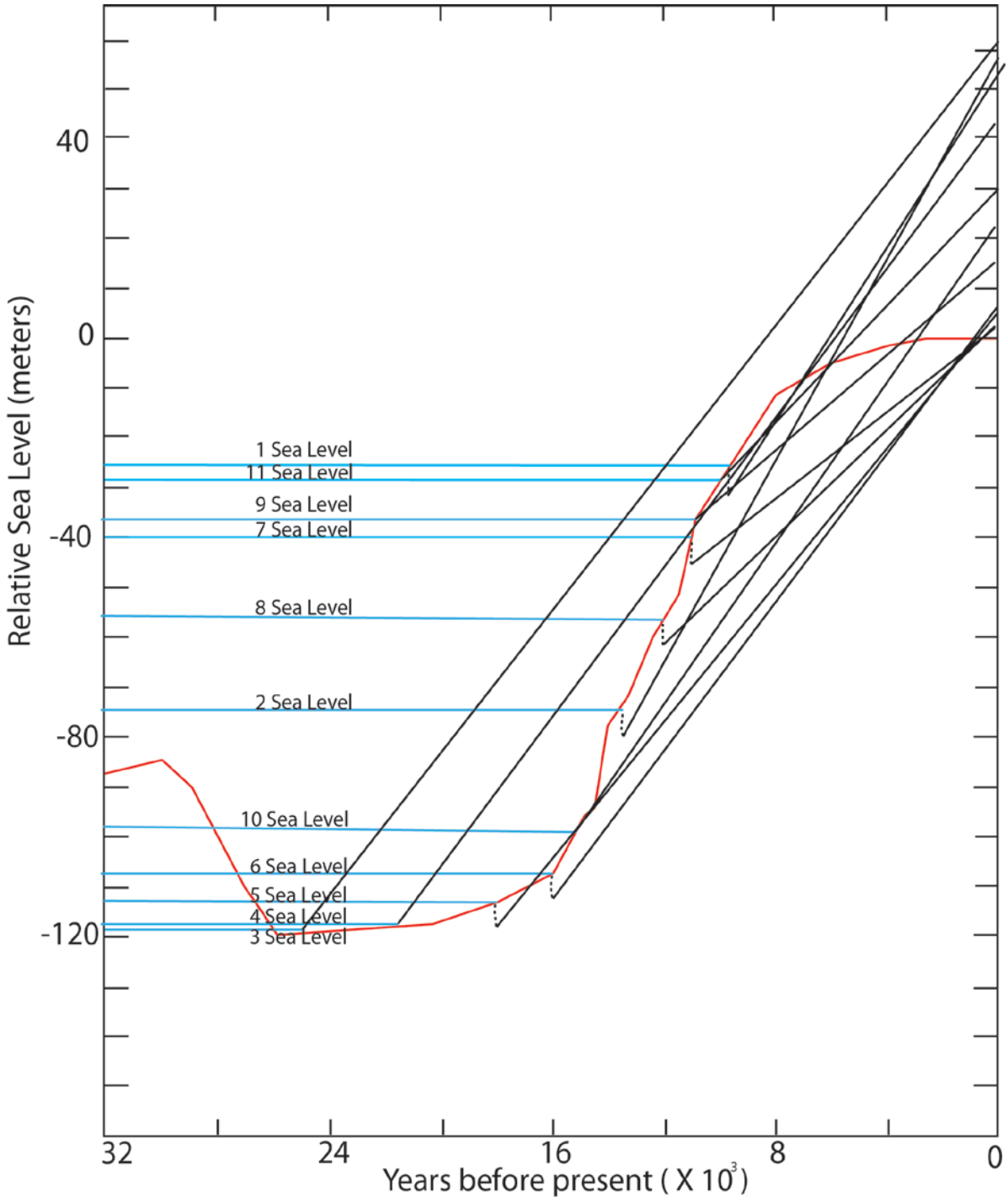

Figure 17 (Uplift Paths for Dated Samples) The sea level curve from Figure 6 displaying calculated uplift paths. The uplift paths were calculated by connecting the line between the paleo sea level sample elevation of depostion and the modern elevation. 0 equals modern sea level. The slope of each line is the time averaged uplift rate for each sample. Dashed line indicates facies depth. See Figure 15 for the paleo sea level sample depostion elevation error.

the peninsula, and correlating the inner edges along terrace to find tilt. The objective of finding an uplift rate from sand and shell samples was not as successful as originally hypothesized. The calculated uplift rates range from 4.2 to 10 m/ka (meters per thousand years). The possible reasons for this wide range are:

1) An incorrect sea level curve was used

2) Possible thrust faults between the terraces were unnoticed

3) Different rates of thrusting have occurred along the peninsula

4) The sample ages were incorrect in giving the age of the marine terrace

5) Or the facies depth is not precise.

The sea level curve used from W. R. Peltier and R.G. Fairbanks (2006) is derived from years of research, has been compared to multiple sea level curves worldwide, and published in a major scientific journal (Quaternary Science Reviews). The error from other world wide data has been accounted for in this thesis. The Barbados sea level curve has been referred to as a credible source worldwide and is not likely the cause of the wide range in uplift rates.

The possibility of thrust faults located between each of the terrace is a possibility for the wide range of uplift rates. However, extensive structural mapping (Morrell et al., 2009) indicates that there are no thrust faults between the terraces (Figure 3). If there were to be thrust fault between the terraces, there would be significant deformation of the marine terraces. Such deformation was not noticed during this research.

The possibility of different rates of uplift along the Peninsula has previously been addressed in this thesis. If different rates of uplift occurred along the Peninsula a noticeable tilt of inner edges would be expected. However, Figure 16 shows no tilt for the terraces on the peninsula.

The possibility of the samples being contaminated is highly probable for some samples. The OSL samples 3, 4, and 10 plot during a sea level low stand. As previously mentioned, marine abrasion platforms are not preserved during sea level low stand so the OSL samples were probably exposed to sunlight after deposition, making them seem younger than the actual deposition. The other OSL samples, 9 and 10 are from Qt 4 and plot on the Holocene sea level rise. Qt 4 is more likely created during the

Marine Isotope Stage 3 (MIS 3 ~38 ka) as previously mentioned (Figure 10 and 11). These sediment samples were probably also exposed to sunlight causing them to seem younger than the actual deposition. The two carbon dates, 1 and 2 are from wood samples dug out of marine sands deposited on Qt 2. These carbon samples also plot within the Holocene high stand, which is also highly unlikely. These samples were probably contaminated by vegetation growth on the terrace surface.

However, four carbon samples (5, 6, 7 and 8) do not show any obvious reasons for contamination. Samples 5 and 6 were found in a river bank outcrop located near transect 3 (See Figure 10 showing outcrop location) below the marine sands of Qt 6 (Figure 18). There is an unconformity between the samples and the overlaying marine sands. The unconformity is visible between the gravel and tilted clay layers. This outcrop became known as Roberto's outcrop. The outcrop was mostly covered in vegetation but a stratigraphic column was constructed to show where the shells were deposited (Figure 18). Because of the dense vegetation at this outcrop a picture could not be shown clearly. Picture taken at nearby outcrop (Figure 19) shows the same features clearly. The shells were deposited below the planar laminated coarse sand and the gravel beach facies of the marine terraces. Both of these shell samples are a part of the Armuelles Formation seen in the stratigraphy column in Figure 3 and are from the wave base facies in Figure 14. These are below an unconformity of the Monte Verde formation, which we are trying to date. Also, the younger sample age is above the older sample age (15.8 ka is above 17.9 ka). These samples have two ages which are not only precise but stratigraphically correct, but they plot on a sea level low stand. The only other possible problem with these data is facies depth. This will be further discussed.

Samples 7 and 8 were found at the Razor Clam outcrop (Figure 20) located south of the Roberto's outcrop in a marine channel eroding into the same formation as Roberto's outcrop (Figure 20). This outcrop is also below the marine sands of Qt 6. This outcrop also shows the gravel and clay unconformity. The samples from the marine channel, however, have an age of 11.1 and 12.5 ka. These sediments are much younger than the Roberto's outcrop and yet both are seen right below the marine sands of Qt 6. The problem with the juxtaposition of these different samples' ages is the original simplistic diagram of how marine terraces form and preserve shells.

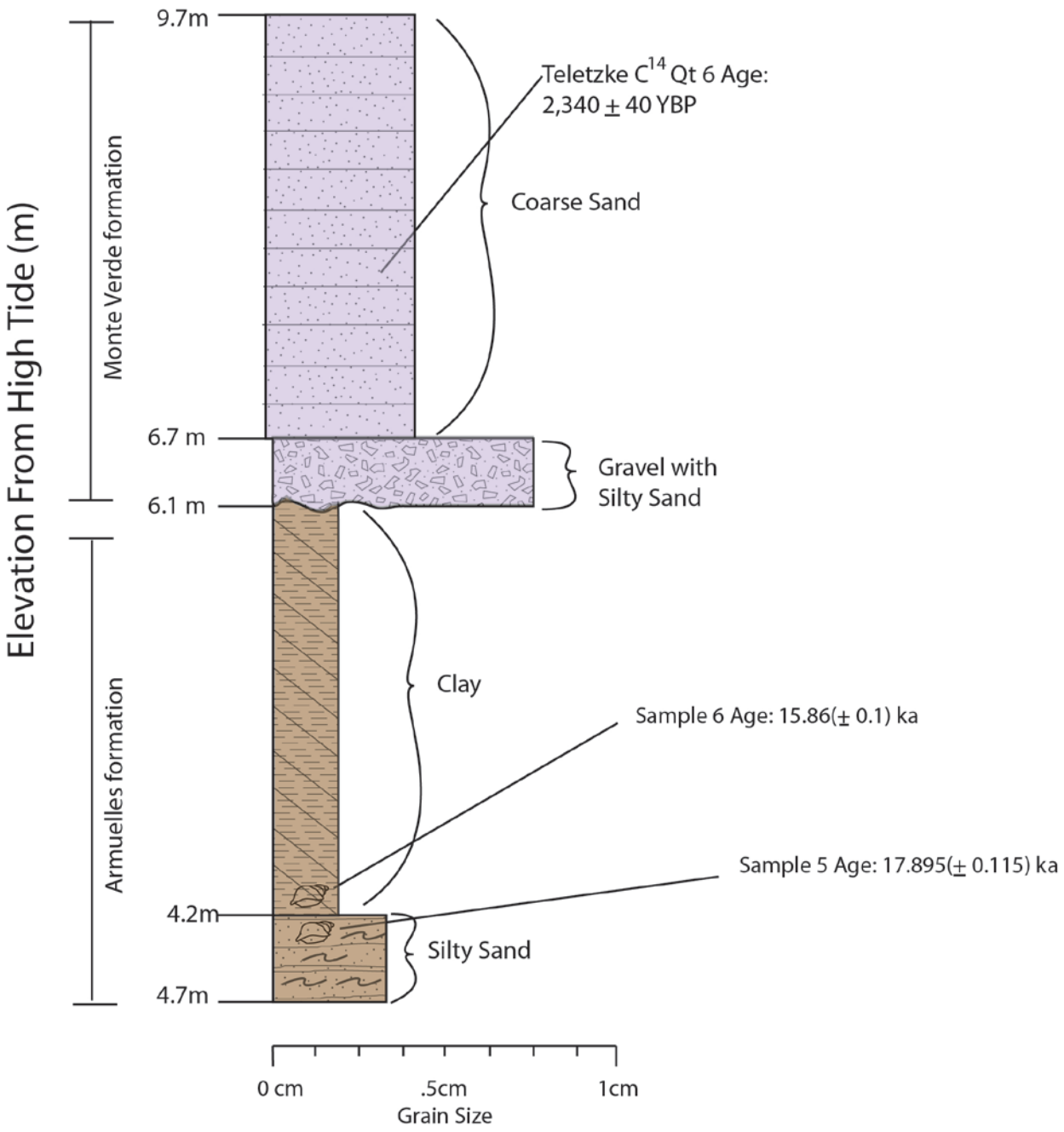

Figure 18 (Roberto's Outcrop) An outcrop near transect 3 with two radiocarbon dates from perserved shells. The locations of these shells are indicated by the shell symbol. The sample number correspond with Plate 1 and Table 1. The age of the samples is listed next to the sample number. Outcrop and layer thickness were done by meauring tape.

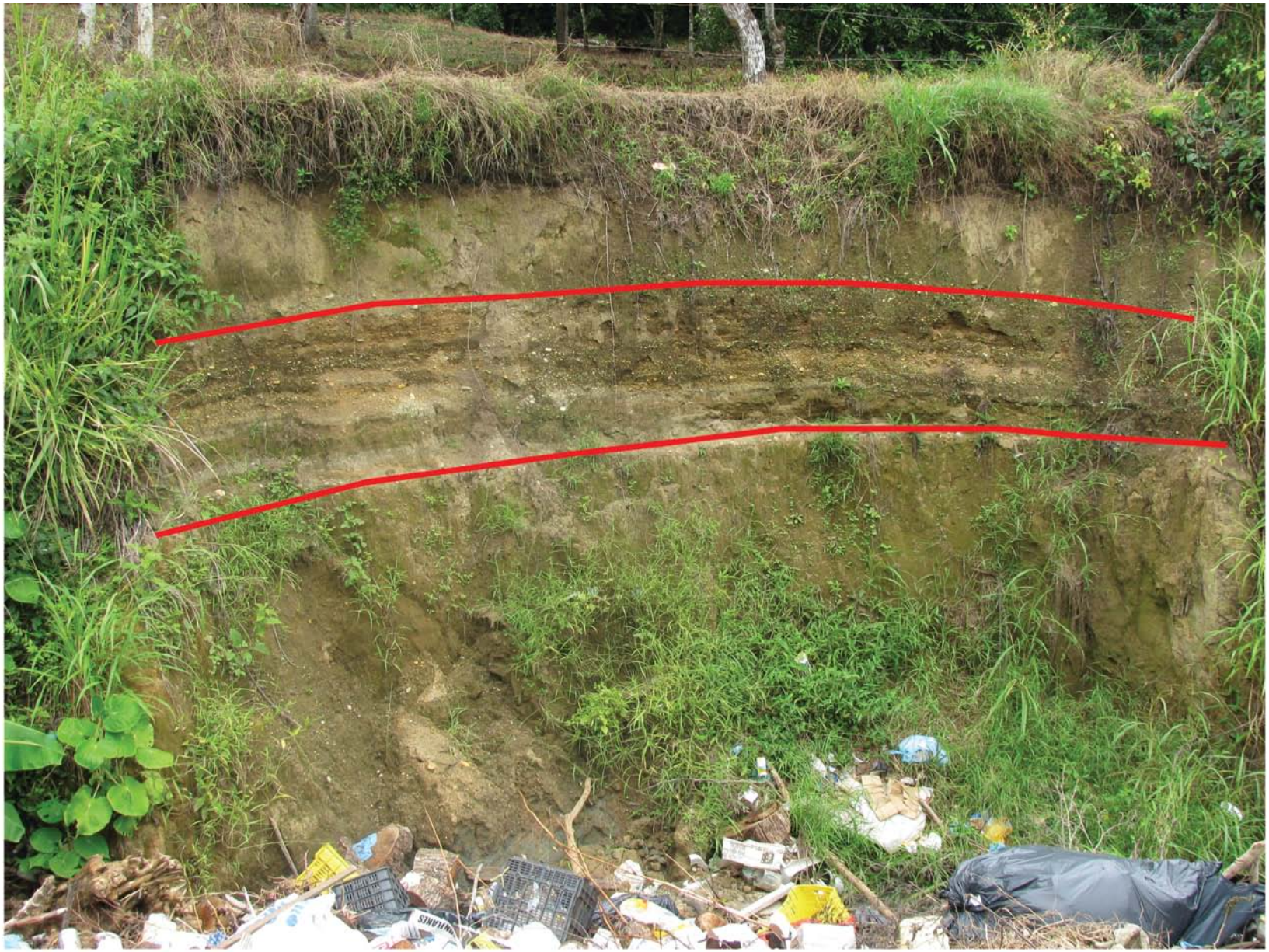

Figure 19 (Trash Dump Outcrop) An outcrop with less vegetation than Roberto's outcrop but shows similar stratigraphy. The red lines seperate the layers and bound the gravel with sand layer of the marine terrace. The layer on the bottom is clay and the layer at the top is coarse sand. There is an unconformity between the clay at the bottom and the gravel deposits at the top.

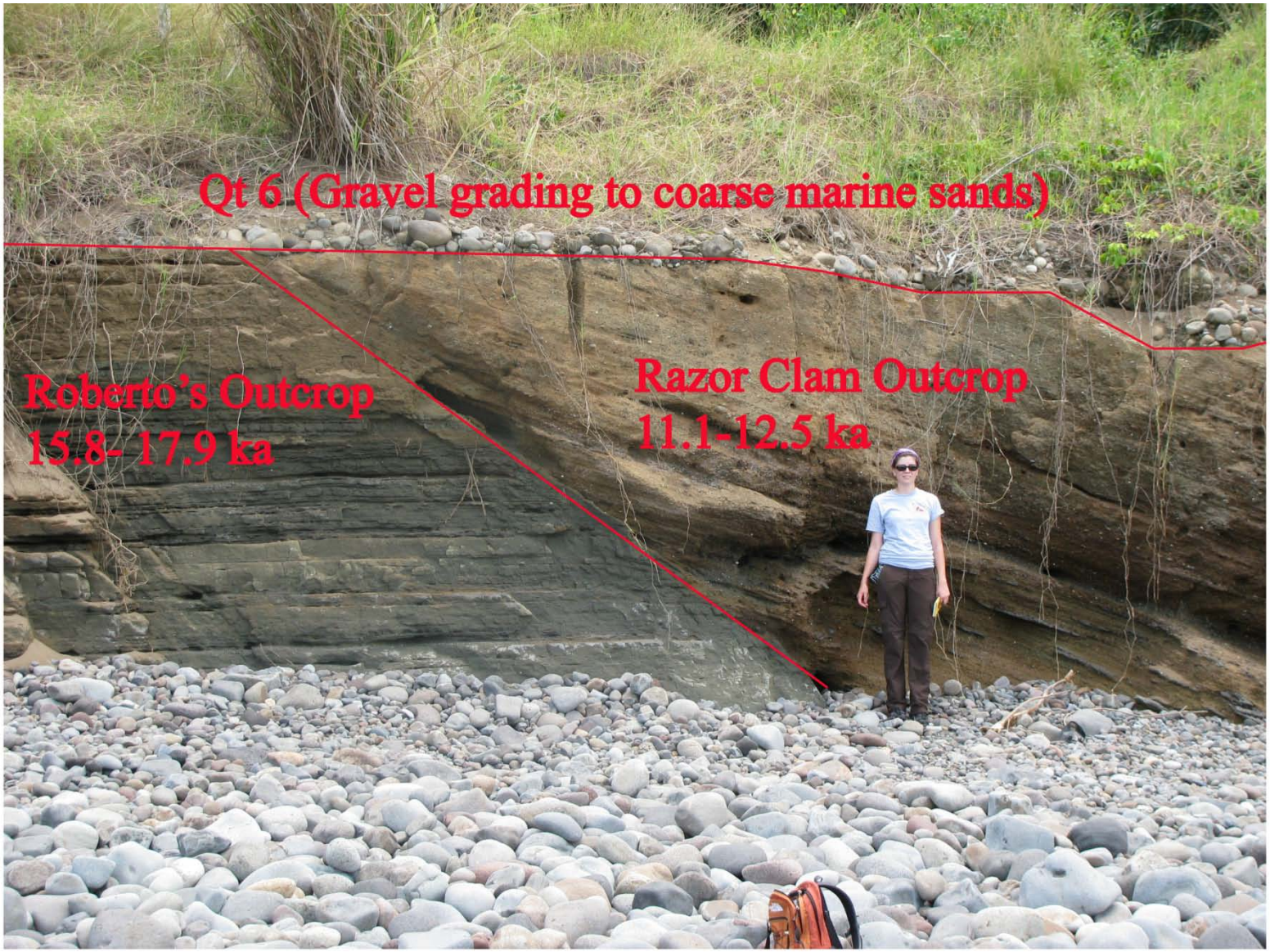

Figure 20 (Razor Clam Outcrop). The angular unconformity in this oucrop is clearly seen and a layer of very coarse gravel marks this unconformity. The gravel layer is similar to the gravel layer visible at the Roberto's Outcrop. The Razor Clam Outcrop is a younger deposit than Robert's Outcrop. The Razor Clam Outcrop most likely was a submarine channel bringing sediments into deeper ocean, which cut and eroded the older Roberto's Outcrop.

Figure 4 is correct in showing how features of terraces form, but is very simplistic when showing how shells are uplifted and preserved. First, as previously mentioned shells are not generally well preserved in the beach facies on the marine terraces. However, shells are preserved in the wave base facies. This means they are most likely from deeper water and more distant than the outer edge of a marine terrace (Figure21). Therefore, a younger terrace could cut into the older terrace's wave base facies. This terrace will also have a wave base deposit which is younger on top of the previous older wave base deposit. Also shells can travel very far from the wave base facies in submarine channels. These channels can carry the shells far past the wave base facies into very deep marine water. Channels are seen off the modern beach for approximately half a kilometer. The shell could have been deposited many meters below another terrace higher in the peninsula because of the capabilities of sediment transport through these marine channels.

However, the shell ages do constrain the age of the overlying marine terrace. A terrace cannot be older than the youngest sediment below. From the data in this research, Qt 6 cannot be older than 11.1 thousand years. My colleague Ally Teletzke's data had shell samples preserved within the marine sands on Qt 6. The sample age range was from 470 $\pm$ 45 to 2,340 $\pm$ 40 YBP (years before present). The Qt6 marine terrace age from Teletzke's data has a wide range in age but fits within the constraints of the shells dated in this research. The oldest shell sample from Teletzke's data (2010) on Qt 6 (2,340 $\pm$ 40 YBP) was a whole bivalve that had no signs of being reworked or contaminated. Using the average height of Qt 6 and the age of Qt 6, the uplift rate calculated is 3.8 $\pm$ .2 m/ka (meters per thousand years).

This uplift rate needs to be compared to the rest of Allison Teletzke's data. Her data show a great example of shell deposits constraining the ages of the marine terrace sands from an accurate OSL age for Qt 4 (Figure 22). Figure 22 shows the stratigraphy of the peninsula in cross section, with sample ages becoming younger up-section towards Qt 4. This constrains the age of Qt 4 to be younger than 40.2 $\pm$ .47 ka. The OSL age was 38.9 $\pm$ 8.3 thousand years, which is consistent with the radiocarbon shell ages.

This OSL age is older than the sea level curve by Peltier and R.G. Fairbanks (2006). A sea level curve of the MIS 3 is needed. Lambeck and Chappell (2001) use worldwide data of uranium-series (^{234}U-

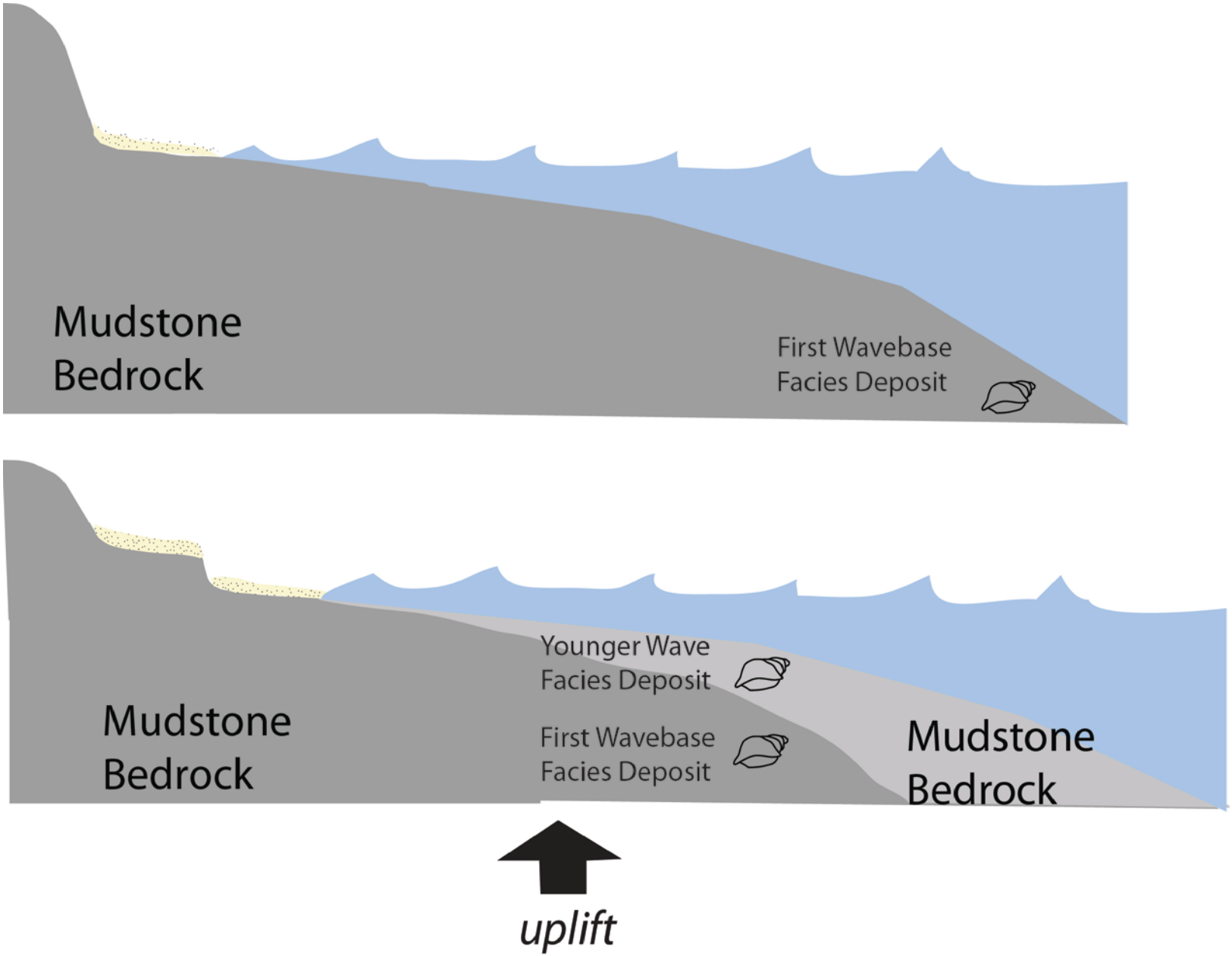

Figure 21 (Wavebase Fossil Preservation) A cartoon showing a more realistic approach of how marine terrace fossils are preserved. The upper cartoon shows a shell deposited in the wavebase facie at deep depths. The cartoon below shows another deposit layering on top of the previous deposit. This is how a younger shell can be deposited on top of an older shell.

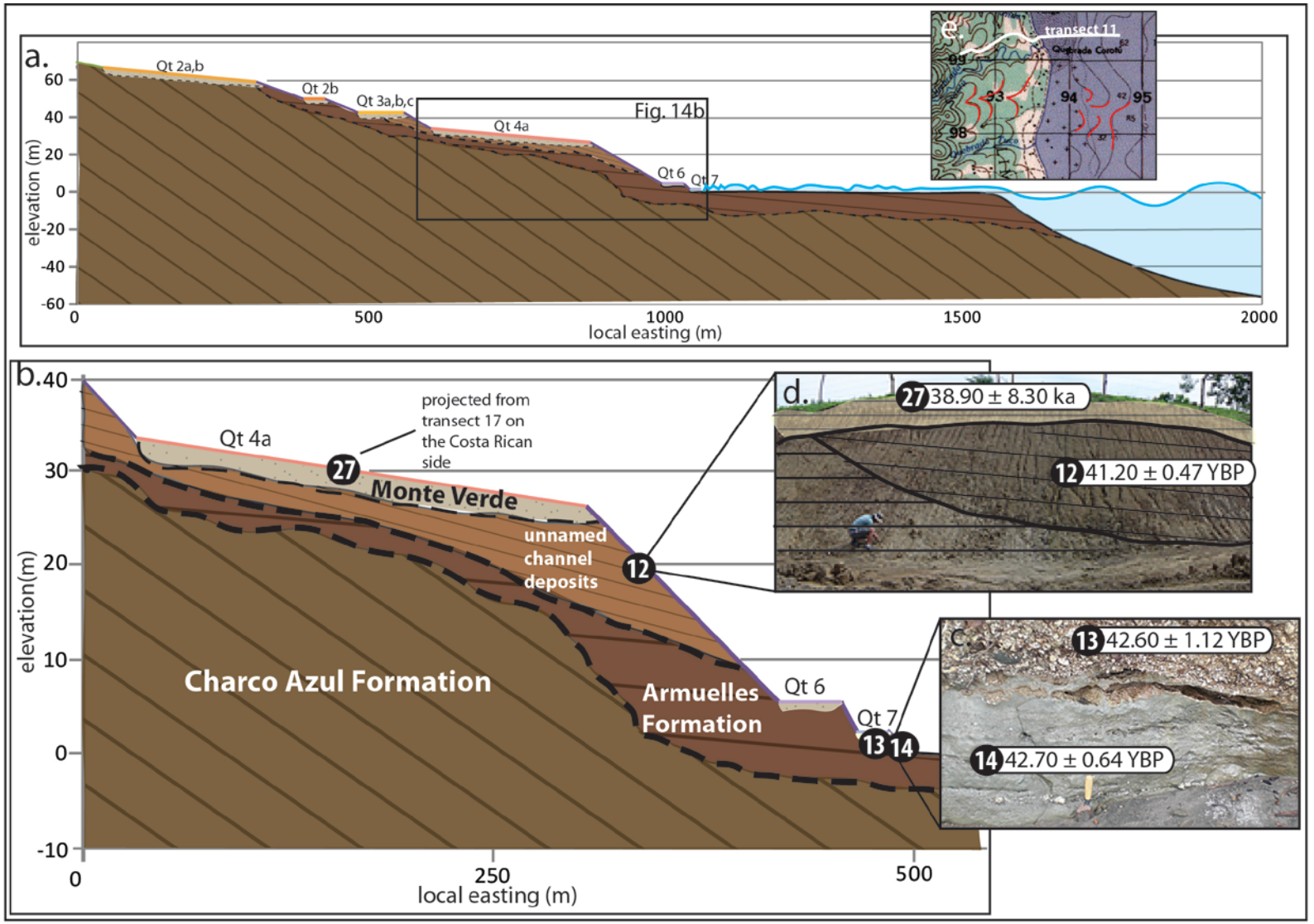

Figure 22 (Teletzke's Sample Ages) Projection of MIS-3 radiocarbon and OSL samples onto transect 11 to show proper stratigraphic sequece of younger over older ages. a) Transect 11 from Teletzke's (2010) data, showing marine terraces and offshore bathymetry b) Expanded cross-section with radiocarbon and OSL ages projected onto it. c) Radiocarbon samples 13 and 14 in marine tidal channeld. d) Radiocarbon sample 12 with OSL sample 27 projected onto the tread from the Costa Rica side. e) Map showing modern tidal channel. Red lines highlight topographic and bathymetric contours.

^{230}Th) dated coral reefs and oxygen isotope ratios of foraminifera from deep sea sediment cores to create a MIS 3 sea level curve. Lambeck and Chappell's (2001) sea level curve created from this data was used to find the paleo sea level of Teletzke's (2010) older OSL ages.

When plotting Teletzke's (2010) age and elevation on the Lambeck and Chappell's (2001) sea level curve, the uplift path yields a time averaged up lift rate of 3.0 m/ka (Figure 23). After plotting lines connecting the average marine terrace elevations above Qt4 to older sea lever high stands, similar uplift paths are seen. This is not a coincidence. Teletzke's (2010) OSL age fits perfectly on a sea level high stand, and there are just are many sea level high stands as there are terraces on the peninsula. This fits the model of terrace forming at stable high stands as originally stated. From this data it can be concluded that the long term uplift rate of the Burica peninsula range between 2.2 and 3.2 m/ka.

The uplift rate calculated from Teletzke's Qt 4 and projected uplift rates gave a range that the uplift rate of Qt 6 does not fit in. The reason for this high uplift rate for Qt 6 is that young terrace uplift paths have not had enough time to be time averaged and the uplift rate is highly affected by the recent seismic activity (coseismic signal). The older terraces have a more accurate long term uplift rate because the uplift rates have been time averaged.

The original hypothesis is that the Panama microplate (Burica Peninsula) is actively being uplifted and forced to step up and over the thick Cocos plate as the Panama Triple Junction migrates along the Middle American Trench. The uplift rates support the original hypothesis of the cause of the Burica Peninsula. This Burica Peninsula did not exist 100,000 years ago and is a direct result of the active uplift of the Panama microplate reacting to subduction of the Cocos plate as the Panama Triple junction migrates down the Middle American Trench. The uplift of the Burica peninsula is on north striking and eastward dipping thrust faults as a response to the subduction of the Cocos plate (Figure 24).

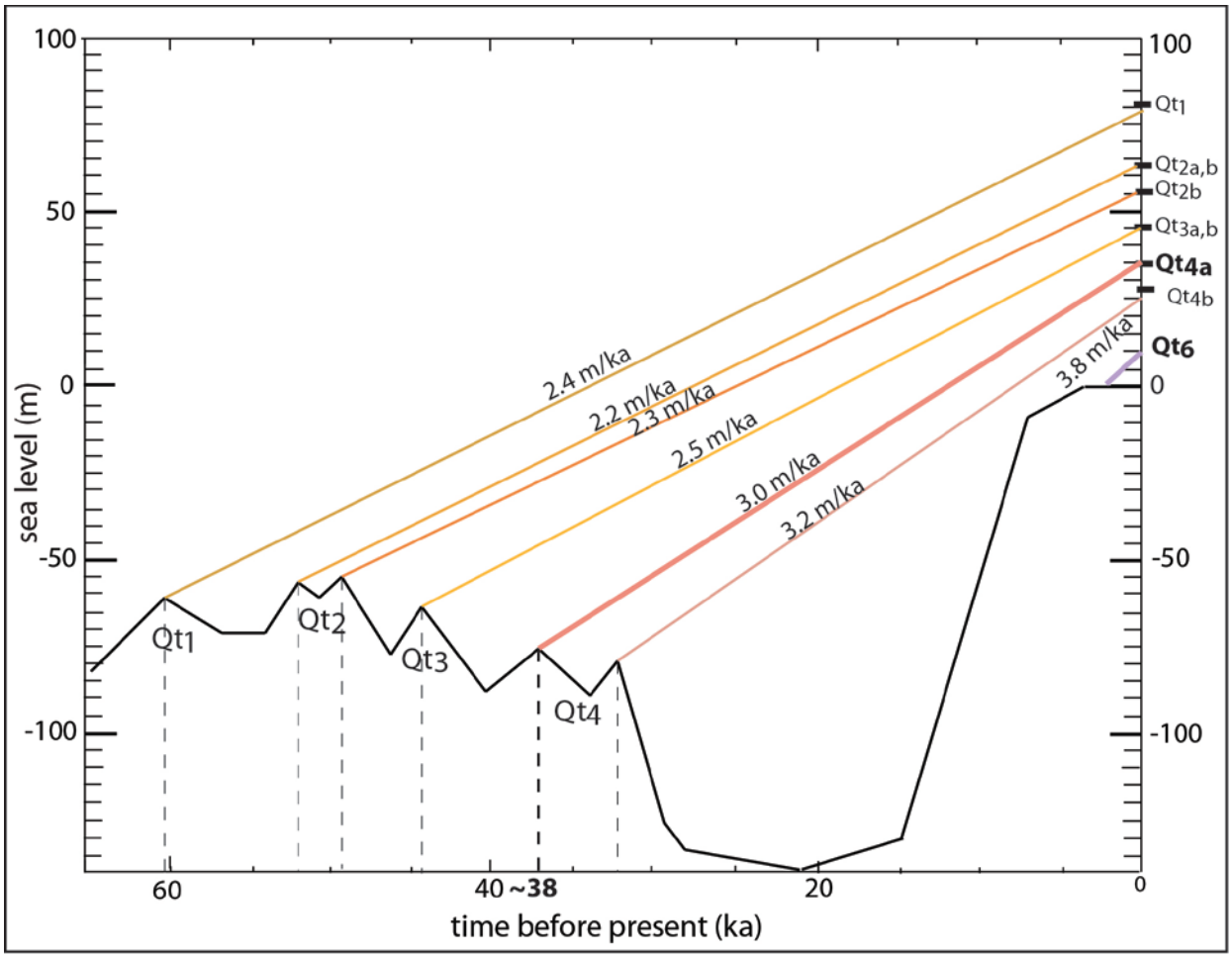

Figure 23 (Final Uplift Paths) Sea level corrleation of MIS-3 marine terrace inner edge elvations. The slope of the line from a peak in the sea level curve to the current elevation of the inner edge of a terrace represents the time-averaged, long-term uplift rate of that terrace. Based on the stratigraphic constraints of the OSL and radiocarbon samples (Fig. 22), Qt 4a must be < 41.2 ka. The OSL age of 38.9 is consistant with that constraint. The other MIS-3 marine terraces are constrained by that age. Projecting the other MIS-3 marine terraces to the other individual sea level peaks produces the range of background uplift rates for the Burica Peninsula. Qt6 is a ^{14}C sample age from Teletzke's data (2010) and is constrained by shell samples from that research. Sea level curve is from Lambeck and Chappell (2001).

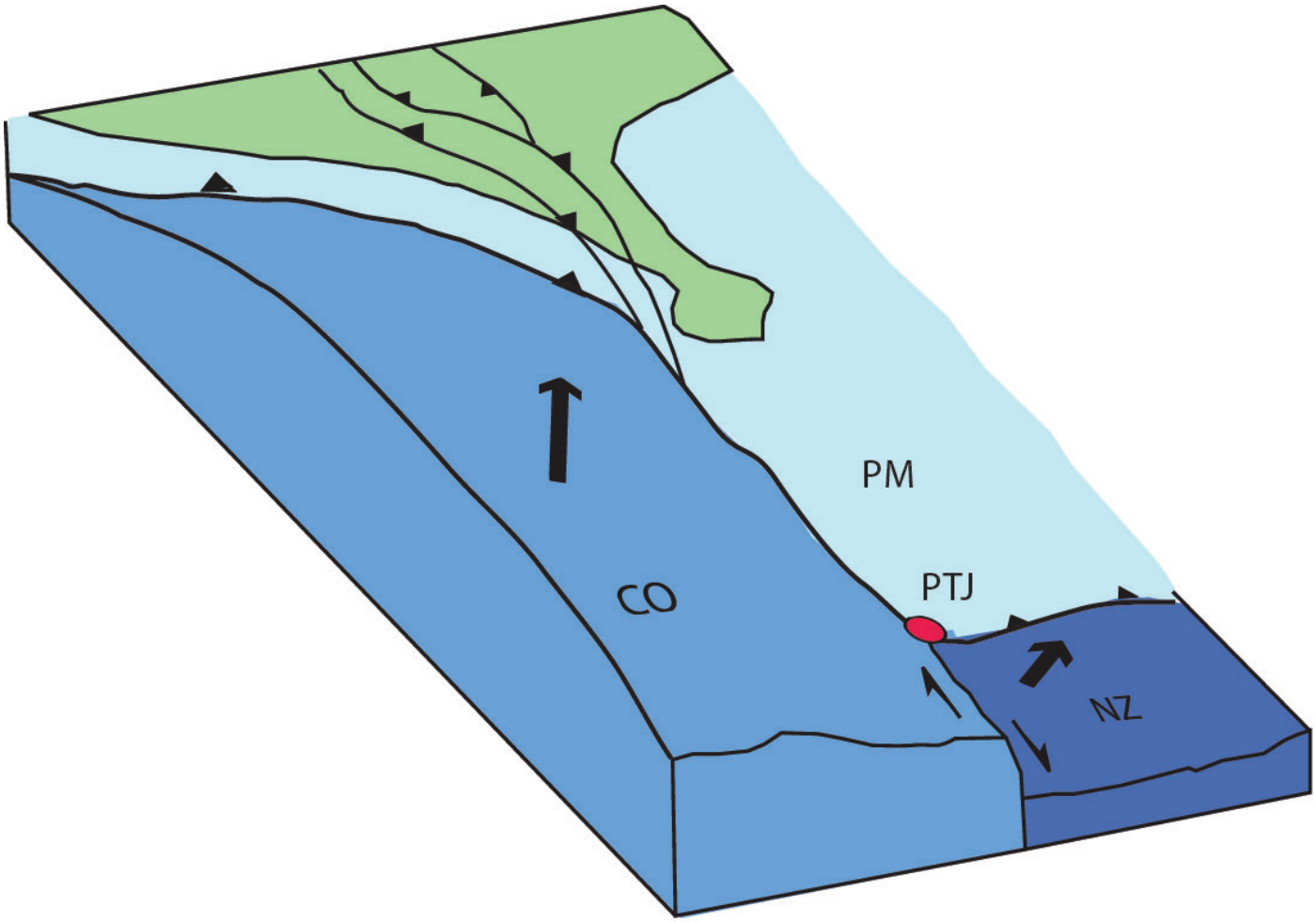

Figure 24 (Final Block Diagram) This cartoon shows the three plates (Cocos plate=CO, Panama microplate=PM, and Nazca plate=NZ) joining together at the Panama Tripple Junction (PTJ). The black arrows are general motions for the CO and NZ with respect to the PM. The figure is showing how with the migration of the PTJ the PM has to step up and over the CO creating north striking and eastward dipping thrust faults, which causes the uplift of the peninsula

SUMMARY AND CONCLUSION

-Radiocarbon and OSL dating and geologic mapping indicate that there are 7 marine terraces on the Burica Peninsula that record uplift since 60,000 years before present.

-An uplift rate calculation from Allison Teletzke's (2010) data and projection uplift paths onto high stand sea levels and average modern elevations for the terraces have yielded a range of 2.2-3.2 m/ka

-The uplift rate calculated from using Allison Teletzke's (2010) data for Qt6 give and uplift rate of 3.8 $\pm$ .2. The reason for this higher uplift rate is from a cosiesmic signal from recent seismic activity.

-The peninsula is being actively uplifted on a north striking, eastward dipping thrust fault at a uniform rate along the peninsula in response to subduction of the Cocos Plate.

REFERENCES

Anderson, R.S., Densmore, A.L., Ellis, M.A., 1999. The generation and degradation of marine terraces. Basin Research 11, 7-19

Bird, P.P., 2003. An updated digital model of plate boundaries. Geochem., Geophys., Geosystems 4, 52 pp.

Bradley, W.C., 1957. The origin of marine-terrace deposits in Santa Cruz area, California. Geol. Soc. Am. Bull. 68, 421-444.

Corrigan, J., Mann, P., Ingle, J.C., 1990. Forearc response to subduction of the Cocos Ridge, Panama-Costa Rica. Geol. Soc. Amer. Bull. 102, 628-652.

DeMets, C., 2001. A new estimate for present-day Cocos–Caribbean plate motion: implications for slip along the Central American volcanic arc. Geophys. Res. Lett. 28, 4043–4046.

DeMets, C.C., Gordon, R.G., Argus, D.F., Stein, S., 1990. Current plate motions. Geophysical J. Int. 101, 425–478.

Fisher, D.M., Gardner, T.W., Sak, P., Sanchez, J.D., Murphy, K., Vannucchi, P., 2004. Active thrusting in the inner forearc of an erosive convergent margin, Pacific coast, Costa Rica. Tectonics 23 13 pp.

Gardner. T.W., Verdnock, D., Pinter, N.M., Slingerland, R.L., Furlong, K.P., Bullard, T.F., Wells, S.G. 1992. Quaternary uplift astride the aseismic Cocos Ridge, Pacific Coast, Costa Rica. Feol. Soc. Amer. Bull. 104, 219-232.

Lambeck, K., Chappell, J., 2001. Sea level change through the last glacial cycle. Science 292, 679-686.

MacMillan, I., Gans, P.B., Alvarado, G., 2004. Middle Miocene to present plate tectonic history of the southern Central American Volcanic Arc. Tectonophycis 392, 325-348.

Mobilegeographics.com, 2009.

Morell, K.D., Fisher, D.M., Gardner, T.W., 2008. Inner forearc response to subduction of the Panama Fracture Zone, southern Central America. Earth and Planetary Science Letters 265, 82-95.

Morell, K.D., Gardner, T.W., Fisher, D.M., Davidson, D., Teletzke, A.L., 2009. Uplift of late Quaternary marine terraces in the forearc of the Middle America Trench due to active thrusting inboard of the Panama Triple Junction, Burica Peninsula, *AGU*, Fall Meet. Suppl., Abstract, T53A-1565.

Peltier, W.R., Fairbanks, R.G., 2006. Global glacial ice volume and Last Glacial Maximum duration from an extended Barbados sea level record. Quaternary Science Reviews 25, 3322-3337.

Ranero, C.R., Phipps Moran, J., McIntosh, K., Reichert, C., 2003. Bending-related faulting and mantle serpentinization at the Middle America trench. Nature 425, 367-373.

Shackleton, N.J., 1967. Oxygen isotope analyses and Pleistocene temperatures re-addressed. Nature 215, 15–17.

Shuanggen, J., Zhu, W., 2004. A revision of the parameters of the NNR-NUVEL-1A plate velocity model. J. Geodyn. 38, 85–92.

Sitchler, J.C., Fisher, D.M., Gardner, T.W., Protti, M., 2007. Constraints on inner forearc deformation from balanced cross sections, Fila Costen˜a thrust belt, Costa Rica. Tectonics

Smith, W. H. F., and D. T. Sandwell, 2003. Global seafloor topography from satellite altimetry and ship depth soundings, Science, v. 277, p. 1957-1962, 26 Sept., 1997.

Teletzke, Allison, 2010, The Late Quaternary Uplift of Marin Terraces on the Burica Peninsula, CostaRica-Panama. Trinity University.

Appendix A

(DGPS Values and Terrace Cross-Sections)

Transect 1a

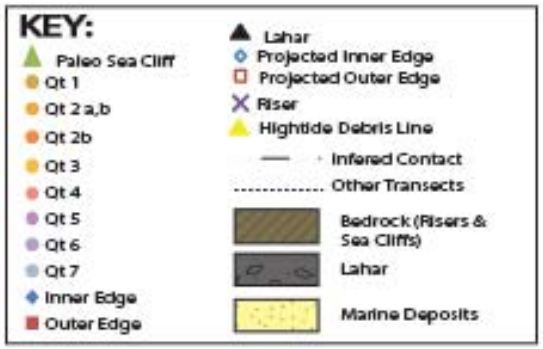
KEY:
Paleo Sea Cliff
Qt 1
Qt 2 a,b
Qt 2b
Qt 3
Qt 4
Qt 5
Qt 6
Qt 7
Inner Edge
Outer Edge
Lahar
Projected Inner Edge
Projected Outer Edge
Riser
Hightide Debris Line
Infered Contact
Other Transects
Bedrock (Risers & Sea Cliffs)
Lahar
Marine Deposits

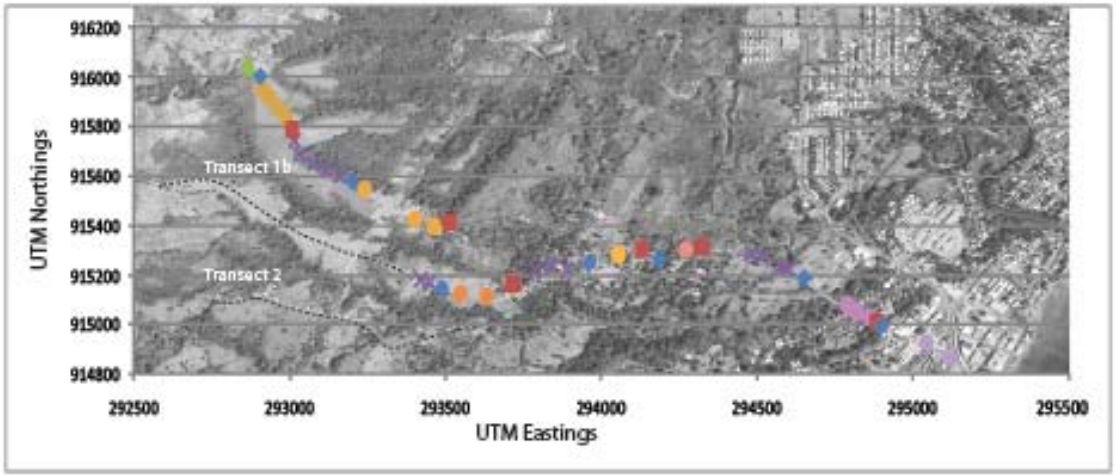
916200
916000
915800
915600
915400
915200
915000
914800
UTM Northings
Transect 1b
Transect 2
292500
293000
293500
294000
294500
295000
295500
UTM Eastings

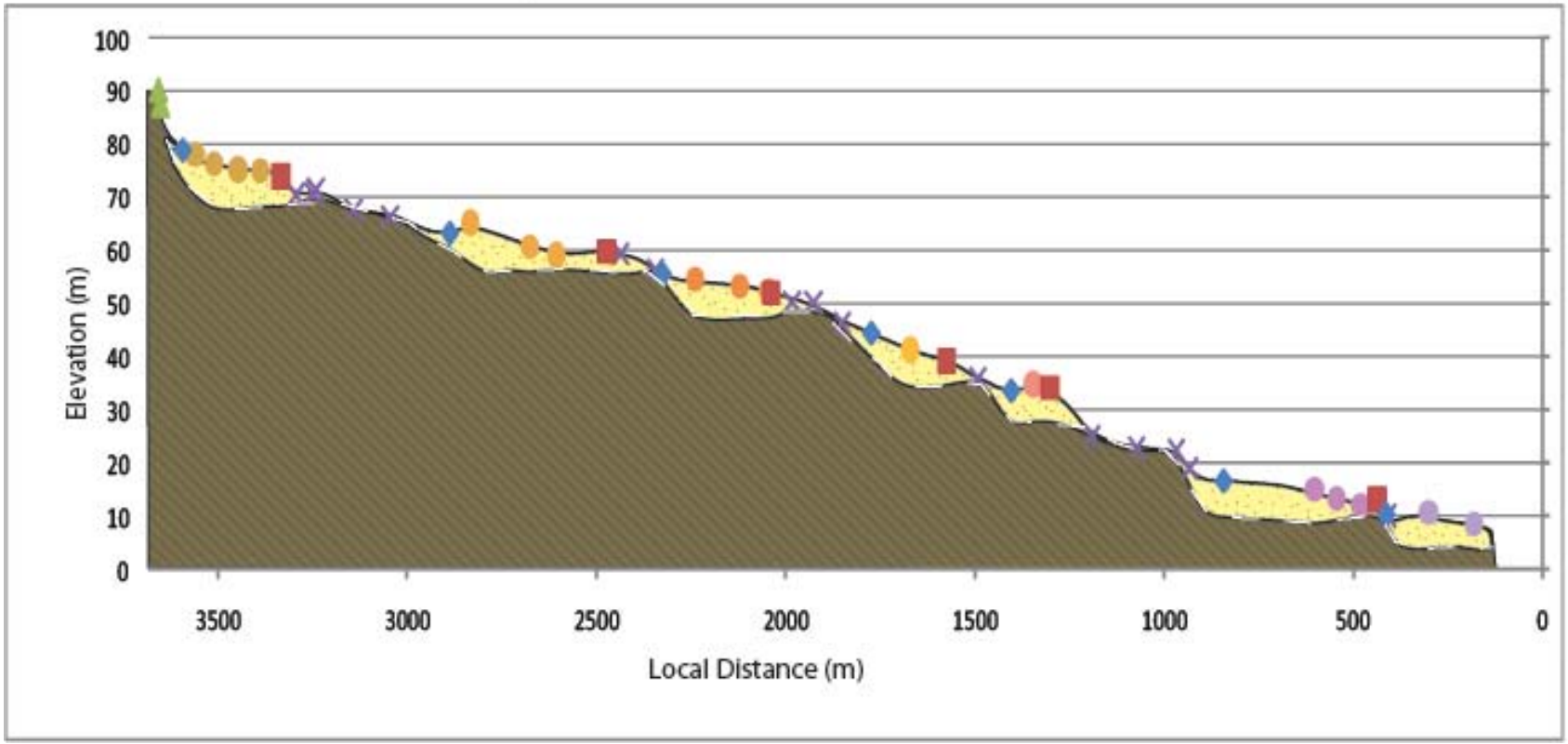
100
90
80
70
60
50
40
30
20
10
0
Elevation (m)
3500
3000
2500
2000
1500
1000
500
0
Local Distance (m)

Transect 1A

Point ID	Comment	Elevation (m)	UTM Easting	UTM Northing	Vertical Precision	Max PDOP	Notes
1	PS	90.099	292865	916058.06	1.9000	3.5000	
2	PS	87.217	292874	916038	1.8000	10.100	
4	IE	78.865	292906	916001.56	1.0000	2.6000	
5	T	78.291	292911	915956.06	1.6000	2.9000	
6	T	76.439	292933	915920.31	1.3000	3.4000	
7	T	75.33	292962	915877.94	1.4000	3.2000	
8	T	75.256	292988	915836.06	1.3000	3.2000	
9	OE	74.06	293007	915786.94	2.1000	3.0000	
10	R	70.5	293016	915740.94	1.9000	3.7000	
11	R	70.732	293033	915686.94	1.5000	3.2000	
12	R	71.676	293076	915649.19	2.2000	3.8000	
13	R	67.633	293118	915625.69	1.6000	2.6000	
14	R	66.414	293161	915602.31	1.8000	3.4000	
15	IE	63.26	293201	915576.75	1.7000	3.6000	
16	T	65.275	293240	915545.44	1.4000	2.0000	
17	T	60.893	293401	915424.44	1.1000	2.1000	
18	T	59.195	293465	915398.56	1.1000	2.7000	
19	OE	59.889	293515	915412.31	1.4000	2.7000	
20	R	59.331	293421	915182.737	1.8000	2.6000	
21	R	56.369	293449	915168.707	0.5000	3.4000	
22	IE	55.549	293490	915148.079	1.4000	3.6000	
24	T	54.74	293547	915127.461	1.1000	2.0000	
25	T	53.412	293633	915114.666	1.1000	2.1000	
26	T	52.548	293712	915157.843	0.8000	2.7000	
27	OE	52.193	293718	915161.963	1.4000	2.7000	
28	R	50.464	293788	915220.179	0.9000	3.0000	
29	R	50.335	293838	915235.115	0.8000	3.7000	
30	R	46.495	293891	915222.589	0.7000	3.2000	
31	IE	44.42	293963	915249.26	0.8000	3.8000	
32	T	41.457	294056	915282.395	1.1000	2.6000	
33	OE	39.292	294129	915303.488	1.4000	2.1000	
34	R	36.043	294140	915299.046	1.8000	2.7000	
35	T	34.928	294188	915264.593	0.5000	2.7000	
36	OE	34.236	294273	915302.81	1.4000	3.0000	
37	IE	33.589	294323	915315.025	1.4000	3.7000	
38	R	25.067	294482	915285.146	0.9000	2.1000	
39	R	22.833	294516	915274.02	0.8000	2.7000	
40	R	22.514	294579	915236.581	0.7000	2.7000	
41	R	18.91	294601	915225.696	0.8000	3.0000	
42	IE	16.591	294654	915188.312	1.0000	3.7000	
43	T	15.02	294788	915081.644	0.3000	2.7000	
44	T	13.237	294820	915051.841	0.9000	3.0000	

45	T	12.15	294859	915029.497	1.5000	3.7000	
46	OE	13.2	294885	915012.148	0.6000	2.1000	
47	OE	10.048	294898	914998.397	0.3000	2.7000	
48	R	10.326	294900	914995.224	0.9000	2.7000	
49	T	10.681	295043	914927.561	1.5000	3.7000	
50	T	8.46	295119	914865.577	0.6000	2.1000	

Transect 1b


KEY:
Paleo Sea Cliff
Qt 1
Qt 2 a,b
Qt 2b
Qt 3
Qt 4
Qt 5
Qt 6
Qt 7
Inner Edge
Outer Edge
Lahar
Projected Inner Edge
Projected Outer Edge
Riser
Hightide Debris Line
Infered Contact
Other Transects
Bedrock (Risers & Sea Cliffs)
Lahar
Marine Deposits

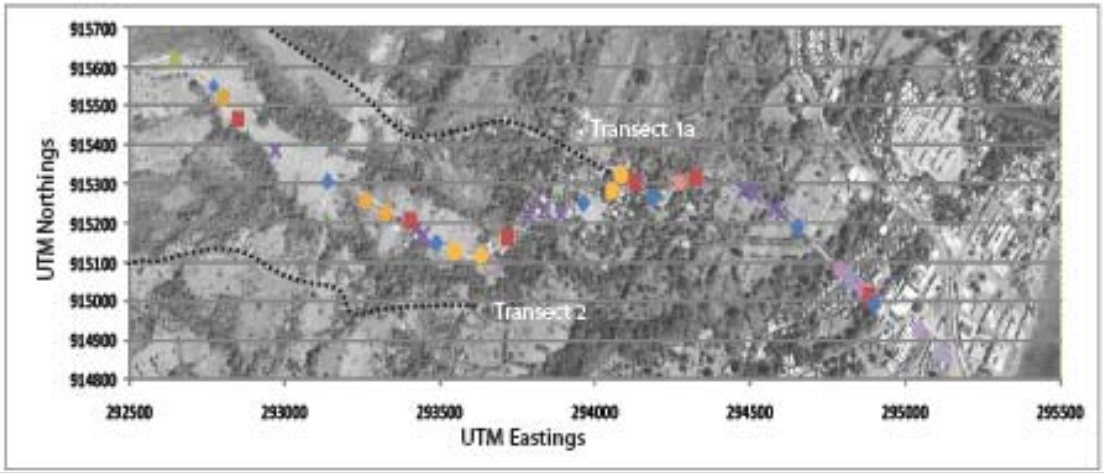
915700
915600
915500
915400
915300
915200
915100
915000
914900
914800
UTM Northings
Transect 1a
Transect 2
292500
293000
293500
294000
294500
295000
295500
UTM Eastings

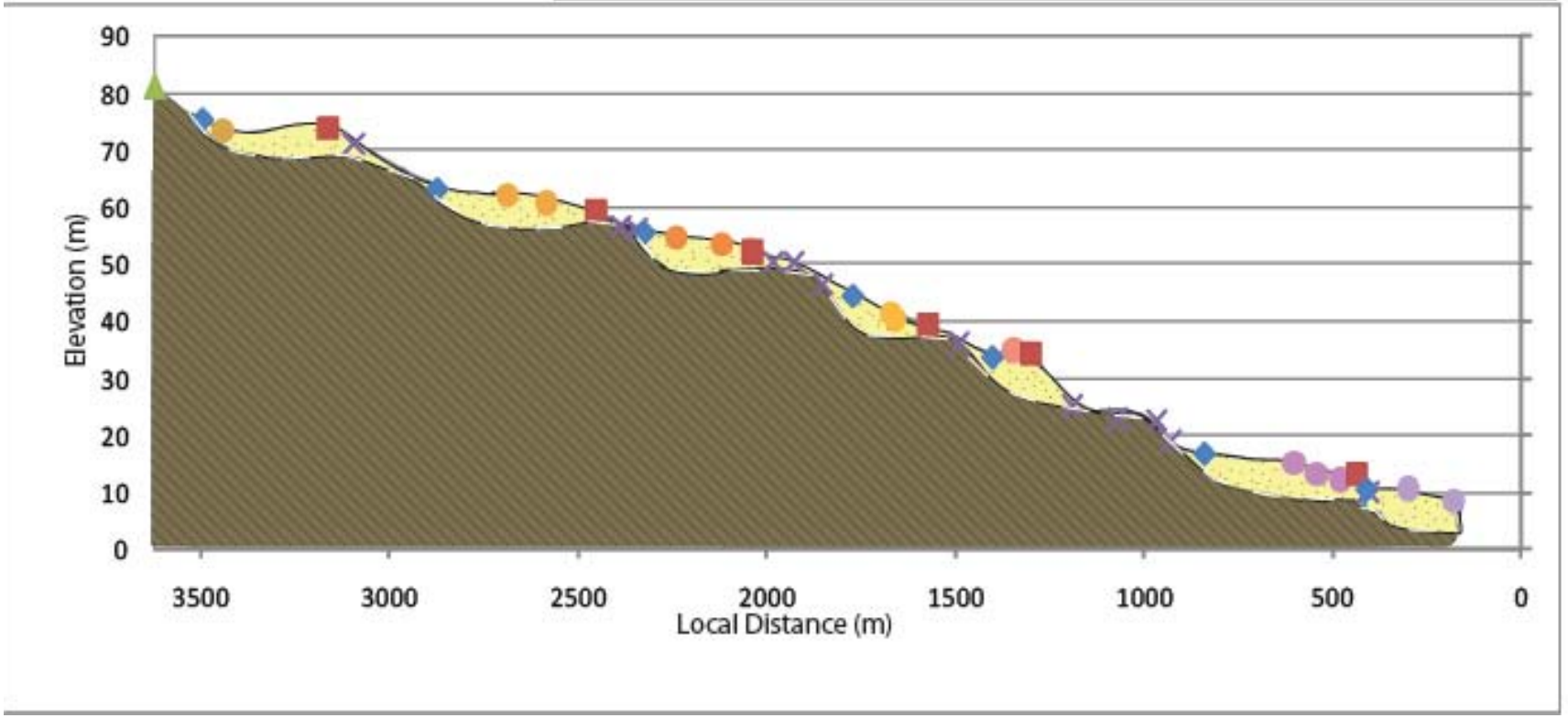
90
80
70
60
50
40
30
20
10
0
Elevation (m)
3500
3000
2500
2000
1500
1000
500
0
Local Distance (m)

Transect 1B

Point ID	Comment	Elevation	UTM Easting	UTM Northing	Vertical Precision	Max PDOP	Notes
1	PS	81.154	292771.5	915548.3	1.5000	3.2000	
2	IE	75.485	293138.8	915304.9	1.4000	3.8000	
3	T	73.498	293489.7	915148.1	1.1000	2.6000	
4	OE	73.585	293962.6	915249.3	1.4000	2.1000	
5	R	71.119	294188	915264.6	0.9000	3.4000	
6	IE	63.199	294653.7	915188.3	1.8000	3.6000	
7	T	60.736	294899.6	914995.2	2.5000	2.0000	
8	T	60.736	292880	915480	1.7000	2.7000	Sample 1&2
9	OE	59.329	292771.5	915548.3	0.9000	3.0000	
10	R	59.331	293421	915182.737	1.8000	2.6000	Below 9 Points are same in 1A
11	R	56.369	293449	915168.707	0.5000	3.4000	
12	IE	55.549	293490	915148.079	1.4000	3.6000	
13	T	54.74	293547	915127.461	1.1000	2.0000	
14	T	53.412	293633	915114.666	1.1000	2.1000	
15	T	52.548	293712	915157.843	0.8000	2.7000	
16	OE	52.193	293718	915161.963	1.4000	2.7000	
17	R	50.464	293788	915220.179	0.9000	3.0000	
18	R	50.335	293838	915235.115	0.8000	3.7000	
19	R	46.495	293891	915222.589	0.7000	3.2000	
31	IE	44.42	293963	915249.26	0.8000	3.8000	
32	T	41.457	294056	915282.395	1.1000	2.6000	
33	OE	39.292	294129	915303.488	1.4000	2.1000	
34	R	36.043	294140	915299.046	1.8000	2.7000	
35	T	34.928	294188	915264.593	0.5000	2.7000	
36	OE	34.236	294273	915302.81	1.4000	3.0000	
37	IE	33.589	294323	915315.025	1.4000	3.7000	
38	R	25.067	294482	915285.146	0.9000	2.1000	
39	R	22.833	294516	915274.02	0.8000	2.7000	
40	R	22.514	294579	915236.581	0.7000	2.7000	
41	R	18.91	294601	915225.696	0.8000	3.0000	
42	IE	16.591	294654	915188.312	1.0000	3.7000	
43	T	15.02	294788	915081.644	0.3000	2.7000	
44	T	13.237	294820	915051.841	0.9000	3.0000	
45	T	12.15	294859	915029.497	1.5000	3.7000	
46	OE	13.2	294885	915012.148	0.6000	2.1000	
47	OE	10.048	294898	914998.397	0.3000	2.7000	

48	R	10.326	294900	914995.224	0.9000	2.7000	
49	T	10.681	295043	914927.561	1.5000	3.7000	
50	T	8.46	295119	914865.577	0.6000	2.1000	

Transect 2

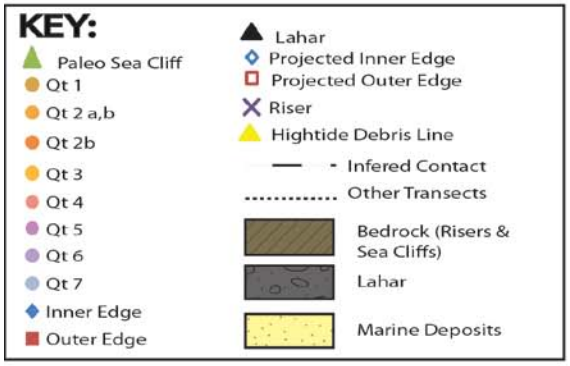
KEY:
Paleo Sea Cliff
Qt 1
Qt 2 a,b
Qt 2b
Qt 3
Qt 4
Qt 5
Qt 6
Qt 7
Inner Edge
Outer Edge
Lahar
Projected Inner Edge
Projected Outer Edge
Riser
Hightide Debris Line
Infered Contact
Other Transects
Bedrock (Risers & Sea Cliffs)
Lahar
Marine Deposits

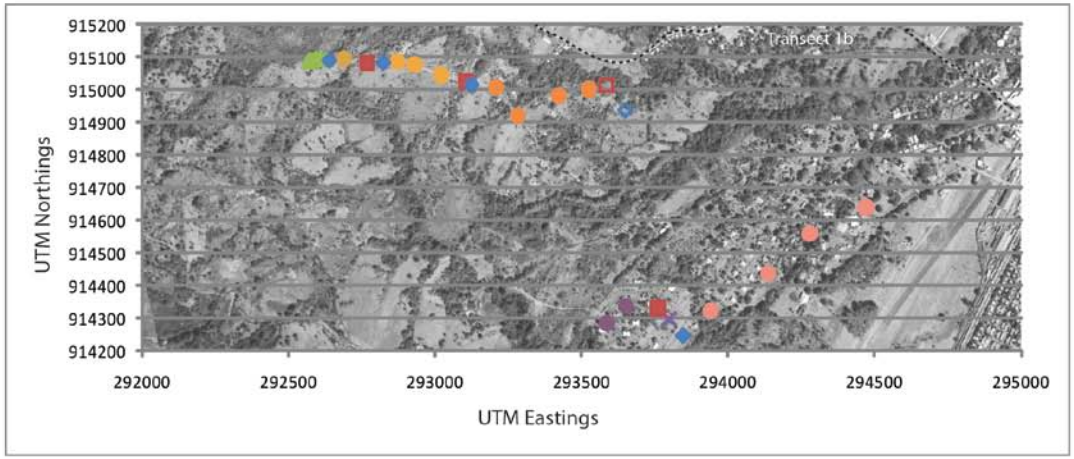
Transect 1b
915200
915100
915000
914900
914800
914700
914600
914500
914400
914300
914200
UTM Northings
292000
292500
293000
293500
294000
294500
295000
UTM Eastings

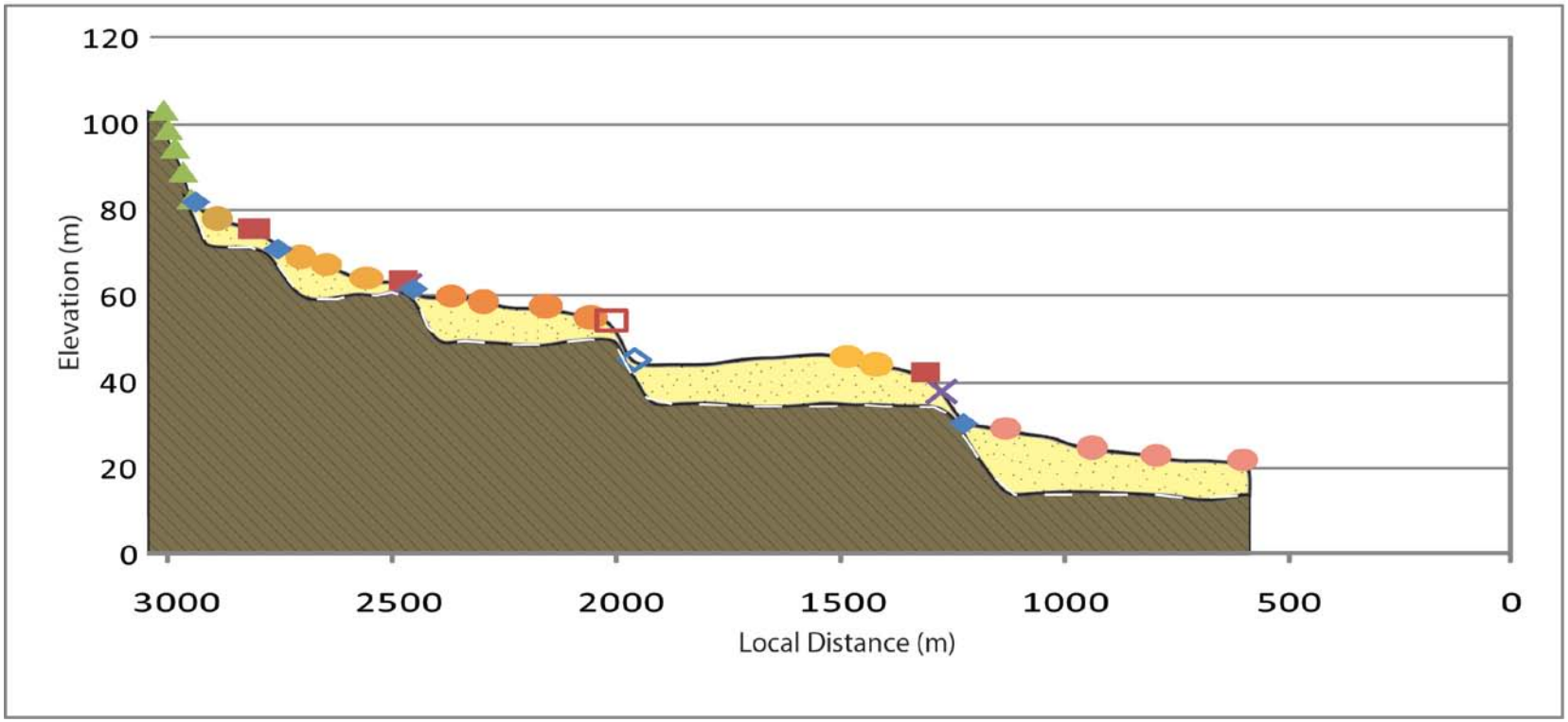
120
100
80
60
40
20
0
Elevation (m)
3000
2500
2000
1500
1000
500
0
Local Distance (m)

Transect 2

Point ID	Comment	Elevation (m)	UTM Easting	UTM Northing	Vertical Precision	Max PDOP	Notes
1	PS	103.24	292567	915086.4	1.1000	1.8000	
2	PS	98.774	292577.1	915089.8	1.3000	3.8000	
3	PS	94.505	292592.1	915094.4	1.1000	3.8000	
4	PS	88.975	292610	915097.9	1.2000	1.6000	
5	PS	82.655	292627.5	915092.1	1.5000	3.1000	
6	IE	81.716	292639.2	915091.8	1.2000	2.5000	
7	T	77.8	292686.8	915093.6	1.5000	4.2000	
8	OE	75.437	292768.2	915081.7	1.3000	3.6000	
9	IE	70.774	292822.8	915084.9	1.0000	2.0000	
10	T	68.996	292870.7	915086.4	1.3000	2.5000	
11	T	67.034	292928.3	915076.3	1.0000	1.8000	
12	T	64.088	293020.1	915044.8	1.1000	2.5000	
13	OE	63.391	293102.7	915025.1	1.1000	2.6000	
14	R	62.543	293110.9	915019	0.9000	4.8000	
15	IE	61.508	293124	915017.2	0.9000	2.5000	
16	T	59.914	293207.7	915009.1	0.9000	2.0000	
17	T	58.478	293282.7	914921.2	0.9000	2.4000	
18	T	57.441	293420.4	914982.4	1.6000	4.4000	
19	T	54.907	293524.4	915001.8	1.0000	3.6000	
20	OE	54	293585.2	914286.9			Projected
21	IE	45.818	293651	914338.2	1.0000	3.0000	
22	T	45	293759.7	914330.7			Projected
23	T	44.008	293797.5	914298.6	0.9000	2.3000	
24	OE	42.169	293844.1	914245.4	1.0000	2.4000	
25	R	37.769	293940.2	914325.7	1.0000	4.3000	
26	IE	30.153	294134.7	914436.7	1.1000	2.4000	
27	T	29.077	294278.2	914558.7	1.1000	3.2000	
28	T	24.55	294469.3	914640.1	1.2000	3.8000	
29	T	22.708	292567	915086.4	1.7000	9.1000	
30	T	21.633	292577.1	915089.8	1.7000	2.3000	

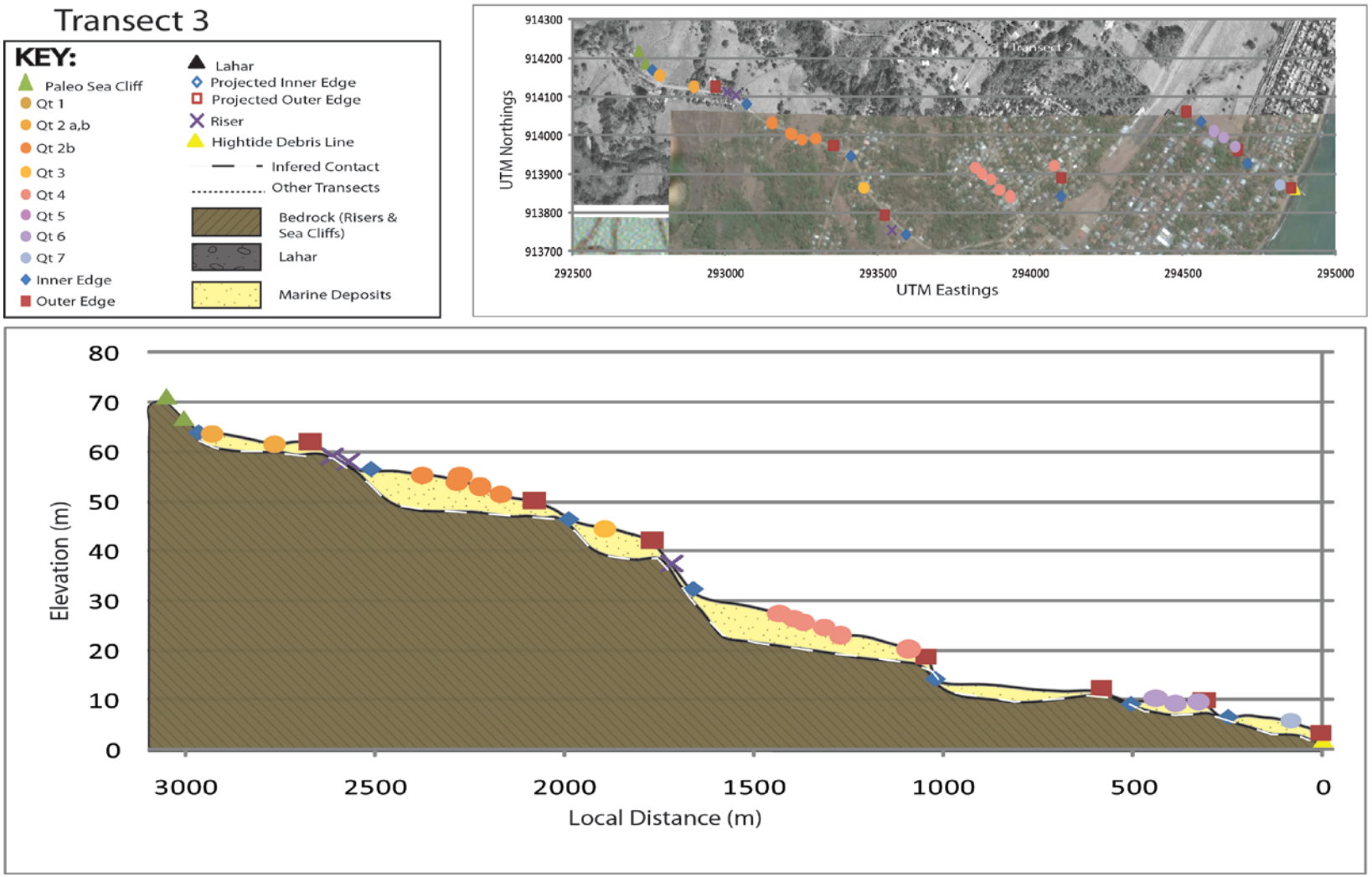
Transect 3
KEY:
Paleo Sea Cliff
Qt 1
Qt 2 a,b
Qt 2b
Qt 3
Qt 4
Qt 5
Qt 6
Qt 7
Inner Edge
Outer Edge
Lahar
Projected Inner Edge
Projected Outer Edge
Riser
Hightide Debris Line
Infered Contact
Other Transects
Bedrock (Risers & Sea Cliffs)
Lahar
Marine Deposits
914300
914200
914100
914000
913900
913800
913700
UTM Northings
292500
293000
293500
294000
294500
295000
UTM Eastings
Transect 2
80
70
60
50
40
30
20
10
0
Elevation (m)
3000
2500
2000
1500
1000
500
0
Local Distance (m)

Transect 3

Point ID	Comment	Elevation (m)	UTM Easting	UTM Northing	Vertical Precision	Max PDOP	Notes
1	PS	71.1	292717.0312	914218.3750	1.9000	12.900	
2	PS	66.723	292739.0313	914186.1875	1.2000	2.8000	
3	IE	64.023	292762.4688	914167.4375	1.0000	3.0000	Sample 3
4	T	63.569	292785.9687	914154.5000	1.7000	6.2000	
5	T	61.375	292898.2500	914126.0000	1.0000	2.4000	
6	OE	62.031	292968.6250	914125.8125	1.1000	2.3000	
7	R	59.081	293007.6250	914111.8125	1.0000	2.5000	
8	R	57.987	293035.1875	914103.5625	2.0000	11.900	
9	IE	56.62	293071.7188	914080.0625	3.5000	5.7000	
10	T	55.325	293154.3750	914031.7500	1.3000	5.7000	
11	T	55.16	293214.5938	914003.9375	1.7000	2.1000	
12	T	53.848	293220.5938	914002.6250	3.0000	5.3000	
13	T	52.962	293253.0312	913988.1250	1.1000	2.4000	
14	T	51.497	293297.2813	913992.0625	0.90000	2.1000	
15	OE	50.129	293356.1563	913973.8750	1.3000	4.2000	
16	IE	46.458	293413.5938	913945.2500	1.0000	2.5000	
17	T	44.447	293454.9062	913863.3125	1.0000	2.8000	Sample 4
18	OE	42.151	293523.4688	913793.5625	0.90000	4.1000	
19	R	37.524	293547.4375	913754.2500	1.0000	4.4000	
20	IE	32.344	293579.3125	913726.5000	1.2000	2.2000	
21	T	27.273	293820.4688	913915.6250	1.0000	3.7000	
22	T	26.251	293843.1562	913900.0625	1.1000	3.0000	
23	T	25.598	293856.5000	913884.5625	1.0000	1.8000	
24	T	24.58	293885.2187	913848.3750	1.1000	1.8000	
25	T	23.038	293906.7813	913820.8125	1.4000	3.6000	
26	T	20.293	294078.5937	913920.2500	1.4000	2.7000	
27	OE	18.619	294102.1562	913888.8750	1.1000	1.9000	
28	IE	14.134	294102.2813	913842.3750	1.4000	3.1000	
29	OE	12.268	294512.0937	914060.6250	1.4000	1.5000	
30	IE	9.934	294561.5937	914034.5000	1.5000	3.6000	
31	T	10.439	294603.1563	914011.0625	1.5000	2.8000	
32	T	9.54	294635.4375	913993.6250	1.5000	2.8000	
33	T	9.216	294671.6875	913971.0000	1.4000	1.9000	
34	OE	9.057	294680.8438	913961.8750	1.6000	2.8000	
35	IE	6.432	294714.0625	913926.3125	1.2000	2.0000	
36	T	5.765	294818.0000	913871.6875	1.6000	3.2000	
37	OE	3.415	294868.5625	913843.0000	1.3000	2.4000	
38	HT	2.086	294868.9687	913835.0000	1.3000	2.5000	

Transect 4

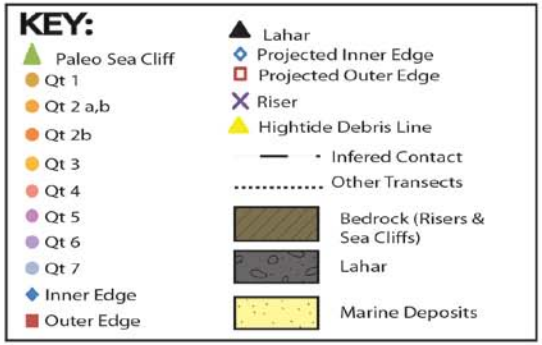
KEY:
Paleo Sea Cliff
Qt 1
Qt 2 a,b
Qt 2b
Qt 3
Qt 4
Qt 5
Qt 6
Qt 7
Inner Edge
Outer Edge
Lahar
Projected Inner Edge
Projected Outer Edge
Riser
Hightide Debris Line
Infered Contact
Other Transects
Bedrock (Risers & Sea Cliffs)
Lahar
Marine Deposits

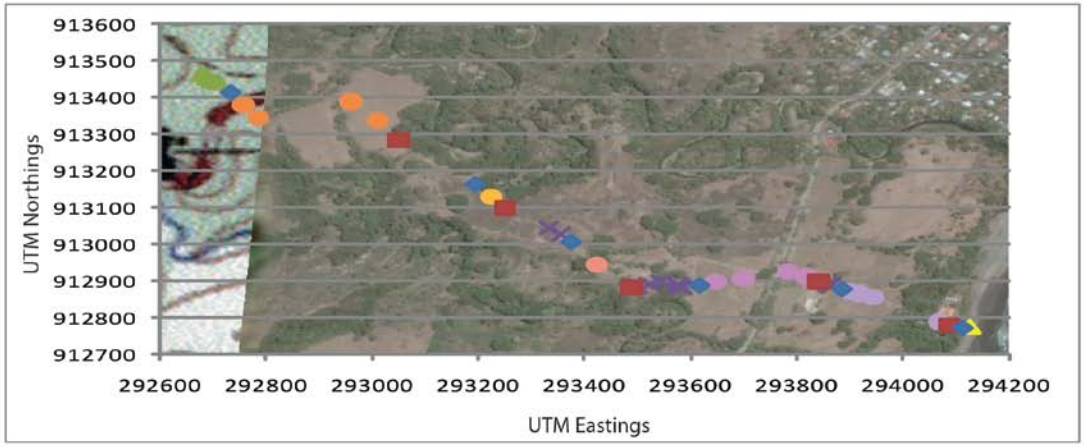
913600
913500
913400
913300
913200
913100
913000
912900
912800
912700
UTM Northings
292600
292800
293000
293200
293400
293600
293800
294000
294200
UTM Eastings

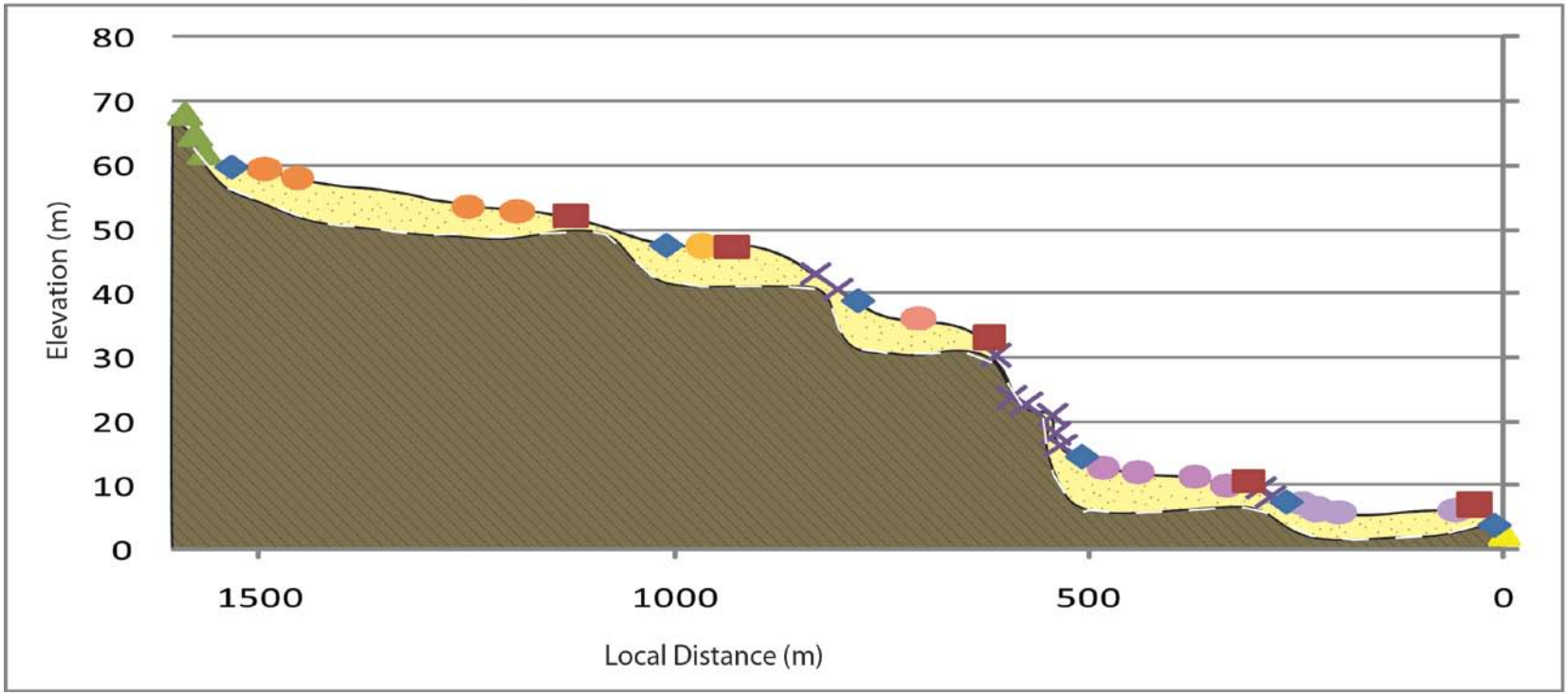
80
70
60
50
40
30
20
10
0
Elevation (m)
1500
1000
500
0
Local Distance (m)

Transect 4

Point ID	Comment	Elevation (m)	UTM Easting	UTM Northing	Vertical Precision	Max PDOP	Notes
1	PS	68.131	292688.7	913454.6	1.0000	2.4000	
2	PS	64.826	292697.8	913447.1	1.0000	2.4000	
3	PS	61.971	292707.9	913442.2	1.4000	6.9000	
4	IE	59.63	292732.1	913415.4	1.1000	5.7000	
5	T	59.314	292757.5	913378.9	1.1000	4.0000	
6	T	57.991	292785.4	913344.1	4.8000	16.000	
7	T	53.5	292959.4	913389.4	1.3000	4.6000	
8	T	52.838	293010.1	913336.9	0.90000	2.0000	
9	OE	52	293049.8	913283.2	1.2000	4.4000	
10	IE	47.396	293192.6	913164.7	1.0000	2.4000	
11	T	47.337	293223.7	913130.4	0.90000	1.9000	
12	OE	47.146	293249.7	913099.6	0.90000	1.5000	
13	R	43.072	293334.1	913045.6	1.0000	1.9000	
14	R	40.662	293356.8	913027.4	1.4000	2.5000	
15	IE	38.74	293373.8	913008	1.3000	2.6000	
16	T	36.022	293423.3	912944.6	2.0000	9.6000	
17	OE	33.179	293488.3	912882.2	2.5000	18.700	
18	R	30.339	293498.9	912885.4	2.0000	5.9000	
19	R	23.738	293523.2	912890.1	1.9000	5.8000	
20	R	22.7	293544.9	912898.9	0.90000	1.9000	
21	R	20.943	293576.2	912890.4	1.1000	1.9000	
22	R	18.126	293579.3	912883.6	1.3000	2.2000	
23	R	16.305	293584.3	912882.3	1.0000	2.2000	
24	IE	14.372	293616	912889.3	0.90000	2.3000	
25	T	12.769	293648.7	912899.7	0.90000	1.9000	
26	T	12.132	293699	912906.5	0.90000	2.4000	
27	T	11.335	293783.7	912925.2	1.5000	3.7000	
28	OE	10.627	293818.4	912912.1	1.1000	2.4000	
29	T	10.018	293842.1	912899.1	1.2000	2.8000	
30	R	9.58	293857.6	912892.3	1.3000	3.7000	
31	R	8.323	293867	912889.3	1.2000	1.8000	
32	IE	7.29	293884.3	912879.2	1.1000	2.3000	
33	T	7.095	293900.9	912871.8	1.2000	2.2000	
34	OE	7	293917.4	912865.6	1.2000	1.9000	
35	T	6.285	293943.1	912857	1.2000	1.9000	
36	T	6.198	294067.3	912788.7	1.4000	2.9000	
37	T	5.879	294087.3	912780	1.6000	4.5000	
38	IE	3.652	294111.5	912773.3	1.6000	8.6000	
39	HT	2.524	294126.2	912776.9	1.9000	4.1000	

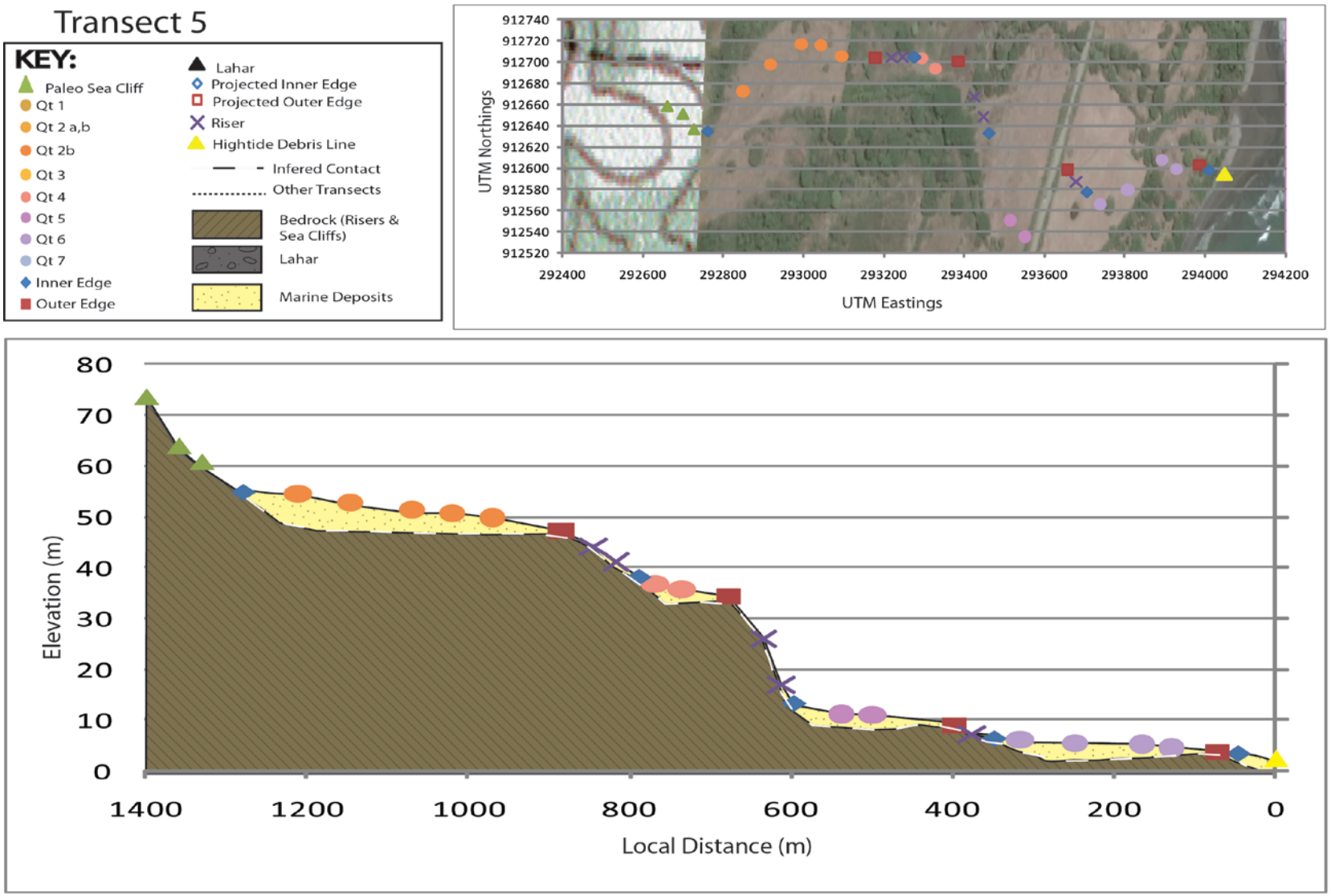
Transect 5
KEY:
Paleo Sea Cliff
Qt 1
Qt 2 a,b
Qt 2b
Qt 3
Qt 4
Qt 5
Qt 6
Qt 7
Inner Edge
Outer Edge
Lahar
Projected Inner Edge
Projected Outer Edge
Riser
Hightide Debris Line
Infered Contact
Other Transects
Bedrock (Risers & Sea Cliffs)
Lahar
Marine Deposits
UTM Northings
912740
912720
912700
912680
912660
912640
912620
912600
912580
912560
912540
912520
292400
292600
292800
293000
293200
293400
293600
293800
294000
294200
UTM Eastings
Elevation (m)
80
70
60
50
40
30
20
10
0
1400
1200
1000
800
600
400
200
0
Local Distance (m)

Transect 5

Point ID	Comment	Elevation (m)	UTM Easting	UTM Northing	Vertical Precision	Max PDOP	Notes
1	PS	73.646	292660.9	912658.4	2.8000	3.3000	
2	PS	63.948	292700.7	912651.3	2.9000	2.7000	
3	PS	60.79	292728.2	912636.9	1.8000	3.9000	
4	IE	54.67	292761.3	912634.3	1.7000	2.2000	
5	T	54.49	292849.6	912672.3	1.7000	2.2000	
6	T	52.738	292917.3	912697.6	1.7000	2.3000	
7	T	51.512	292995.1	912716.6	1.6000	2.3000	
8	T	50.717	293044.4	912715.6	1.6000	2.3000	
9	T	49.887	293095	912705.6	2.2000	3.5000	
10	OE	47.162	293178.7	912703.9	3.3000	6.0000	
11	R	43.989	293219.2	912704.1	3.1000	4.4000	
12	R	41.12	293247.7	912704.8	3.2000	4.1000	
13	IE	38	293276.7	912704.8	2.8000	4.1000	
14	T	36.68	293295.5	912703.2	2.6000	2.2000	
15	T	35.725	293327.9	912693.6	2.8000	3.2000	
16	OE	34.301	293386.1	912700.4	2.3000	3.2000	
17	R	25.983	293427	912666.8	2.5000	2.7000	
18	R	17.012	293448.2	912648.4	2.3000	2.9000	
19	IE	13.244	293462.7	912632.5	2.4000	3.6000	
20	T	11.189	293515.5	912550.8	1.6000	2.4000	
21	T	11.071	293552.2	912535.6	1.5000	2.2000	
22	OE	8.85	293658.5	912598.8	1.5000	2.5000	
23	R	7.11	293679.3	912587.3	1.6000	2.2000	
24	IE	6.337	293706.7	912576.9	1.4000	2.5000	
25	T	6.166	293738.2	912566.1	1.4000	2.2000	
26	T	5.504	293807.8	912579.5	1.3000	2.1000	
27	T	5.255	293892	912607.7	2.4000	3.5000	
28	T	4.621	293928.6	912599.4	2.9000	2.5000	
29	OE	3.729	293986.5	912603.2	2.9000	5.0000	
30	IE	3.406	294010.6	912597.4	2.0000	8.1000	
31	HT	2.529	294057.9	912590.3	1.5000	2.6000	

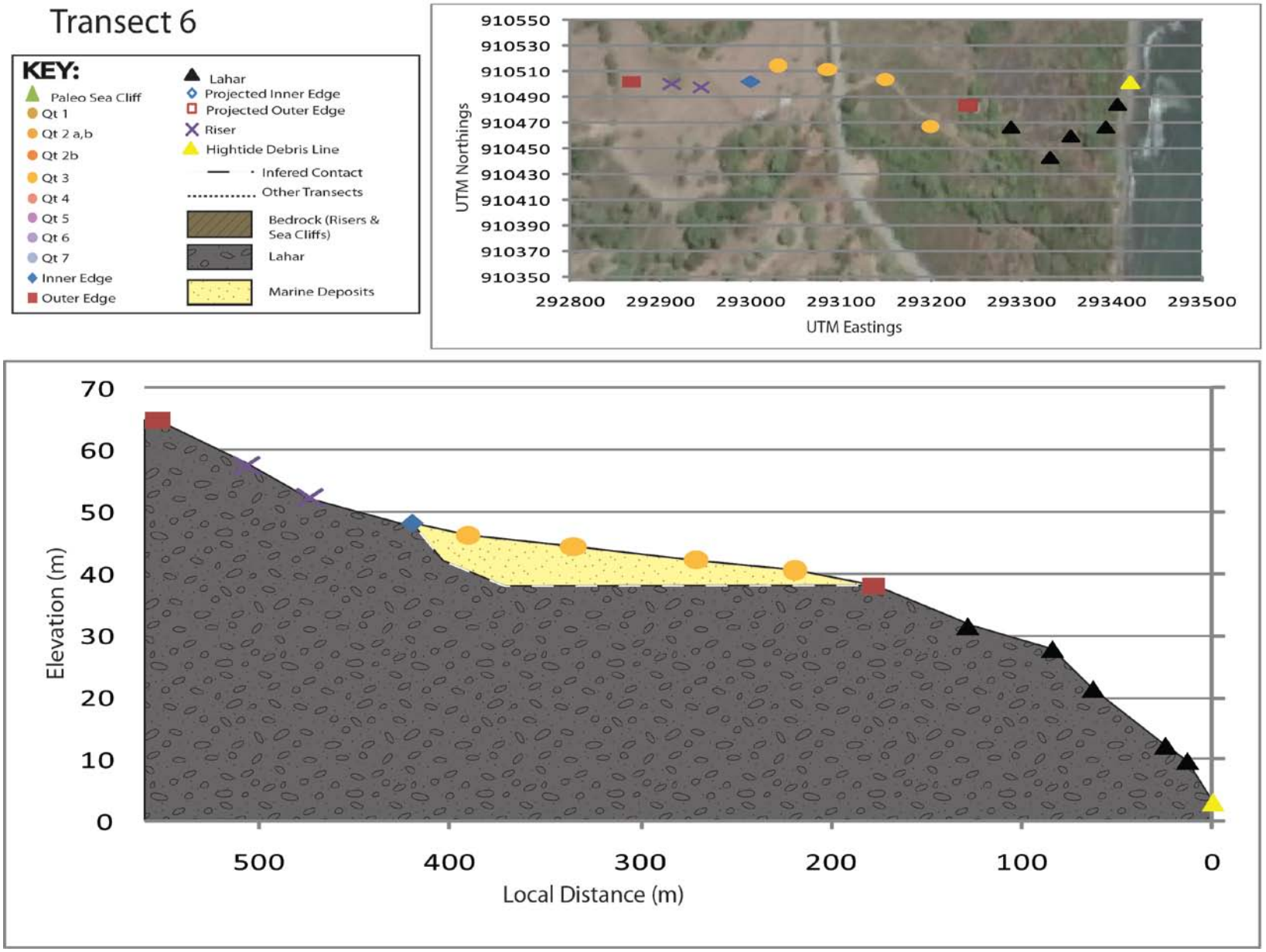
Transect 6
KEY:
Paleo Sea Cliff
Qt 1
Qt 2 a,b
Qt 2b
Qt 3
Qt 4
Qt 5
Qt 6
Qt 7
Inner Edge
Outer Edge
Lahar
Projected Inner Edge
Projected Outer Edge
Riser
Hightide Debris Line
Infered Contact
Other Transects
Bedrock (Risers & Sea Cliffs)
Lahar
Marine Deposits
910550
910530
910510
910490
910470
910450
910430
910410
910390
910370
910350
UTM Northings
292800
292900
293000
293100
293200
293300
293400
293500
UTM Eastings
70
60
50
40
30
20
10
0
Elevation (m)
500
400
300
200
100
0
Local Distance (m)

Transect 6

Point ID	Comment	Elevation (m)	UTM Easting	UTM Northing	Vertical Precision	Max PDOP	Notes
1	OE	64.783	292866.4	910505.3	3.6000	5.6000	
2	R	57.468	292912.8	910500.2	1.3000	2.6000	
3	R	52.236	292945.8	910497.6	1.3000	2.5000	
4	IE	48.201	292999.9	910502.1	1.4000	2.6000	
5	T	46.122	293030.4	910514.5	1.4000	2.6000	
6	T	44.276	293085.6	910511.8	1.8000	3.0000	
7	T	42.325	293149.8	910504	1.2000	2.6000	
8	T	40.529	293199.3	910466.9	1.7000	3.0000	
9	OE	37.9	293241.1	910483.7	1.9000	3.9000	
10	L	31.424	293289.5	910466.7	1.7000	3.4000	
11	L	27.72	293332.5	910443.2	1.3000	1.8000	
12	L	21.315	293355.2	910459.9	2.8000	7.1000	
13	L	12.224	293393.8	910466.8	7.3000	9.0000	
14	L	9.739	293406.6	910484.5	6.3000	9.2000	
15	HT	3.1200	293421.2	910501.4	4.7000	5.7000	

Transect 7

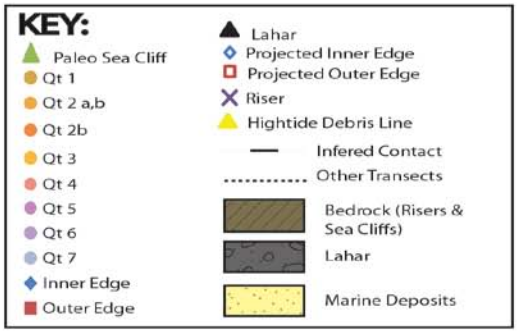
KEY:
Paleo Sea Cliff
Qt 1
Qt 2 a,b
Qt 2b
Qt 3
Qt 4
Qt 5
Qt 6
Qt 7
Inner Edge
Outer Edge
Lahar
Projected Inner Edge
Projected Outer Edge
Riser
Hightide Debris Line
Infered Contact
Other Transects
Bedrock (Risers & Sea Cliffs)
Lahar
Marine Deposits

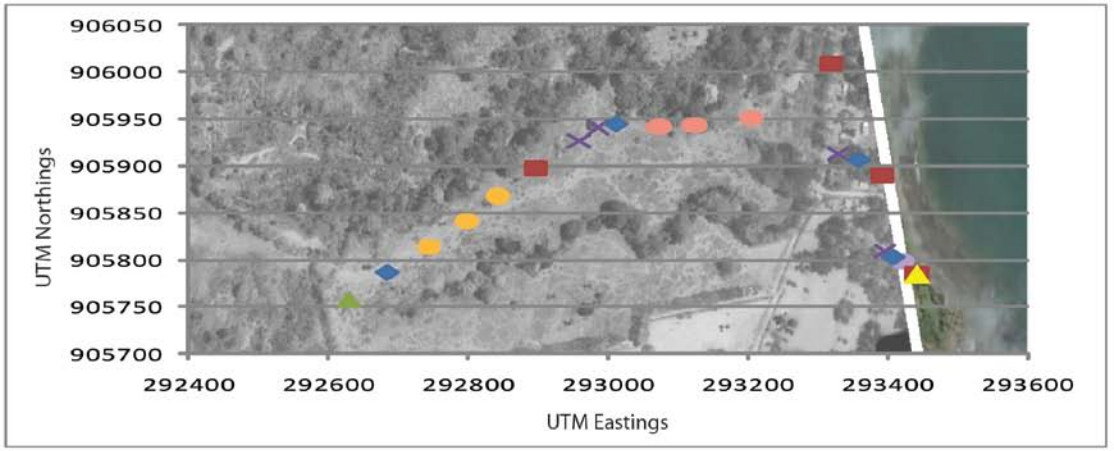
906050
906000
905950
905900
905850
905800
905750
905700
UTM Northings
292400
292600
292800
293000
293200
293400
293600
UTM Eastings

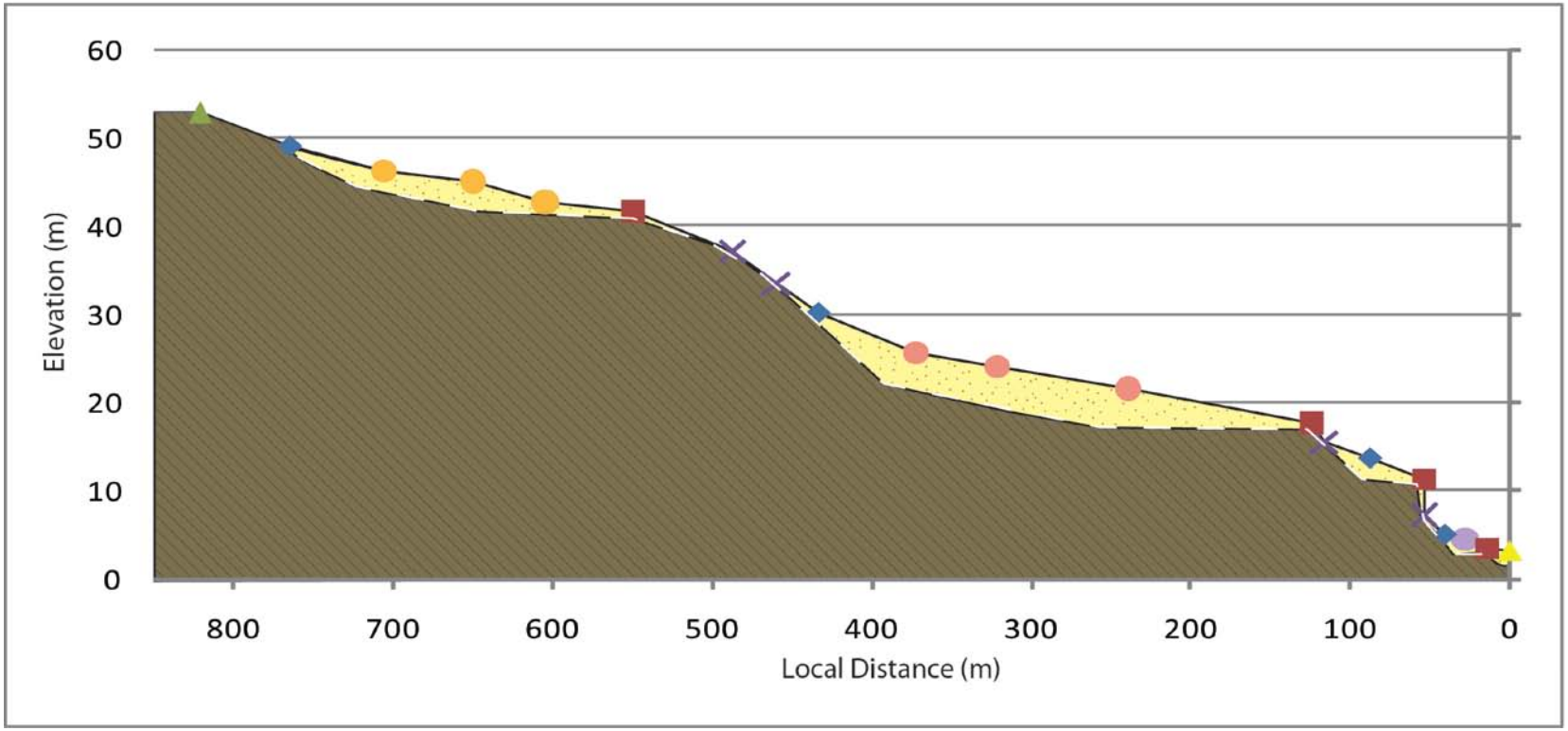
60
50
40
30
20
10
0
Elevation (m)
800
700
600
500
400
300
200
100
0
Local Distance (m)

Transect 7

Point ID	Comments	Elevation (m)	UTM Easting	UTM Northing	Vertical Precision	Max PDOP	Notes
1	PS	52.849	292630	905757.4	1.4000	2.9000	
2	IE	49.009	292685	905786.6	1.2000	2.4000	
3	T	46.118	292743.6	905813.4	1.0000	1.7000	
4	T	44.995	292798.5	905841.4	1.0000	1.7000	
5	T	42.649	292842.9	905867.9	1.0000	1.8000	
6	OE	41.641	292897.1	905897.4	1.0000	2.3000	
7	R	37.145	292959.7	905926.3	1.1000	2.3000	
8	R	33.363	292986.1	905940.8	0.90000	1.4000	
9	IE	30.124	293012.7	905944.8	1.0000	1.8000	
10	T	25.525	293073.9	905941.8	0.90000	2.0000	
11	T	23.942	293124.4	905943.1	0.90000	1.7000	
12	T	21.512	293206.3	905950.5	0.90000	1.9000	
13	OE	17.641	293320.5	906008.9	0.90000	1.9000	Sample 9
14	R	15.418	293330.1	905912.6	1.9000	5.1000	
15	IE	13.651	293359.8	905906.7	1.2000	2.2000	
16	OE	11.233	293393.9	905889.9	1.4000	1.9000	
17	R	7.207	293396	905808.8	3.1000	14.000	
18	IE	5	293409.4	905802.9			Projected
19	T	4.507	293421.6	905798.1	1.2000	1.9000	
20	OE	3.334	293435.8	905790.6	1.7000	3.7000	
21	HT	3.0860	293436.9	905792.8	1.8000	2.5000	

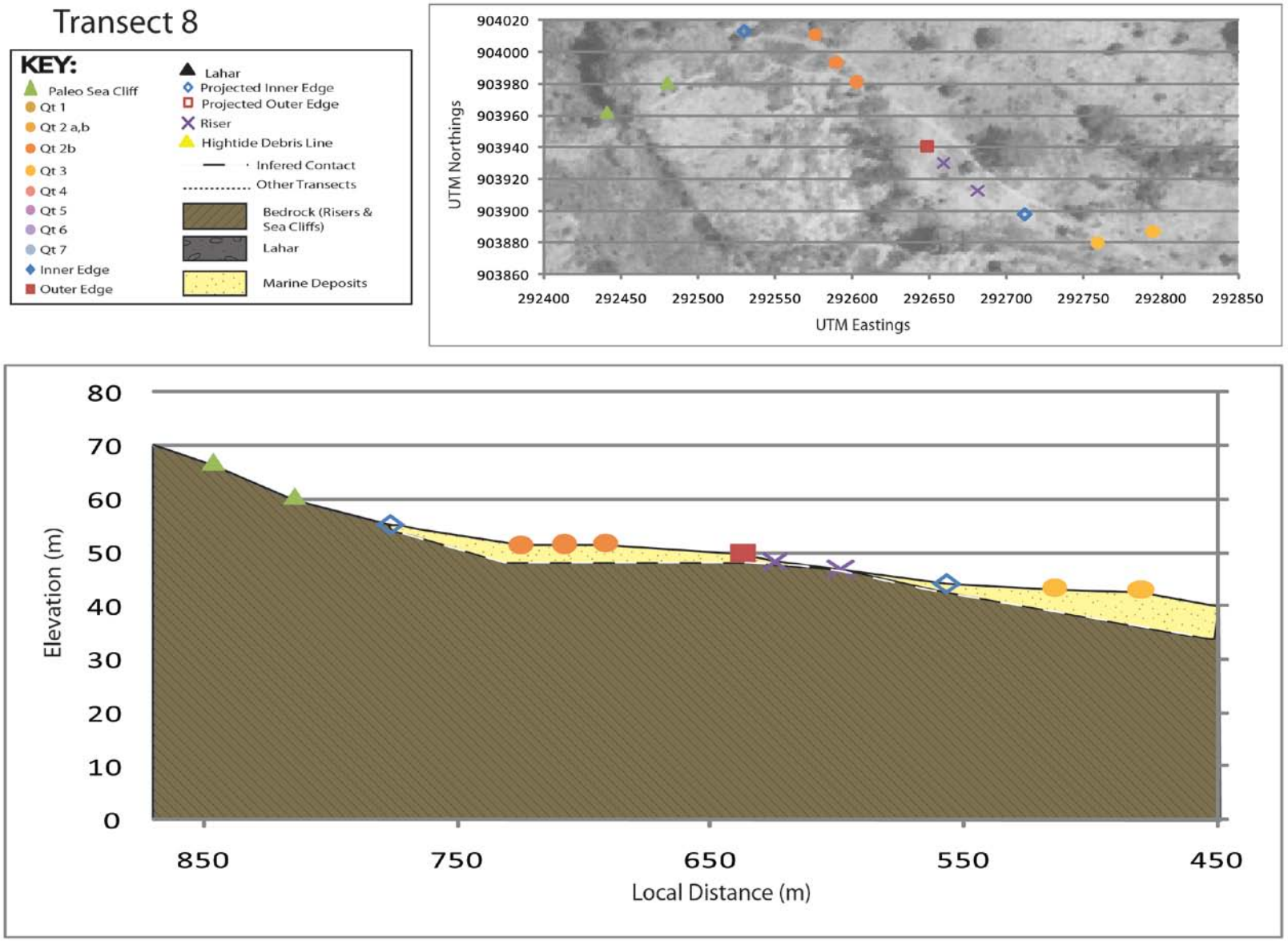
Transect 8
KEY:
Paleo Sea Cliff
Qt 1
Qt 2 a,b
Qt 2b
Qt 3
Qt 4
Qt 5
Qt 6
Qt 7
Inner Edge
Outer Edge
Lahar
Projected Inner Edge
Projected Outer Edge
Riser
Hightide Debris Line
Infered Contact
Other Transects
Bedrock (Risers & Sea Cliffs)
Lahar
Marine Deposits
UTM Northings
904020
904000
903980
903960
903940
903920
903900
903880
903860
292400
292450
292500
292550
292600
292650
292700
292750
292800
292850
UTM Eastings
Elevation (m)
80
70
60
50
40
30
20
10
0
850
750
650
550
450
Local Distance (m)

Transect 8

Point ID	Comment	Elevation	UTM Easting	UTM Northing	Vertical Precision	Max PDOP	Notes
1	PS	66.825	292648.3	903940.7	1.1000	2.3000	
2	PS	60.485	292659.2	903930.3	0.90000	1.8000	
3	IE	55	292681.1	903912.6			Projected
4	T	51.314	292589.4	903993.2	1.0000	2.4000	
5	T	51.627	292602.8	903981.3	1.0000	2.0000	
6	T	51.763	292758.7	903880.1	1.0000	2.0000	
7	OE	49.886	292794.7	903887	1.0000	2.9000	
8	R	48.375	292576	904011	0.90000	1.9000	
9	R	46.863	292441	903962	1.0000	1.9000	
10	IE	44	292480	903981			Projected
11	T	43.495	292530	904013	1.1000	1.6000	
12	T	43.144	292712	903898	1.0000	1.9000	

Transect 9

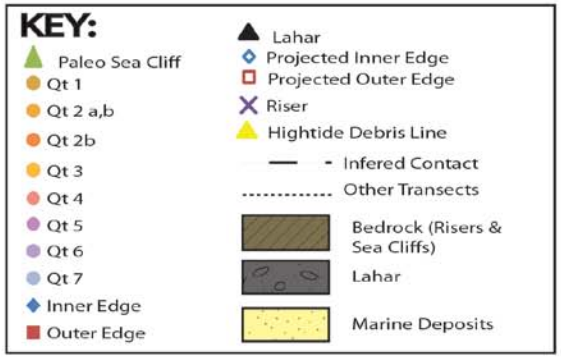
KEY:
Paleo Sea Cliff
Qt 1
Qt 2 a,b
Qt 2b
Qt 3
Qt 4
Qt 5
Qt 6
Qt 7
Inner Edge
Outer Edge
Lahar
Projected Inner Edge
Projected Outer Edge
Riser
Hightide Debris Line
Infered Contact
Other Transects
Bedrock (Risers & Sea Cliffs)
Lahar
Marine Deposits

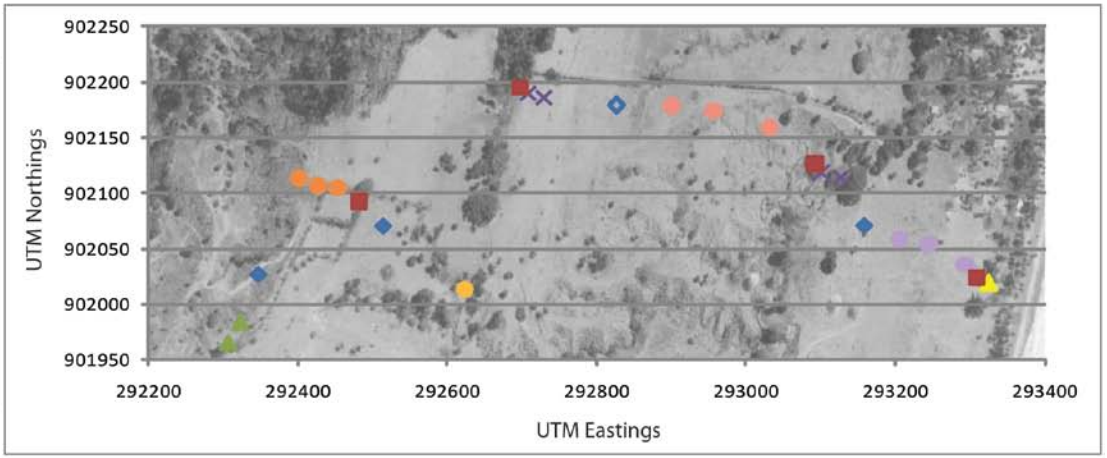
902250
902200
902150
902100
902050
902000
901950
UTM Northings
292200
292400
292600
292800
293000
293200
293400
UTM Eastings

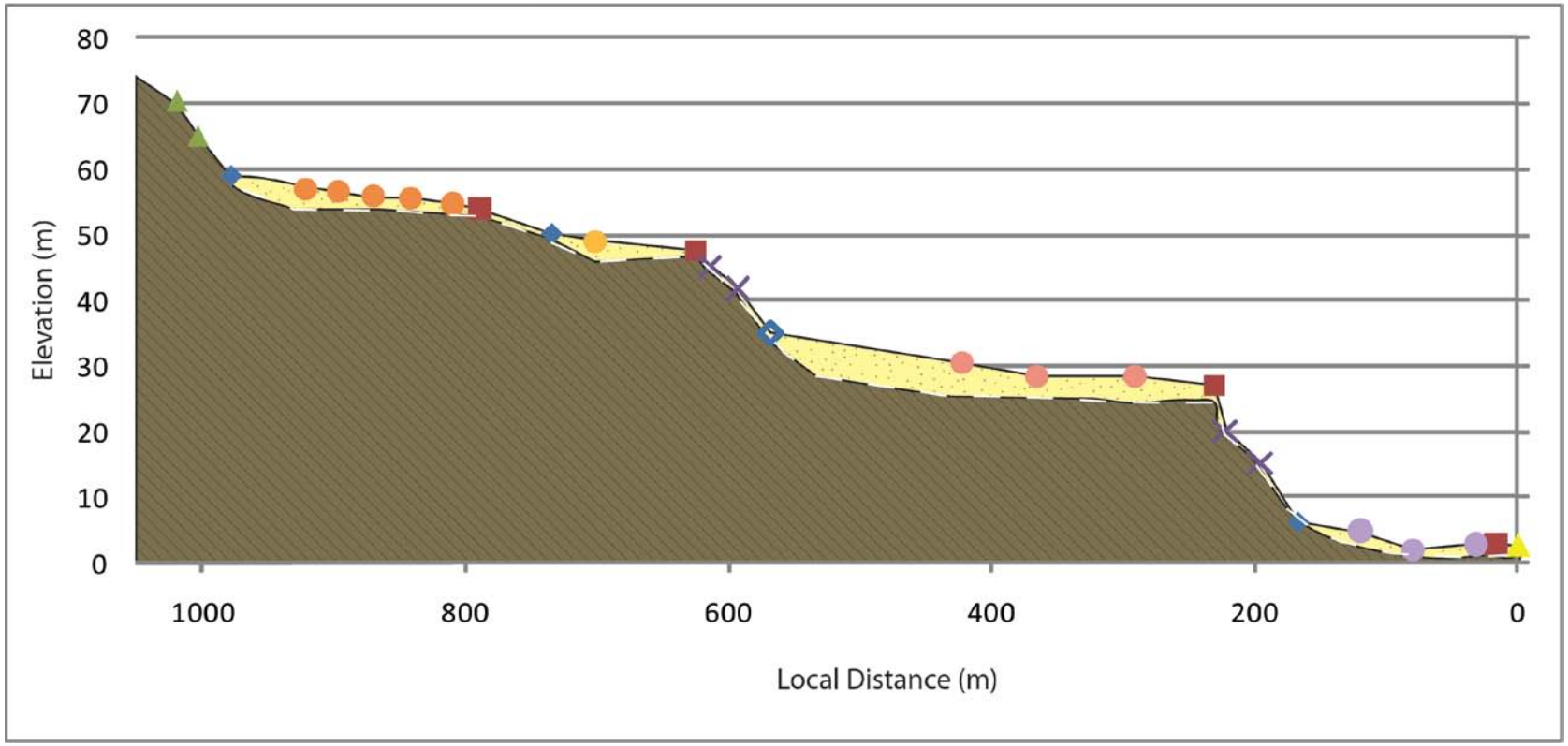
80
70
60
50
40
30
20
10
0
Elevation (m)
1000
800
600
400
200
0
Local Distance (m)

Transect 9

Point ID	Comment	Elevation (m)	UTM Easting	UTM Northing	Vertical Precision	Max PDOP	Notes
1	PS	70.323	292306.6	901964.9	1.3	3.1	
2	PS	64.986	292322.7	901983.9	1.5	4.4	
3	IE	58.826	292346.9	902026.6	1.2	2.9	
4	T	57.062	292402.3	902113.3	1.4	2.8	
5	T	56.66	292427.4	902107	1.1	2.1	
6	T	55.862	292453.4	902104.5	1.2	2.9	
7	OE	55.679	292482.2	902092.5	1.4	2.3	
8	IE	54.708	292514	902070.1	1.2	2.4	
9	T	49.027	292623.8	902013.9	1.3	2.3	
10	OE	47.477	292697.3	902194.6	1.6	2.7	
11	R	45.071	292708.3	902189.4	1.1	2.1	
12	R	41.829	292728.9	902185.9	1.2	2.1	
13	IE	30	292827	902179			Projected
14	T	28.447	292900.3	902178.7	1.2	2.2	
15	T	28.383	292957.1	902174.3	1.9	3	
16	T	26.962	293031.8	902159.1	1.6	2.6	
17	OE	20.146	293092.5	902126.4	1.5	2.2	
18	R	15.097	293100.9	902118.5	1.3	2	
19	R	6.071	293127.4	902113.7	1.4	4.3	
20	IE	4.913	293157.6	902070.6	1.5	2.7	
21	T	2.094	293204.7	902058.4	1.6	2.7	
22	T	2.84	293244.6	902053.8	2.3	4.8	
23	T	2.896	293293.3	902035.4	2.2	2.1	
24	OE	2.696	293308.3	902024.1	1.3	2.3	
25	HT	70.323	293324.8	902019.2	1.3	3.1	